

1-1-2009

# Flow behaviour of water-in-oil emulsions stabilized by wax crystals

Roomana Aafaqi

Follow this and additional works at: <http://digitalcommons.ryerson.ca/dissertations>

 Part of the [Chemical Engineering Commons](#)

---

## Recommended Citation

Aafaqi, Roomana, "Flow behaviour of water-in-oil emulsions stabilized by wax crystals" (2009). *Theses and dissertations*. Paper 1069.

This Thesis is brought to you for free and open access by Digital Commons @ Ryerson. It has been accepted for inclusion in Theses and dissertations by an authorized administrator of Digital Commons @ Ryerson. For more information, please contact [bcameron@ryerson.ca](mailto:bcameron@ryerson.ca).

6175 6271X  
TP  
156  
EG  
A74  
2009

# FLOW BEHAVIOUR OF WATER-IN-OIL EMULSIONS STABILIZED BY WAX CRYSTALS

by

**Roomana Aafaqi**

Master of Science, USM, Malaysia  
Bachelor of Engineering, UPM, Malaysia

A thesis

presented to Ryerson University

in partial fulfillment of the  
requirements for the degree of

**Master of Applied Science**

in the Program of  
Chemical Engineering

Toronto, Ontario, Canada, 2009

©Roomana Aafaqi 2009

I hereby declare that I am the sole author of this thesis or dissertation.  
I authorize Ryerson University to lend this thesis or dissertation to other  
institutions or individuals for the purpose of scholarly research.

-----  
\* Signature

I further authorize Ryerson University to reproduce this thesis or dissertation  
by photocopying or by other means, in total or in part, at the request of other  
institutions or individuals for the purpose of scholarly research.

-----  
\*Signature

# Abstract

## FLOW BEHAVIOUR OF WATER-IN-OIL EMULSIONS STABILIZED BY WAX CRYSTALS

©Roomana Aafaqi

Master of Applied Science, Department of Chemical Engineering  
Ryerson University, Toronto, Canada, 2009

The large temperature gradients experienced by crude oil emulsions in pipelines found in colder environments can lead to the precipitation, deposition and build-up of wax-like species from the crude oil onto the pipe wall that result in flow assurance problems. The objective of this thesis was to understand the rheological behaviour of model water-in-oil emulsions stabilized by wax crystals.

The microstructure, phase transitions and rheology of model emulsions consisting of water, mineral oil, paraffin wax and the emulsifier polyglycerol polyricinoleate (PgPr) were investigated. Changes in emulsion flow behaviour (steady state and dynamic) as a function of composition, temperature and passage through a laboratory-scale flowloop were investigated, with these parameters significantly affecting shear flow, yield stress and viscoelasticity. The gelation temperature of wax-containing ('waxy') oil was slightly lower than that of its equivalent emulsion due to differences in the structure of the gelled emulsion network. Overall, this study successfully showed that there exist significant differences in the microstructure and flow behaviour of model crude oil emulsions when wax and a dispersed aqueous phase are present.

# Acknowledgements

I would like to express my deepest gratitude to my supervisor, Dr. D errick Rousseau, for his supervision, patience and guidance throughout my studies. His comments and suggestions throughout the research and during the thesis revisions are highly appreciated.

I wish to thank the contributing members of Chevron Corporation (Houston, Texas, USA) and Chevron Canada Resources (Calgary, Alberta, Canada) team for their assistance and support, namely Dr. Alberto Montesi, Dr. Rama Venkatesan, Mr. Lee Rhyne, Mr. Mark Williams and Mr. David Buckley for their invaluable and thought-provoking discussions during the tenure of this work.

I also thank the administrative and technical staff of the Department of Chemical Engineering for their support throughout the duration of my studies. Furthermore, I would like to thank Dr. Supratim Ghosh for his extensive contributions to the work, especially in the microscopy sections. Special thanks are also due to Professor Farhad Ein-Mozaffari for the extensive usage of his rheometer.

The support of friends and fellow graduate students is also highly appreciated. Finally, I would like to extend my deep gratitude to my family for their support and patience.

# Table of contents

<b>ABSTRACT.....</b>	<b>III</b>
<b>ACKNOWLEDGEMENTS .....</b>	<b>IV</b>
<b>TABLE OF CONTENTS .....</b>	<b>V</b>
<b>LIST OF FIGURES.....</b>	<b>IX</b>
<b>LIST OF SYMBOLS .....</b>	<b>XIII</b>
<b>CHAPTER 1: INTRODUCTION .....</b>	<b>1</b>
<b>1.1 Model System Justification .....</b>	<b>1</b>
1.1.1 Fundamental Concepts.....	2
1.1.1.1 Wax Appearance Temperature (WAT).....	2
1.1.1.2 Gelation Temperature (Pour Point).....	3
1.1.2 Wax Deposition Mechanisms .....	5
1.1.2.1 Molecular Diffusion.....	5
1.1.2.2 Brownian Diffusion .....	6
1.1.2.3 Gravity Settling.....	6
1.1.2.4 Shear Dispersion .....	7
1.1.3 Pigging.....	8
<b>1.2 Crude Oil Emulsions .....</b>	<b>9</b>
<b>1.3 Research Objectives.....</b>	<b>10</b>
<b>1.4 Thesis Structure .....</b>	<b>10</b>
<b>CHAPTER 2: LITERATURE REVIEW .....</b>	<b>13</b>
<b>2.1 Crude Oil .....</b>	<b>13</b>
2.1.1 Classification of Crude Oils.....	14
2.1.2 Saturates/Aromatics .....	17
2.1.3 Asphaltenes.....	17
2.1.4 Resins.....	18
2.1.5 Solids .....	18
2.1.6 Wax.....	18
2.1.7 Crude Oil Emulsions.....	21

<b>2.2 Emulsion Characteristics .....</b>	<b>22</b>
2.2.1 Basic Principles.....	22
2.2.2 Emulsifying Agents .....	23
2.2.2.1 Surfactants .....	23
2.2.2.2 Solid Particles .....	26
2.2.3 Emulsion (In)stability .....	28
2.2.3.1 Creaming/Settling .....	28
2.2.3.2 Flocculation/Aggregation .....	30
2.2.3.3 Coalescence .....	30
2.2.3.4 Ostwald Ripening .....	31
2.2.4 Treatment of Emulsions.....	31
<b>2.3 Rheology of Emulsions .....</b>	<b>32</b>
2.3.1 Factors Involving the Dispersed Phase that Affect Emulsion Rheology .....	33
2.3.2 Factors Involving the Continuous Phase that Affect Emulsion Rheology .....	34
<b>2.4 Crude Oil Emulsion Studies.....</b>	<b>35</b>
2.4.1 Crude Oil Emulsion Stability.....	35
2.4.2 Effect of Solids on Crude Oil Emulsion Stability.....	36
2.4.2.1 Effect of Solids Size and Concentration .....	36
2.4.2.2 Effect of Solids Shape and Density .....	37
2.4.2.3 Effect of Solids Wettability .....	38
2.4.3 Crude Oil Rheology .....	39
2.4.4 Factors Affecting Rheological Behaviour .....	39
2.4.4.1 Thermal History .....	40
2.4.4.2 Shear History .....	41
2.4.4.3 Time Dependency .....	41
2.4.4.4 Effect of Water Droplets.....	42
2.4.5 Modelling Crude Oil Emulsions.....	44
<b>CHAPTER 3: EXPERIMENTAL.....</b>	<b>47</b>
<b>3.1 Materials .....</b>	<b>47</b>
3.1.1 Mineral Oil.....	47
3.1.2 Water.....	49
3.1.3 Surfactant .....	49
3.1.4 Paraffin Wax .....	50
<b>3.2 Model Crude Oil Emulsion Preparation .....</b>	<b>51</b>
<b>3.3 Laboratory Flowloop.....</b>	<b>52</b>
<b>3.4 Analytical Methods .....</b>	<b>54</b>
3.4.1 Pulsed Field Gradient Nuclear Magnetic Resonance (PFG-NMR) .....	54
3.4.2 Confocal Laser Scanning Microscopy (CLSM) .....	54

3.4.3 Polarized Light Microscopy (PLM).....	56
3.4.4 Differential Scanning Calorimetry (DSC) .....	56
3.4.5 Bohlin C-VOR Rheometer .....	56
<b>CHAPTER 4: WAX CRYSTALLIZATION IN A MODEL CRUDE OIL</b>	<b>58</b>
<b>4.1 Introduction.....</b>	<b>58</b>
<b>4.2 Materials and Methods.....</b>	<b>59</b>
<b>4.3 Results and Discussions .....</b>	<b>60</b>
4.3.1 Wax Crystallization in Wax-Containing Oil .....	60
4.3.1.1 Differential Scanning Calorimetry (DSC) .....	60
4.3.1.2 Confocal Laser Scanning Microscopy (CLSM) .....	62
4.3.1.3 PFG-NMR results .....	65
4.3.2 Wax Crystallization in Emulsion.....	66
4.3.2.1 Sedimentation Behaviour.....	66
4.3.2.2 Droplet Size Distribution .....	68
4.3.2.3 CLSM of Emulsions .....	69
<b>4.4 Conclusion .....</b>	<b>70</b>
<b>CHAPTER 5: BASELINE FLOW CONDITIONS FOR MODEL CRUDE OIL EMULSIONS IN A LAB-SCALE FLOWLOOP .....</b>	<b>72</b>
<b>5.1 Introduction.....</b>	<b>72</b>
<b>5.2 Materials and Methods.....</b>	<b>74</b>
<b>5.3 Results and Discussion .....</b>	<b>75</b>
5.3.1 Determination of $\Delta P$ and the Rate of Cooling .....	75
5.3.2 Theoretical Shear Rate in the Flowloop .....	78
5.3.3 Shear Plateau Determination .....	78
<b>5.4 Conclusion .....</b>	<b>82</b>
<b>CHAPTER 6: RHEOLOGICAL BEHAVIOUR OF CRUDE OIL EMULSIONS .....</b>	<b>83</b>
<b>6.1 Introduction.....</b>	<b>83</b>
<b>6.2 Material and Methods .....</b>	<b>85</b>
<b>6.3 Results and Discussion .....</b>	<b>87</b>
6.3.1 Viscosity Profiles.....	87
6.3.2 Flow Behaviour of Model Crude Oil Emulsions in a Lab-scale Flowloop.....	91

6.3.2.1 Steady State Rheological Behaviour.....	91
6.3.2.2 Dynamic Rheological Behaviour.....	99
<b>6.4 Conclusions.....</b>	<b>104</b>
<b>CHAPTER 7: YIELDING AND GELLING OF MODEL CRUDE OIL EMULSIONS .....</b>	<b>105</b>
<b>7.1 Introduction.....</b>	<b>105</b>
<b>7.2 Materials and Methods.....</b>	<b>108</b>
<b>7.3 Results and Discussion .....</b>	<b>109</b>
7.3.1 Yielding of Model Crude Oil Emulsions.....	109
7.3.1.1 Effect of Temperature.....	109
7.3.1.2 Effect of Shear History .....	110
7.3.1.3 Effect of Ageing.....	112
7.3.2 Gelation of Model Crude Oil Emulsions.....	114
7.3.2.1 Effect of Cooling Rate .....	114
7.3.2.2 Crude Oil Emulsion vs. Waxy Oil Gelation .....	117
7.3.2.3 Effect of PgPr.....	117
<b>7.4 Conclusion .....</b>	<b>118</b>
<b>CHAPTER 8: CONCLUSIONS AND RECOMMENDATIONS.....</b>	<b>120</b>
<b>8.1 Conclusions.....</b>	<b>120</b>
<b>8.2 Recommendations.....</b>	<b>122</b>
<b>REFERENCES .....</b>	<b>124</b>

# List of Figures

Figure 1.1 Schematic of wax network structures of crude oil at various temperatures (a) just below WAT (b) between WAT and gelation temperature (c) just below gelation temperature .....	4
Figure 1.2 Cross-sectional view of a plugged pipeline.....	8
Figure 2.1 SARA separation scheme for crude oil .....	15
Figure 2.2 Molecular structures schematics of wax. ....	19
Figure 2.3 Micellization of surfactant molecule .....	24
Figure 2.4 Wettability of water-oil surfaces .....	27
Figure 2.5 Natural emulsion destabilization processes (a) creaming and sedimentation (b) flocculation/aggregation (c) coalescence and (d) Ostwald ripening .....	29
Figure 3.1 High temperature gas chromatogram of light mineral oil .....	48
Figure 3.2 Critical micelle concentration (CMC) determination of PgPr at a planar water/oil interface. ....	50
Figure 3.3 Carbon distribution of paraffin wax using HTGC.....	51
Figure 3.4 Schematic of the laboratory flowloop system .....	53
Figure 3.5 Effect of added dyes on the droplet size distribution of model emulsions. The 2.5%, 50% and 97.5% values are the volume-weighted % of the water droplets smaller than the corresponding droplet diameter.....	55
Figure 4.1 DSC thermogram of pure paraffin wax.....	61
Figure 4.2 DSC thermogram of mineral oil, wax and emulsifier mixtures (from 4 to 70 °C at 5 °C min <sup>-1</sup> ).....	61
Figure 4.3 Enthalpies of fusion of wax crystals in oil with and without added emulsifier (from 4 to 70 °C at 5 °C min <sup>-1</sup> ).....	62
Figure 4.4 Micrographs of wax-oil-PgPr mixtures (T=25 °C) after 0, 1 and 7 days of storage. Wax crystals appear as white needles dispersed in the oil phase, which appears dark. The size bar represents 25 µm. ....	63

Figure 4.5 Total crystal area in mixtures of light mineral oil and wax at different wax concentrations and in the absence/presence of PgPr (T=25°C). .....	64
Figure 4.6 Mean crystal length in mixtures of light mineral oil and wax at different wax concentrations and in the absence/presence of PgPr (T=25°C).....	65
Figure 4.7 Sedimentation of water-in-oil emulsions containing 2.5% PgPr, 20% water and either (a) 3% wax or (b) 5% wax in the oil phase as a function of storage time at 25 °C. ....	67
Figure 4.8 Droplet size distribution of emulsions containing 3% wax and 2.5% PgPr (closed symbol) vs. 5% wax and 2.5% PgPr (open symbol). ....	69
Figure 4.9 CLSM pictures of model emulsions containing 3 or 5% (w/w) wax. The size bar represents 20 µm. ....	70
Figure 5.1 Typical flowloop data for the model crude oil emulsion passed through a 5 m loop. ....	76
Figure 5.2 Typical flowloop data for the model crude oil emulsion passed through a 10 m loop. ....	76
Figure 5.3 Shear plateau determination with different measuring times for model crude oil emulsions consisting of 5 % (w/w) wax. ....	79
Figure 5.4 Viscosity of model crude oil emulsions containing 5 % (w/w) wax as a function of shear rate at a cooling rate of 1 °C/min (error bars omitted for clarity).....	81
Figure 6.1 Temperature-dependent viscosity profile of mineral oil. ....	88
Figure 6.2 Temperature-dependent viscosity profile of a mineral oil-PgPr (2.5% w/w) mixture.....	88
Figure 6.3 Temperature-dependent viscosity profiles of mineral oil-wax mixture and the corresponding model emulsion consisting of mineral oil and water (4:1) and 5 % (w/w) wax. ....	89
Figure 6.4 Water DSD of the fresh and final emulsions after the application of shear rate of 200 s <sup>-1</sup> . ....	91
Figure 6.5 Viscosity profiles of emulsions as a function of temperature (shear rate = 200 s <sup>-1</sup> , rate of cooling = 1 °C/min). Error bars omitted for clarity. ....	92

Figure 6.6 Droplet size distribution of the emulsions' dispersed phase when passed through different lengths of the flowloop. ....	93
Figure 6.7 Yield stress determination of emulsions flowed through different flowloop lengths using a shear sweep method (0.5-8 Pa).....	94
Figure 6.8 Creep recovery tests for 5m loop-flowed emulsions. Error bars omitted for clarity. ....	96
Figure 6.9 Creep recovery tests for 10m loop-flowed emulsions. Error bars omitted for clarity. ....	96
Figure 6.10 Steady-state flow curves for the emulsions passed through different lengths of flowloop (symbols). The corresponding lines are the Herschel–Bulkley model fit. ....	98
Figure 7.1 Effect of cooling shear rates on the yield stress of an emulsion consisting of mineral oil and water (4:1) and 5 % (w/w) wax to a temperature of 4 °C.....	111
Figure 7.2 Wax crystal microstructure of the model emulsions with different shear histories (a) 0 s <sup>-1</sup> (static) and (b) 10 s <sup>-1</sup> . The scale bars represent 20 μm. ....	111
Figure 7.3 Effect of ageing time on the yield stress of emulsion (T = 14 °C). ....	113
Figure 7.4 Wax crystal evolution with ageing time (a) 0 hrs (b) 8 hrs. The size bar represents 25 μm. ....	113
Figure 7.5 Effect of cooling rates on the gelation of waxy oil (strain = 0.005, f = 1Hz) .....	115
Figure 7.6 Effect of cooling rates on the gelation of model emulsions (strain = 0.005, f = 1Hz).....	115
Figure 7.7 Isothermal change in G' of emulsion with time (T = 14 °C, strain = 0.005, f = 1 Hz).....	116
Figure 7.8 Effect of PgPr on the gelation of waxy oil (T = 14 °C, strain = 0.005, f = 1 Hz).....	118

# List of Tables

Table 2.1 SARA fractionation of Alberta and international bitumen and heavy oils.....	17
Table 2.2 Emulsions in the petroleum industry (Schramm, 1992). W/O refers to water-in-oil emulsions and O/W refers to oil-in-water emulsions .....	22
Table 4.1 Hydrogen nuclei diffusion coefficients ( $10^{-9}$ m <sup>2</sup> /s) for waxy oil.....	66
Table 5.1 Process conditions of the model emulsions as it passes through the flowloop.....	77
Table 5.2 Parameters used in the calculation of shear rate .....	78
Table 6.1 Outlet temperatures of the emulsions passed through different flowloop lengths .....	86
Table 6.2 Wax appearance temperatures (WAT) using rheometry (viscometry and oscillatory) and DSC.....	90
Table 6.3 Herschel-Bulkley model parameters for model emulsions.....	98
Table 7.1 Yield stress of model emulsions vs. wax % .....	110
Table 7.2 Comparison of gelation points of waxy oil and model emulsion....	117

# List of Symbols

$\gamma$	shear rate ( $s^{-1}$ )
$\delta$	phase angle ( $^{\circ}$ )
$\alpha$	shape factor
$\gamma$	resultant strain rate (%)
$\eta$	Newtonian dynamic viscosity (Pa·s)
$\eta_{\infty}$	infinite-shear rate viscosity (Pa·s)
$\eta_B$	Bingham viscosity coefficient
$\eta_c$	Casson viscosity coefficient
$\eta_o$	zero-shear rate viscosity (Pa·s)
$\eta_r$	relative viscosity
$\mu$	dynamic viscosity (Pa·s)
$\zeta$	thickness of gel layer (m)
$\pi$	mathematical constant (3.14)
$\rho_d$	density of the solid wax deposit ( $g/m^3$ )
$\sigma_1$	critical stress (Pa)
$\sigma_2$	apparent yield stress (Pa)
$\sigma_{HB}$	yield stress in Herschel-Bulkley model
$\tau_{gel}$	shear stress applied to the wax-oil mixture during gelation (Pa)
$\tau_y$	yield stress of the fluid (Pa)
$\phi$	volume fraction of the dispersed phase
$\omega$	radial frequency (Hz)
$A$	area of wax deposition ( $m^2$ )
$C$	volume fraction concentration of wax in oil
$d$	internal diameter of the pipe (m)
$D_e$	molecular diffusivity of wax in oil
$D_m$	diffusion coefficient of wax in oil
$dT/dt$	cooling rate applied during gelation ( $^{\circ}C/min$ )
$E_a$	activation energy (kJ/mol)
$g$	deformation (%)
$G'$	storage modulus (Pa)
$G''$	loss modulus (Pa)
$J_c$	creep compliance (1/Pa)
$J_r$	recoverable compliance (1/Pa)
$K$	consistency factor
$k_l$	Einstein's coefficient
$L$	length of pipe (m)
$m_m$	mass of deposited wax (g)
$n$	shear rate index
$Nu$	Nusselt number
$Q$	volumetric flow rate ( $m^3/h$ )
$r$	radial coordinate
$R$	universal gas constant
$s$	solid wax content

$T$	absolute temperature (°C)
$T_o$	bulk temperature (oil) (°C)
$T_w$	temperature at the pipe wall (°C)
$V$	velocity of fluid (m/s)
$\Delta P$	pressure drop (Pa)
$\Delta t$	time shift (s)

# Chapter 1

## Introduction

An unresolved difficulty facing the chemical, petroleum, food and pharmaceutical industries is the unwanted surface deposition of dissolved or suspended solids during fluid flow operations (Bott, 1997; Lee *et al.*, 1997; El-Hattab, 1985). For the crude oil industry, production, transportation and processing of petroleum is considerably affected by the deposition of asphaltenes, hydrates and wax in pipelines, with significant economic consequences (Venkatesan *et al.*, 2005).

### 1.1 Model System Justification

Crude oil is a complex mixture of hydrocarbons consisting of numerous components such as paraffins, aromatics, naphthenes, resins and asphaltenes. Amongst these, high molecular weight paraffin waxes as well as hydrates and asphaltenes are responsible for process inefficiencies during the production, separation, transport and refining of the oil, as these can deposit on the inner wall of pipelines and/or mass-congeal, thereby requiring high startup pressures, perhaps beyond the well capacity. In their native environment, most crude oil components are in the liquid state as the local temperature maintains them above their solidification temperatures. Below a critical temperature, higher-

melting components (*e.g.*, long-chain paraffin waxes) will precipitate as their solubility decreases, altering viscosity and thus fluid flow. This behaviour is very difficult to predict, thus complicating oil processing.

Crude oils from diverse origins will exhibit differences in density, viscosity, interfacial tension, interparticle interactions and thus solids deposition behaviour. As a result, rather than studying many different oils or selecting more representative oils, in this research, model oils and emulsions with known compositions were explored, so that the interplay between overall composition, rheology, and the role of shear and temperature on product stability and deposition behaviour could be pinpointed.

## **1.1.1 Fundamental Concepts**

### **1.1.1.1 Wax Appearance Temperature (WAT)**

Depending on their composition (*e.g.*, aliphatic chain length) and structure (*e.g.*, chain branching), wax solubility in aromatic and naphthalenic compounds may be low, and may decrease drastically with decreasing temperatures. The highest temperature below which paraffin wax start to precipitate as crystals is defined as the wax appearance temperature (WAT).

When measuring the WAT, the key is to preheat the oil sample to a high enough temperature to fully solubilize all pre-existing wax crystals and remove the presence of crystal history. There are several techniques available for WAT measurements, including viscometry, differential scanning calorimetry, cross polarization microscopy, filter plugging, and Fourier transform infrared energy scattering. Typically, the WAT is measured using more than one technique as it

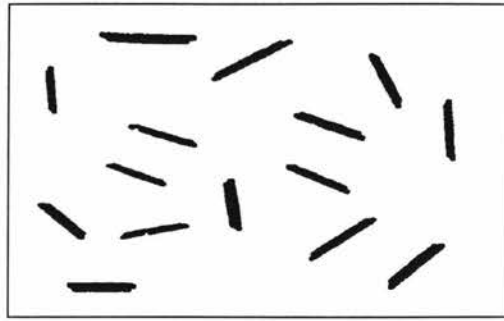
may differ by more than 10 °C when using different techniques (Monger-McClure *et al.*, 1999; Hammami and Raines, 1997). Figure 1.1(a) shows the proposed organization of wax crystals at temperatures just below WAT under stagnant conditions. Once wax nucleates, there is crystal growth and the development of a network. The properties of this network will strongly influence flow efficiency in a pipeline.

### **1.1.1.2 Gelation Temperature (Pour Point)**

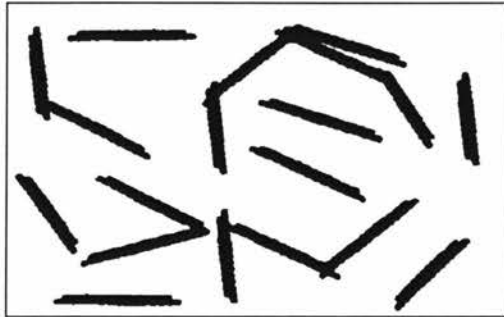
Wax-like species will precipitate from the crude oil once the temperature is below the WAT. The precipitated wax may deposit on the pipe wall and/or form a wax-oil gelled continuous network (Venkatesan *et al.*, 2002).

The gel deposit consists of wax crystals that entrap a portion of the oil. As the temperature is decreased, more wax will precipitate and the thickness of the waxy gel will increase, causing gradual solidification ('gelling') of the crude, eventually causing the oil to congeal and no longer flow. The temperature at which oil movement stops is defined as the crude gelation temperature (Figure 1.1). Because seawater temperatures are normally well below the gelation temperature of the crude, waxy gels may form after temporary pipeline shutdown. In this case, the crude oil is cooled during quiescent (static) conditions, resulting in significantly different properties compared to cooling under dynamic conditions (Paso *et al.*, 2005). Quantitative structural and rheological information on the gel strength may help to direct potential remediation approaches to break down the gel structure.

(a)



(b)



(c)

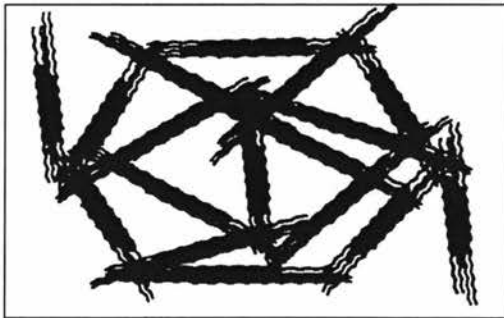


**Figure 1.1** Schematic of wax network structures of crude oil at various temperatures (a) just below WAT (b) between WAT and gelation temperature (c) just below gelation temperature (adapted from Singh *et al.*, 2001)

## 1.1.2 Wax Deposition Mechanisms

Wax deposition is a complex problem involving fluid dynamics, mass and heat transfers, and thermodynamics (Burger *et al.*, 1981; Brown *et al.*, 1993; Creek *et al.*, 1999; Hsu *et al.*, 1999; Singh *et al.*, 1999). It is now generally accepted that molecular diffusion of wax-like species from the crude oil towards the pipeline wall surface is the dominant deposition mechanism. Other mechanisms such as Brownian motion, gravity settling, and shear dispersion have also been mentioned as potentially influencing wax deposition, though their importance is now considered secondary (Guo *et al.*, 2005).

### 1.1.2.1 Molecular Diffusion

When waxy crude flows in pipelines, the temperature at the centre of the pipeline is the hottest and that at the pipe wall is the coldest, resulting in a radial temperature profile. Since wax solubility in the oil decreases as a function of temperature, when the temperature is lower than the WAT, wax crystals will start to appear. Thus, the radial temperature gradient will produce a concentration gradient of wax in the oil with the molten wax concentration lowest closest to the pipe wall. The concentration gradient will thus result in mass transfer of wax from the centre of the pipe to the pipe wall by molecular diffusion (Guo *et al.*, 2005). Fick's second law of diffusion can be used to estimate this wax flux:

$$\frac{dm_m}{dt} = \rho_d D_m A \frac{dC}{dr} \quad 1.1$$

where  $m_m$  is the mass of deposited wax,  $\rho_d$  is the density of the solid wax deposit,  $D_m$  is the diffusion coefficient of the molten wax species in the oil,  $A$  is the area of wax deposition,  $C$  is the volume fraction concentration of molten wax in oil and  $r$  is the radial coordinate.

### **1.1.2.2 Brownian Diffusion**

Certain regions within oil flowing in a pipeline may be at temperatures below the cloud point (WAT). In this case, wax crystals will precipitate and be suspended in the oil. Such crystals may collide with thermally-agitated oil molecules, giving rise to an irregular ‘wiggling’ motion of the crystals. In the presence of a solid wax concentration gradient, there will be diffusive transport of wax crystals towards regions of lower crystal concentration. Many researchers (Brown *et al.*, 1993; Burger *et al.*, 1981; Hsu *et al.*, 1998; Hunt, 1962; Majeed *et al.*, 1990; Singh *et al.*, 1999) have claimed that the contribution of Brownian diffusion to wax deposition is small, since it is compensated by the drag of the fluid.

### **1.1.2.3 Gravity Settling**

Wax crystals tend to be denser than the solvent oil (Azevedo *et al.*, 2003); therefore, gravity settling is a possible mechanism for deposition. Studies conducted by Burger *et al.* (1981) under centrifugal fields determined typical size distributions of crystals and terminal settling velocities. For typical operating conditions encountered in pipelines, these velocities did not

significantly contribute to the formation of wax deposits. Further experimental studies conducted by the same authors confirmed these predictions.

#### **1.1.2.4 Shear Dispersion**

As with Brownian diffusion, wax deposition by shear dispersion is a means of cross-stream transport of solid particles in suspension. In general, the motion of solid particles depends on their size, relative density and concentration (Azevedo *et al.*, 2003). Several studies on concentrated solid wax have indicated that the motion of particles (*e.g.*, crystals) in a shear field will be in the direction of decreasing shear and will not affect wax deposition (Brown *et al.*, 1993; Burger *et al.*, 1981; Hsu *et al.*, 1998; Hunt, 1962).

Crude oil flow behaviour is highly composition-dependent, with certain crude varieties more susceptible to deposition and plugging, particularly high-wax crudes. Thus, if the oil temperature drops below the WAT, wax-like materials may start to precipitate and deposit on the pipe's internal surface. Continued deposition will lead to a reduction in the pipe's internal diameter, effectively resulting in a higher pressure drop. In extreme cases, wax deposition may be so severe that prevention methods, such as pigging (described below), may be required. In certain situations, the plugging of pipelines may lead to shutdown or even complete abandoning of the operation (Wang *et al.*, 2005). This is particularly so with transportation and production of waxy crude oils, as the ambient temperature is often well below their WAT or gelation temperatures (Venkatesan *et al.*, 2005).

Figure 1.2 shows a cross-sectional view of a pipeline severely affected by paraffin deposition. As shown in Figure 1.2, the area available for crude oil flow is drastically reduced. Under such circumstances, the portion of the pipeline that is plugged would have to be replaced, resulting in significant operational costs. According to the US Department of Energy, remediation of pipeline blockage in water depths of about 400m can cost \$1 million/mile (Venkatesan *et al.*, 2005).

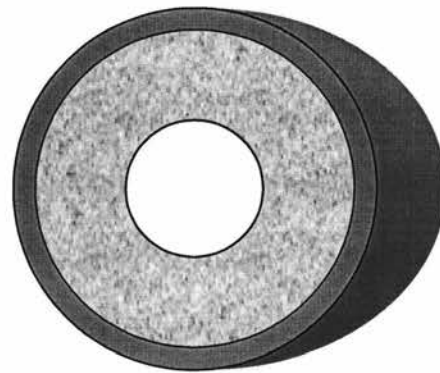


**Figure 1.2** Cross-sectional view of a plugged pipeline (adapted from Venkatesan *et al.*, 2005)

### 1.1.3 Pigging

Pigging is the standard industrial process of using ‘scraper’ devices to remove the wax deposits from the pipe walls. During mechanical pigging, wax deposits in pipelines may be scraped out by pigs, which are forced through the pipeline by the flowing crude oil. These usually consist of steel bodies, potentially with attachments such as brushes to help in cleaning (Hsu *et al.*, 1998). There are numerous types of pigs, *e.g.*, simple spheres, foam pigs, and smart pigs. The pig is sent into a pipeline using a pig launcher, and is pushed by

the crude itself or other material such as gas. The pig mechanically scrapes the wax from the pipe wall and re-deposits it back into the crude. This method requires knowledge on the hardness of the deposit, which depends on the ageing time, wax composition and thermal and shear history of the wax deposit or gel.

## 1.2 Crude Oil Emulsions

Emulsions can be encountered at many stages during drilling, producing, transporting and processing of crude oils and in many locations such as in hydrocarbon reservoirs, well bores, surface facilities, transportation systems and refineries (Langevin *et al.*, 2004). Water, which is naturally present in oil reservoirs, mixes with crude oil to form potentially stable emulsions due to the presence of very high shear rates and zones of turbulence encountered in choke valves. In most cases, water-in-crude oil (W/O) emulsions are created given the oil-soluble nature of the native surfactants (such as asphaltenes and resins) and the presence of small solid particles (crystallized waxes and clays, for example). In oilfield operations, the water content of the emulsion can be as high as 60-70% in volume, while in the refinery the amount is generally much smaller (1-6%) (Ronningsen *et al.*, 1992).

While the rheological behaviour of waxy crude oil is well characterized, very little work has been done on the potential impact of emulsified water on crude oil flow behaviour. A thorough understanding of the rheological behaviour of crude oil emulsions is necessary when attempting to diminish the operational problems these can cause.

## **1.3 Research Objectives**

The overall goal of this research was to understand the rheological behaviour of crude oil emulsions stabilized by wax crystals. This understanding was intended to provide insight on wax deposition in pipelines and a basis for remediation.

The objectives of this research were to:

- (1) understand wax crystallization processes in model emulsions representative of crude oil emulsions;
- (2) characterize the model crude oil emulsions' rheological behaviour;
- (3) determine the changes in the rheological behaviour of the model crude oil emulsion flowed through a laboratory-scale flowloop;
- (4) investigate the yielding and gelation behaviour of the model crude oil emulsions;
- (5) correlate rheology with the crystal growth and microstructure of the wax under various conditions.

## **1.4 Thesis Structure**

The chapters of this thesis have been written to be read independently, with each chapter providing relevant background knowledge, as well as experimental and theoretical details. Because of this format, there is some repetition of introductory material from chapter to chapter. An overview of each chapter is as follows:

*Chapter2.* This chapter serves as an introduction to the subject of water-in-crude oil emulsions. First, crude oil composition, with a focus on native oilfield solids is discussed. Second, basic emulsion principles, emulsifiers, emulsion stabilization mechanisms and the methods used to commercially treat oilfield emulsions are introduced. Finally, the flow behaviour of crude oil is reviewed.

*Chapter3.* This chapter describes the materials, properties examined and the instruments used in the present work, namely: droplet size distribution and solid wax content (using pulsed NMR), wax crystallization behaviour (using DSC), microstructure of wax crystals (using confocal and light microscopy) and rheology (using a controlled shear rheometer). The operating principles of these instruments are also discussed.

*Chapter4.* This chapter focuses on the wax crystallization behaviour of a model waxy oil and emulsions. It also compares the crystallization properties of wax as its concentration changes in model systems.

*Chapter5.* The focus of this chapter is the theoretical determination of the emulsions' in-pipe flow conditions and the development of an experimental protocol for rheological measurements that mimics pipeline flow conditions in a rheometer.

*Chapter6.* This chapter presents the rheological behaviour of model crude oil emulsions. First, the viscosity profiles of the model systems are presented. Secondly, the change in their flow behaviour following transport in a model flowloop are ascertained. This comprises steady-state, oscillatory and creep recovery measurements.

*Chapter 7.* This chapter explains the yielding behaviour of model emulsions and how this changes with time, stress and temperature-dependent wax crystallization. Gelation behaviour is also discussed.

*Chapter 8.* This chapter summarizes the main findings of this study and suggests recommendations for future research.

# Chapter 2

## Literature Review

### 2.1 Crude Oil

Crude oil is a complex mixture of hydrocarbons consisting of numerous components such as paraffins, aromatics, naphthenes, resins and asphaltenes. (Oliveira *et al.*, 2007). The approximate carbon chain range for these components is  $C_5H_{12}$  to  $C_{18}H_{38}$  (Oliveira *et al.*, 2007). Shorter hydrocarbons are considered natural gas while longer hydrocarbon chains are more solid, and the longest chained-species are referred to as coal. In its naturally occurring form, crude oil may also contain other non-metallic elements such as sulphur, oxygen, and nitrogen. It is usually black or dark brown in colour (although it may be yellowish or even greenish), but varies greatly in appearance, depending on composition (Singh *et al.*, 2001). The origin of the crude oil can have a significant effect on composition, resulting in oils varying widely in volatility, density, viscosity, colour and flow behaviour (Khan *et al.*, 1996).

Crude oil remains an abundant commodity. Globally, some 650 billion barrels of oil have been produced. According to a recent source (Hou *et al.*, 2007), there remains another trillion barrels of proved reserves to be produced.

An additional 10 trillion barrels of oil resources await development, assuming the price of oil someday justifies production. Petroleum is also the raw material for many chemical products, including solvents, fertilizers, pesticides and plastics (Schramm, 1992).

Conventional crude oil refers to oil that can be produced through primary recovery without the addition of heat, chemicals or solvents. These can be produced through pumping operations because of their low viscosity and density (Speight, 1999). Oil that is significantly more viscous and has a lower API gravity (higher density) is called “heavy crude oil”. These oils require some heat input or the addition of solvents to reduce viscosity during production. Extra heavy crude oils (bitumens) are even denser and more viscous than heavy oil and usually contain significantly higher quantities of metallic groups and heteroatoms (sulphur, nickel, vanadium, lead *etc.*). They are solid or near-solid materials that do not flow freely under ambient conditions and are usually produced through mining of oilsand deposits (Speight, 1999).

### **2.1.1 Classification of Crude Oils**

The petroleum industry generally classifies crude oil by the geographic location it is produced in (*e.g.*, West Texas, Brent, or Oman), its API gravity (an oil industry measure of density), and by its sulphur content (Irani *et al.*, 1982). Crude oil may be considered *light* if it has low density or *heavy* if it has high density; and it may be referred to as *sweet* if it contains relatively little sulphur or *sour* if it contains substantial amounts of sulphur (Aske *et al.*, 2001).

Given their complex composition, crude oils are most commonly classified on the basis of their polarity and solubility. The four solubility classes are saturates, aromatics, and resins (collectively known as maltenes) as well as asphaltenes. Their method of separation is called SARA fractionation (the abbreviation is made up of the first letter of each solubility class) and is shown in Figure 2.1.

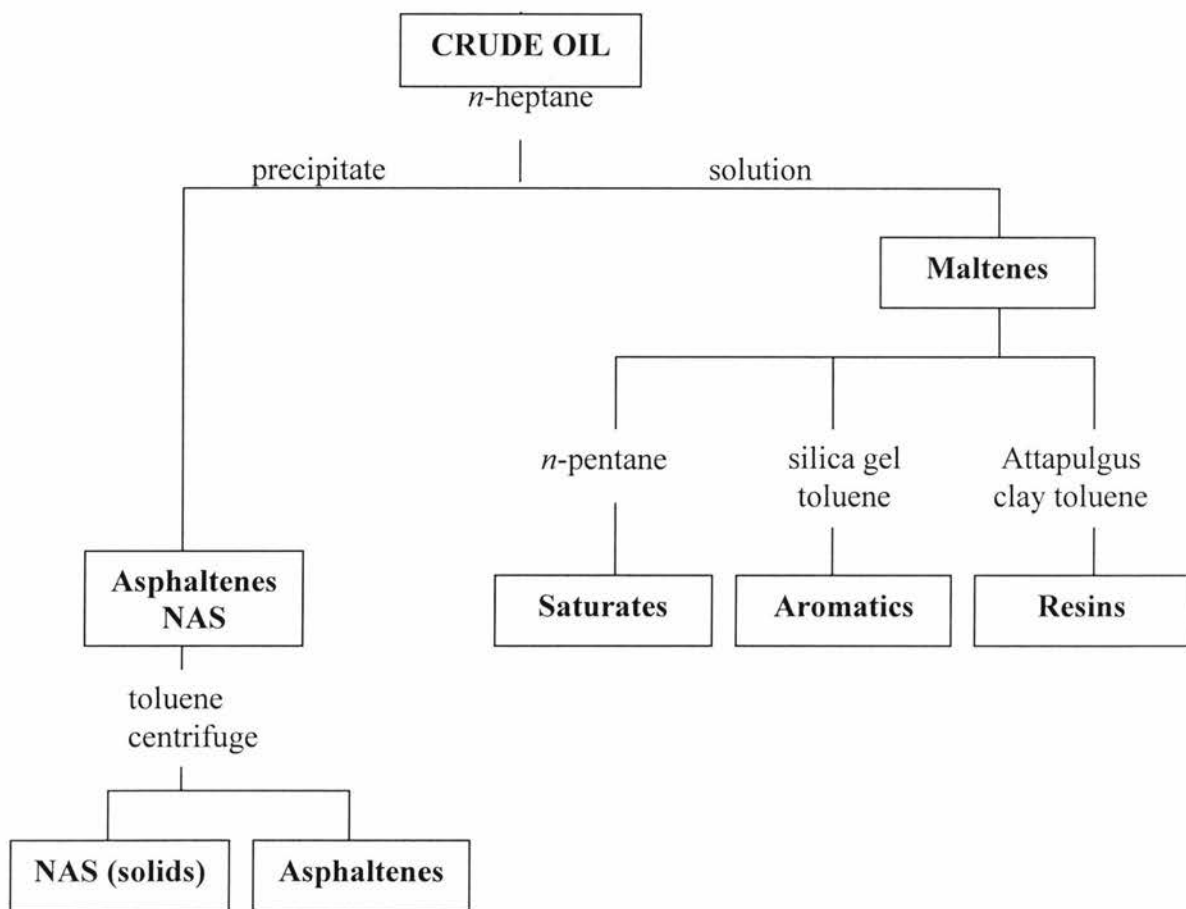


**Figure 2.1** SARA separation scheme for crude oil (Aske *et al.*, 2001)

The first SARA fractionation step is the separation of the asphaltenes from crude oil. Asphaltenes are precipitated by adding 40 volumes of *n*-heptane to 1 volume of crude oil. The mixture is usually stirred, allowed to settle, and filtered. The dark brown/black powder remaining in the filter paper comprises the asphaltenes. The maltenes passing through the filter are concentrated by evaporating the associated pentane and then separated into saturates, aromatics and resins through clay-gel adsorption chromatography. Resins adsorb onto Attapulugus clay (which is surface-active), aromatics adsorb on silica gel, and saturates elute directly. The resins are separated from the clay with a 50/50 (w/w) mixture of toluene and pentane whereas the aromatics are separated with a mixture of 50/50 (w/w) toluene and acetone. The solvents are evaporated to concentrate each component.

A putative SARA analysis of Alberta and international bitumen and heavy oil is given in Table 2.1 (Peramanu *et al.*, 1999; Akbarzadeh *et al.*, 2004). Note that other solvents may be used for deasphalting oil. Pentane is used if one requires all four solubility classes for use; however, asphaltenes are often precipitated with hexane or heptane if their recovery alone is desired.

**Table 2.1** SARA fractionation of Alberta and international bitumen and heavy oils.

Source	Saturates (wt%)	Aromatics (wt%)	Resins (wt%)	Asphaltenes (wt%)
<b>Western Canadian</b>				
Athabasca	17.3 <sup>(a)</sup> , 16.3 <sup>(b)</sup>	39.7 <sup>(a)</sup> , 39.8 <sup>(b)</sup>	25.8 <sup>(a)</sup> , 28.5 <sup>(b)</sup>	17.3 <sup>(a)</sup> , 14.7 <sup>(b)</sup>
Cold Lake	20.7 <sup>(a)</sup> , 19.4 <sup>(b)</sup>	39.2 <sup>(a)</sup> , 38.1 <sup>(b)</sup>	24.8 <sup>(a)</sup> , 26.7 <sup>(b)</sup>	15.3 <sup>(a)</sup> , 15.5 <sup>(b)</sup>
Lloydminster <sup>(b)</sup>	23.1	41.7	19.5	15.3
<b>International</b>				
Venezuela <sup>(b)</sup>	15.4	44.4	25.0	15.2
Russia <sup>(b)</sup>	25.0	31.1	37.1	6.8
Indonesia <sup>(b)</sup>	23.2	33.9	38.2	4.7

(a) Peramanu *et al.*, 1999; (b) Akbarzadeh *et al.*, 2004)

## 2.1.2 Saturates/Aromatics

Saturates are defined as non-polar hydrocarbons that include straight and branched alkanes and cycloparaffins compounds (naphthalenes). Wax (long-chained paraffins) is also classified as a sub-class of saturates. As the name implies, aromatics are composed of structures containing aromatic rings. They include monoaromatics, substituted naphthalenes, and phenanthrenes. Saturates and aromatics generally are the lightest fraction of the crude oil (Sjöblom *et al.*, 2002).

## 2.1.3 Asphaltenes

Asphaltenes are defined as the crude oil fraction insoluble in *n*-heptane, but soluble in toluene (Daniel-David *et al.*, 2008). These are defined as large, polar, polynuclear molecules consisting of condensed aromatic rings, aliphatic side chains and various heteroatom groups (Strausz *et al.*, 1992; Watson and Barteau, 1994). As a result, these are the highest molecular weight and most polar compounds of crude and are responsible for the high density and viscosity

of some heavy crude oils and bitumens. The chemical characteristics of asphaltenes render them amphiphilic and thus surface-active (Taylor, 1992; Schildberg *et al.*, 1995).

#### **2.1.4 Resins**

Resins in crude oil consist mainly of naphthalenic aromatic hydrocarbons, with aromatic ring systems and alicyclic chains. Hence, resins contain molecules similar to those found in aromatics, except that they are generally larger and contain more sulphur, oxygen and nitrogen. The crude oil resins are to some extent interfacially-active and are effective as a dispersant of asphaltenes (Aske *et al.*, 2001).

#### **2.1.5 Solids**

Some of the most stable oilfield emulsions contain a relatively large amount of solids, often consisting of non-asphaltenic solids (NAS) < 1  $\mu\text{m}$  in size. Solids may be clays or silicates present in the crude (native solids), corrosion products, or precipitated material such as chemical additives that have become insoluble.

#### **2.1.6 Wax**

Crude oil can contain a significant quantity of wax, which can crystallize during production, transportation and storage of oil. This leads to flow restriction and plugging in pipelines. The presence of solid wax below the WAT affects the prediction and evaluation of the oil's flow properties.

Wax concentration and compositional distribution in crude oil depends on the oilfield. The molecular weight distribution of the wax typically ranges

from 10 to 100 carbons. As a term, wax includes *n*-alkane/paraffins, *iso*-paraffins and *cyclo*-paraffins. Figure 2.2 illustrates the molecular structure of each kind of wax.

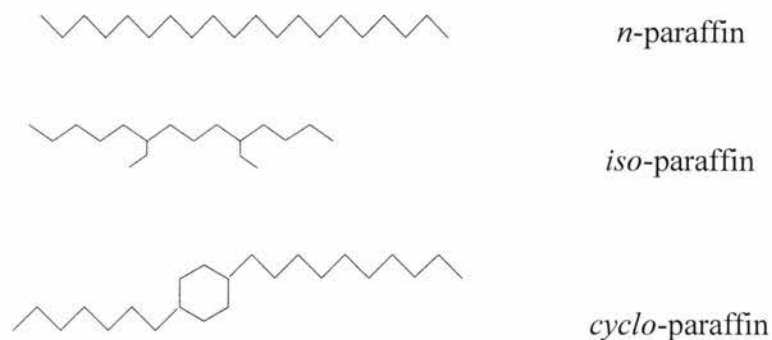


**Figure 2.2** Molecular structures schematics of wax (Speight, 1999).

Wax crystallization is a complex phenomenon. Paraffins crystallize as long needles/plates whereas *iso*- and *cyclo*-paraffins crystallize as amorphous masses (Ronningsen *et al.*, 1992). Paraffins are found to have a sharp transition in gel strength at the pour point (PP). Extensive studies report that very small amounts (1-6%) of wax solids are able to cause oil gelation (Kané *et al.*, 2003, Speight, 1999, Visintin *et al.*, 2005). However, the gel strength build-up in *iso*-paraffins is a gradual process (Visintin *et al.*, 2005).

At high temperatures, wax is in liquid state and crude oil behaves as a Newtonian fluid. As the waxy crude cools to below the WAT, wax will start to crystallize, agglomerate and entrap the liquid oil into its structures. The crystallization of wax significantly increases crude oil viscosity, altering the flow behaviour of the crude to non-Newtonian behaviour.

An understanding of the microstructural organization of the individual wax crystals and their association into flocs and into a network is important to ascertain deposition behaviour. It has been proposed that the growth of platelet-like crystallites leads to a crystalline or gel-like structure with entrapped liquid oil (Dirand *et al.*, 1998; Holder and Winkler, 1965), where molecular diffusion is the dominant mechanism for wax deposition from crude oil (Ramirez-Jaramillo *et al.*, 2001; Akbarzadeh and Zougari, 2008). The importance of heat transfer in the formation and growth of wax deposition has also been shown (Bidmus and Mehrotra, 2004; Fong and Mehrotra, 2007). Fogler's group (Venkatesan *et al.*, 2005; Singh *et al.*, 2000) proposed that wax deposition proceeds initially via the formation of a gel-like deposit, noting that its structure and composition are dependent on the thermal and shear conditions, though wax compositional variety also promotes gelation (Paso *et al.*, 2005). Visintin *et al.* (2005) found similarities between gelation (below the PP) and deposit formation (far above the PP), suggesting that wax solids formed in the oil at the pipewall will be rapidly frozen into open aggregate structures incorporating a large volume of liquid oil. These mechanically-weak structures would be substantially altered by the shear regime near the pipeline walls. The presence of an aqueous phase on wax crystallization, gelling and deposition has not been extensively studied.

Visintin *et al.* (2005) formulated an elegant model regarding the gelling behaviour of crude oils, invoking attractive interactions between the wax crystal network's individual crystallites as accounting for many properties of the gels,

including their ability to partly re-form following shearing. Rather than being a diffusion-limited process, the authors suggested that competition exists between wax crystal growth and crystallite aggregation. With the associating particles not initially present in the fluid, they form and grow in size at a rate determined by crystal nucleation and growth (NG), which is distinct from diffusion-limited gelation. In a complex system such as crude oil, NG will be heterogeneous as impurities present serve as nucleation sites for crystallization. After primary nucleation, crystals may behave as secondary nucleation sites and promote further crystallization. However, under the influence of mixing, mass transfer will be accelerated, implying that NG and crystallite aggregation or gelation will concurrently take place, as explored by Merino-Garcia *et al.* (2007).

### **2.1.7 Crude Oil Emulsions**

Crude oil is often recovered as an emulsified system due to the presence of water and surface-active hydrocarbons in crude oil combined with the shear caused by the flow through piping, valves and chokes.

Water (brine) and oil (light hydrocarbons) can mix as either water-in-oil (W/O) or oil-in-water (O/W) emulsion forms (Table 2.1). However, W/O emulsions are more common in the petroleum industry. W/O emulsions can also form during the refining, storage and distribution operations. In these cases, the water content in emulsion is usually low (6-10%) (Farah *et al.*, 2005). The viscosity of such W/O emulsions is strongly augmented by increasing its water content ('cut') and by decreasing temperature (Krieger and Dougherty, 1959).

**Table 2.2** Emulsions in the petroleum industry (Schramm, 1992). W/O refers to water-in-oil emulsions and O/W refers to oil-in-water emulsions

Occurrence	Usual Type
<i>Undesirable Emulsions</i>	
Well head emulsions	W/O
Oil sand floatation process, froth	W/O or O/W
Oil spill emulsions	W/O
<i>Desirable Emulsions</i>	
Heavy oil pipeline emulsions	O/W
Oil sand floatation process, slurry	O/W
Emulsion drilling fluid:	
Oil-emulsion mud	O/W
Oil-based mud	W/O
Asphalt emulsions	O/W
Enhanced oil recovery in-situ emulsions	O/W

## 2.2 Emulsion Characteristics

An emulsion is a mixture of two immiscible liquids in which one liquid is dispersed in the other in the form of droplets. The dispersed phase is called internal phase whereas the continuous phase is called external phase. Emulsions are found in a number of products, including pharmaceuticals, cosmetics, food, insecticides and crude oils (Rousseau, 2000).

### 2.2.1 Basic Principles

There are three conditions required to form an emulsion:

- (1) The presence of two immiscible liquids;
- (2) The presence of agitation;
- (3) The presence of surfactants promoting emulsion formation.

In order to form an emulsion with a short-term stability, the liquids must be thoroughly agitated to produce sufficiently small droplets. The formation of these droplets results in the increase in the contact surface area between the two liquids, thereby increasing the excess free energy. The increased energy associated with the increased contact area is supplied by the mechanical energy of agitation.

For an emulsion to be stable, the droplets of the internal phase must be prevented from coming together and coalescing. Substances used to help form the emulsion (called surface-active agent, surfactant, emulsifier, stabilizer, *etc.*) must also help prevent the droplets from coming together either by forming a rigid film around the droplets, or by imparting a charge to the droplets causing them to repel each other.

## **2.2.2 Emulsifying Agents**

Emulsifying agents such as surfactants or surface-active solids can stabilize emulsions (Aveyard *et al.*, 2003).

### **2.2.2.1 Surfactants**

Surfactants are wetting agents that lower the surface tension of a liquid, allowing easier spreading, and lower the interfacial tension between two liquids. They are the most commonly-used emulsion stabilizers.

Many surfactants can also assemble in the bulk solution into aggregates. Examples of such aggregates are micelles. The concentration at which surfactants begin to form micelles is known as the critical micelle concentration (CMC). When micelles form in water, their tails form a hydrophobic core

whereas their (ionic/polar) heads form an outer shell that maintains favourable contact with water. The CMC is observed by a sharp break in an interfacial tension (or surface pressure) versus concentration curve (Figure 2.3).

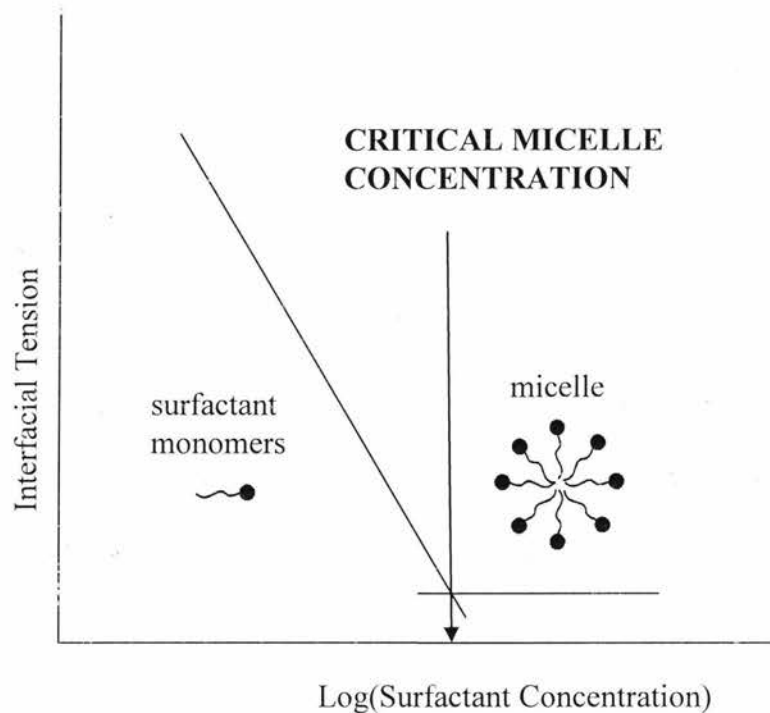


**Figure 2.3** Micellization of surfactant molecule (adapted from Tambe *et al.*, 1993)

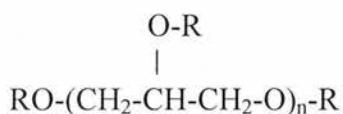
At concentrations below CMC, surfactants exist in the form of individual molecules that aggregate into micellar structures as the concentration increases above CMC. The break in the plot reflects the change in apparent molar mass of the solute (*i.e.*, surfactants grouped as micelles) in solution (Lyklema, 1994).

A surfactant can be classified by the presence of a charged group in its head. The head of an ionic surfactant carries a net charge. If the charge is negative, the surfactant is called anionic; if the charge is positive, it is called cationic. If a surfactant contains a head with two oppositely-charged groups, it

is termed zwitterionic. Common ionic surfactants are based on sulphate, sulphonate or carboxylate anions (such as  $-\text{COO}^-$ ,  $-\text{SO}_4^-$ ,  $-\text{SO}_3^-$ , *etc.*) whereas cationic surfactants are based on quaternary ammonium cations (such as  $-\text{NH}_3^+$ ,  $-\text{N}^+$ , tetrabutyl ammonium bromide, benzyltributyl ammonium chloride *etc.*). Examples of zwitterionic include alkyl betaine, which contains a positive group,  $-\text{N}^+$  and a negative group,  $-\text{COO}^-$  (Schramm, 1992).

In non-ionic surfactants, there are no charged groups present in the headgroup. Examples of such surfactants include alkyl poly(ethylene oxide), alkyl polyglucosides, fatty alcohols, polyglycerol polyricinoleate (PgPr), *etc.*

PgPr is a yellowish, viscous liquid composed of polyglycerol esters of polycondensed fatty acids from castor or soya bean oil. PgPr is strongly lipophilic, soluble in fats and oils and insoluble in water and ethyl alcohol (Wilson *et al.*, 1998). It is very commonly used in food products such as chocolates due to its tendency to improve flow behaviour during chocolate production. It is a bulky, branched surfactant with a molecular weight of  $\sim 7000\text{g/mole}$  (Knoth *et al.*, 2005). The general structure of PgPr is represented as below:



where  $\text{R}=\text{H}$  or a fatty acyl group derived from polycondensed ricinoleic acid and 'n' is the degree of polymerization of glycerol. In a study on the crystallization effects of surfactants on triglycerides (TG), Rousseau and Hodge (2004) found that PgPr did not affect the final crystal polymorph or morphology

under stagnant crystallization conditions. However, under shear and quench-cooling to 5 °C, it led to less stable crystal polymorphs and looser crystal flocs.

PgPr has also been used in studies with multiple emulsions, as it appears to be the most effective hydrophobic emulsifier available (Wilson *et al.*, 1998). PgPr is also used in the pharmaceutical industry for the dispersion and release of bioactive components (Knoth *et al.*, 2005).

#### **2.2.2.2 Solid Particles**

The presence of solid particles can either stabilize or destabilize emulsion droplets. If particles are present in the continuous phase, they can potentially stabilize emulsion droplet by adsorbing at the water/oil interface directly or by adsorbing onto an existing surfactant film. Such solid particles, also known as Pickering crystals, create a steric barrier between adjacent water droplets thereby hindering droplet collisions, film drainage and coalescence (Tambe and Sharma, 1993; Tadros and Vincent, 1983). They can also contribute to the mechanical rigidity and viscosity of the emulsion if a tightly packed network structure is created and there are strong particle-particle interactions (Tambe and Sharma, 1993; Tadros and Vincent, 1983; Menon and Wasan, 1984; Tambe and Sharma, 1994; Abend *et al.*, 1998; Binks and Kirkland, 2002; Aveyard *et al.*, 2003).

The key factors that determine the influence of solid particles on emulsion stabilization are particle size and location, microstructure, interfacial film rheology and wettability (Rousseau, 2000). In the concentration range where they are typically encountered, emulsion stability will increase with

decreasing particle size and increasing particle concentration. Solid particles should be at least 10 times smaller than the size of the droplet in order to be an effective stabilizer (Binks and Kirkland, 2002; Aveyard *et al.*, 2003). They should also be locally biwetable, containing some surfaces preferably wetted by water and some by oil (Aveyard *et al.*, 2003). A water-wet solid has an apparent contact angle  $\theta$  as measured through the water phase  $< 90^\circ$  whereas  $\theta$  for an oil-wet is  $> 90^\circ$  (Figure 2.4).

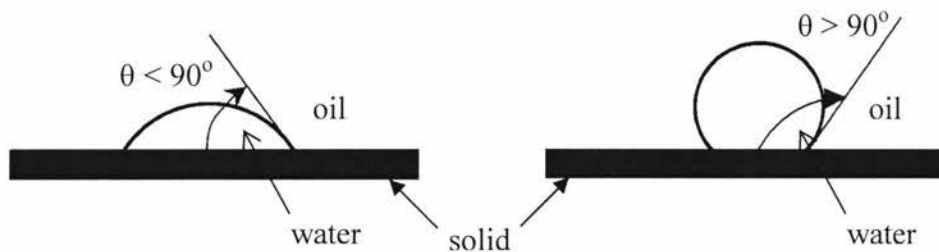


**Figure 2.4** Wettability of water-oil surfaces (adapted from Aveyard *et al.*, 2003)

The formation of wax networks plays a vital role in the stabilization of crude oil emulsions (Schramm *et al.*, 1992). However, there remains insufficient fundamental and applied knowledge of wax networking and its role in wax crystallization in crude oil emulsions. Miskandar *et al.* (2004) worked on tablespreads such as butter and margarine (W/O emulsions) and showed that their flow behaviour during key unit operations (*e.g.*, transport, packaging, *etc.*) was considerably affected by crystalline fat content (Miskandar, Man, Yusoff and Rahman 2004). They showed that a slower in-pipe flow rates induced more rapid crystallization in butter, and hence led to an increase in butter's yield

stress. It was proposed that its yield stress and viscoelastic behaviour were due to its 3D fat crystal network (held together by van der Waals forces) and its close association with the continuous oil and aqueous phases (Wright, Scanlon, Hartel and Marangoni 2001). Applying a force greater than the yield stress of butter would cause instantaneous breakdown of the crystalline network followed by a gradual decrease in viscosity with applied shear. Though at different solids contents and in a completely different system, fundamentally this type of behaviour may be quite similar to that of crude oil in the presence of a wax crystalline network, and may be used to gain further insight on its low-temperature flow behaviour.

### **2.2.3 Emulsion (In)stability**

The formation of emulsion is a thermodynamically unfavourable process due to the increase in interfacial area following emulsification. Emulsions tend to break into separate liquid phases over time (Rousseau, 2000). There are five main mechanisms that can contribute to emulsion instability: (1) creaming/settling; (2) flocculation; (3) Ostwald ripening; (4) coalescence; and (5) phase inversion. Figure 2.5 shows different types of emulsion (in)stability processes.

#### **2.2.3.1 Creaming/Settling**

Creaming and settling are due to differences in density between the two phases under the influence of gravity, which eventually leads to phase separation.

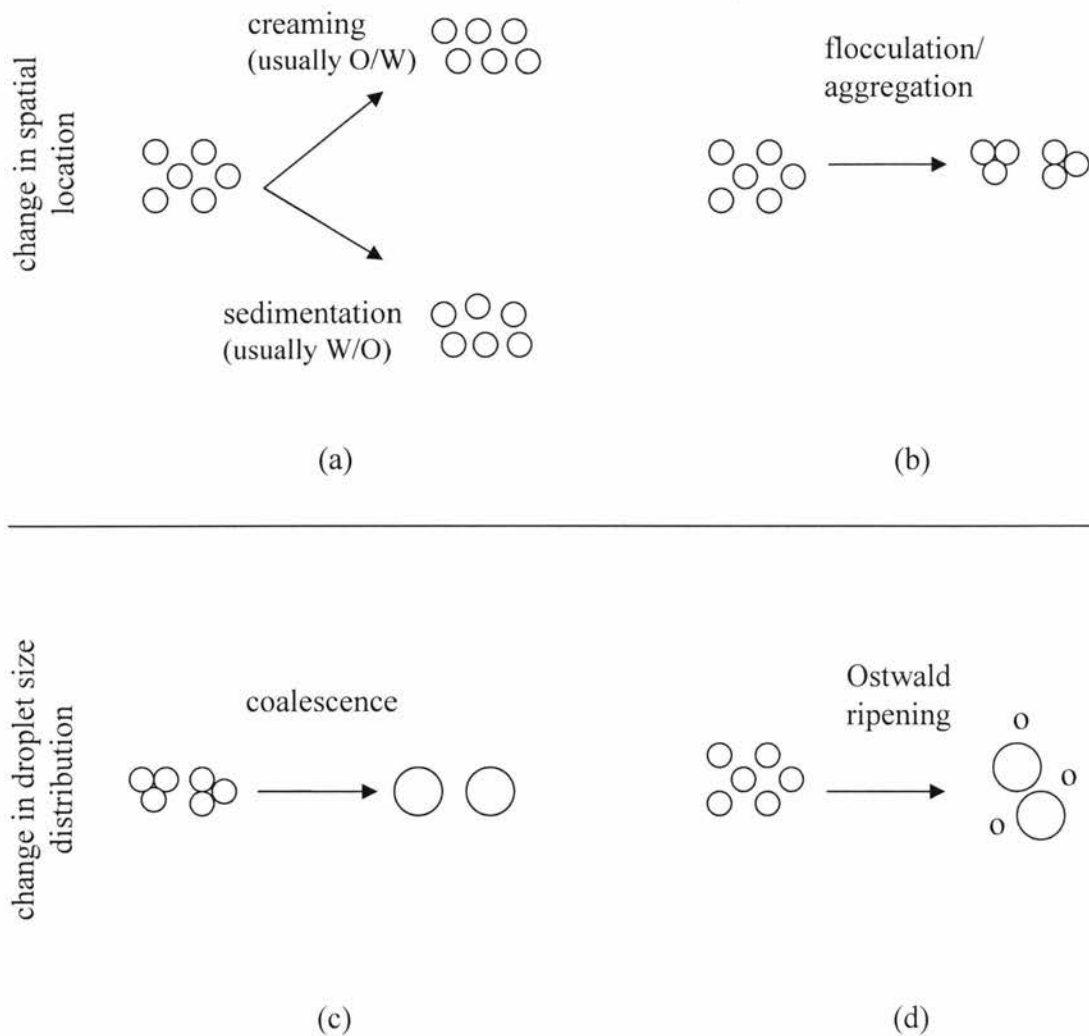


**Figure 2.5** Natural emulsion destabilization processes (a) creaming and sedimentation (b) flocculation/aggregation (c) coalescence and (d) Ostwald ripening (adapted from Yan *et al.*, 1999)

Since the density of water is higher than that of oil, O/W emulsions undergo creaming whereas W/O emulsions undergo settling process. It is typical for an emulsion to undergo creaming/settling process unless the density difference between the phases is very small and/or the viscosity of the continuous phase is very high (Fechner, 2007).

### **2.2.3.2 Flocculation/Aggregation**

Flocculation is the aggregation of droplets due to weak attractive forces between colloids. It depends on the interaction energy between two particles as a function of interparticle distance. The interaction energy is defined as the combination of attractive and repulsive forces. In emulsions, attraction comes from London-van der Waals forces and repulsion is often due to surfactants present at the interface (Becher, 1965).

### **2.2.3.3 Coalescence**

When two colliding droplets form a single larger droplet, the process is called coalescence. Complete coalescence occurs if the droplets are fully liquid whereas the process is said to be partial if the droplets contain crystalline matter. Partial coalescence can lead to phase inversion where an O/W emulsion transitions towards W/O type, as during the churning of butter (Rousseau, 2000).

#### **2.2.3.4 Ostwald Ripening**

Ostwald ripening is the growth of larger droplets at the expense of smaller ones (Dickinson *et al.*, 1999), where mass is transferred through the continuous phase between droplets of disparate size. The concentration of dispersed phase at the surface of a droplet is inversely proportional to its radius of curvature (Kabalnov and Shchukin, 1992). This means that larger particles, with their lower surface to volume ratio, results in a lower energy state (and have a lower surface energy). As the system tries to lower its overall energy, molecules on the surface of a small (more energetically unfavourable) particle will tend to diffuse through solution and add to the surface of larger particle (Dickinson *et al.*, 1999). Therefore, mass transfer occurs from smaller droplets to larger droplets, resulting in the shrinkage of the smaller droplets and growth of larger ones, with the smaller droplets eventually disappearing. This phenomenon is usually of little importance in crude oil given the lack of miscibility between the aqueous and oil phases.

#### **2.2.4 Treatment of Emulsions**

Oilfield emulsions are treated in a number of ways in order to destabilize the emulsions formed during processing, including gravity settling, heating, electrostatic coalescing and chemical demulsifiers.

Gravity settling is used only for relatively unstable emulsions, and is very slow especially when the continuous phase viscosity is high, the density difference between oil and water is small and the average droplet size is small. This approach is rarely used alone (Smith and Arnold, 1987).

Heating reduces the bulk emulsion viscosity, which facilitates drainage of the continuous phase from between droplets and may also reduce the rigidity of the interface, which results in coalescence (Smith and Arnold, 1987). For waxy oils, adsorbed solid wax particles may become dissolved upon heating, causing the emulsion film to break down.

Electrostatically-enhanced coalescence is also used to increase the resolution of water and oil. In an electrostatic coalescer, a high-voltage electric field is applied to water-in-crude oil emulsions, which polarizes the water droplets (Smith and Arnold, 1987). Contact between the positive and negative poles of the droplets leads to coalesce.

In addition to heating and electrostatic coalescence, chemical demulsifiers are also used to destabilize emulsions. Most commercial demulsifiers are flocculants aimed at promoting rapid settling. In order to be effective, they must be mixed thoroughly in the emulsion so as to reach the water/oil interface, where they displace the existing stabilizers and promote coalescence. For adsorbed solids, demulsifiers may alter the wettability and promote particle desorption. Examples include polyglycol esters, sulfonates, polymerized oils and esters, alkanolamine condensates and polyamine derivatives (Smith and Arnold, 1987).

## **2.3 Rheology of Emulsions**

Knowledge of the flow behaviour of emulsions is required for unit operations such as mixing, pumping, filling or packaging (Barnes *et al.*, 1994).

In qualitative terms, emulsions range from low viscosity milk-like Newtonian liquids through thicker shear-thinning, cream-like materials with apparent yield stresses. At a fundamental level, the rheology of emulsions is a direct manifestation of the various interaction forces that occur in the system. The different mechanisms of emulsion (in)stability such as creaming and sedimentation, flocculation, coalescence, Ostwald ripening and phase inversion may be investigated using various rheological techniques (Tadros, 1994).

## **2.3.1 Factors Involving the Dispersed Phase that Affect Emulsion Rheology**

### **2.3.1.1 Volume Fraction of the Dispersed Phase ( $\phi$ )**

One of the most important factors that affects emulsion rheology is the volume fraction of the dispersed phase ( $\phi$ ). In dilute emulsions ( $\phi < 0.01$ ), the relative viscosity ( $\eta_r$ ) of the system is related to  $\phi$  using Einstein's equation:

$$\eta_r = 1 + 2.5\phi \quad 2.1$$

As the volume fraction of the emulsion is gradually increased, the relative viscosity becomes a more complex function of  $\phi$ , and may be represented by a polynomial equation:

$$\eta_r = 1 + k_1\phi + k_2\phi^2 + k_3\phi^3 + \dots \quad 2.2$$

where  $k_1$  is Einstein's coefficient (equal to 2.5 for hard spheres), and  $k_2$  and  $k_3$  are coefficients that account for hydrodynamic interaction between the droplets (Tadros, 1994).

### 2.3.1.2 Droplet Size Distribution

The droplet size distribution of the dispersed phase affects emulsion rheology, particularly at high volume fractions ( $\phi > 0.6$ ). In this case,  $\eta_r$  (Equation 2.2) is inversely proportional to the reciprocal of the mean droplet diameter (Richardson and Tyler, 1933). The average separation distance between two droplets,  $h_m$ , is related to the droplet diameter  $d_m$  by the following equation:

$$h_m = d_m [(\phi_{\max} / \phi)^{1/3} - 1] \quad 2.3$$

where  $\phi_{\max}$  is the maximum packing fraction, equal to 0.74 for hexagonally packed mono-dispersed spheres (droplets). However, with most emulsions,  $\phi_{\max}$  reaches a value higher than 0.74 as a result of polydispersity (Tadros, 1994).

### 2.3.2 Factors Involving the Continuous Phase that Affect Emulsion Rheology

There are several factors related to continuous phase that affect emulsion rheology, including the viscosity of the medium, which will be affected by additives such as excess emulsifier. The second property of the medium that affects emulsion rheology is composition, and how it affects properties such as polarity and pH. These in turn will affect the surface charge on the droplets and hence their attraction/repulsion. A third property is the nature and concentration of electrolytes in the system, which is commonly referred to as electroviscous effects (Tadros, 1994). The magnitude of the electroviscous effect is proportional to  $\phi$ . This effect may cause a great increase in viscosity.

Emulsion rheology also depends on the interfacial rheology of the

emulsifier film surrounding the droplets. When shear is applied to an interfacial film, its molecules as well as the molecules of the oil and water phases are displaced from their equilibrium positions. The stress that develops depends on the associated molecular rearrangement. This will have an effect on the interfacial viscosity of the film and hence on the bulk rheology of the emulsion. For emulsions in which the droplets deform under shear, viscosity will increase more rapidly with  $\phi$  than for the emulsions of identical droplet size (Tadros, 1994). When dispersed droplets are very small, deformation is less likely and the effect of interfacial rheology becomes less significant. In some cases, the chemical nature of the emulsifier can affect relative viscosity, particularly at high  $\phi$  values. The nature of the emulsifier, in particular its solubility and distribution in both phases, also has a large effect on rheology (Barnes, 1994; Menon and Wasan, 1988).

## **2.4 Crude Oil Emulsion Studies**

### **2.4.1 Crude Oil Emulsion Stability**

Above and beyond the factors described above, the stability of crude oil emulsions will depend on many parameters, including: oil composition (Ahmed *et al.*, 1999; Elgibaly *et al.*, 1997), salinity and pH of the aqueous phase (Plegue *et al.*, 1986), oil:water ratio (Sun and Shook, 1996), droplets size and polydispersity (Ahmed *et al.*, 1999; Sun and Shook, 1996), temperature (Sun and Shook, 1996; Sharma *et al.*, 1998), surfactant presence, type and concentration (Zaki *et al.*, 2000), and mixing regime (Ahmed *et al.*, 1999). A large number of studies, mostly experimental in nature, have been carried out on

crude oil-water emulsions. However, the results of these studies have not always been consistent. A good review using formulation-composition maps of heavy hydrocarbon emulsions was presented by Salager *et al.* (2001), who described the morphology of an emulsion using a formulation-composition map based on hydrophilic-lipophilic deviation (HLD) concept. The formulation component groups parameters such as temperature, types and amounts of electrolytes present in water, types of oil and emulsifiers and the nature of alcohol and its concentration whereas the composition component represents the fraction of oil or water of an emulsion (Salager *et al.* 2001).

## **2.4.2 Effect of Solids on Crude Oil Emulsion Stability**

As mentioned earlier, solids can adsorb at the water/oil interface, onto an existing surfactant-stabilized film, or become trapped between water droplets. Adsorption or trapping will reduce film drainage, increase film viscosity and potentially increase the bulk viscosity of the emulsion. The extent to which solids increase overall emulsion stability depends strongly on the size and concentration of solids, their shape, morphology and density, and their wettability. As described earlier, crude oil emulsion stabilization likely results from the interplay between the crystal network and surface-active crystals.

### **2.4.2.1 Effect of Solids Size and Concentration**

Assuming an ideal system, emulsion stability increases with decreasing colloidal particle size and increasing concentration (Menon and Wasan, 1988; Yan *et al.*, 1999; Tambe and Sharma, 1993; Menon and Wasan, 1984; Abend *et*

*al.*, 1998; Schulman and Leja, 1954; Bowman, 1967; Gelot *et al.*, 1984; Yan and Masliyah, 1995; Binks and Lumsdon, 2001; Sullivan and Kilpatrick, 2002).

The size of the solids in relation to water droplets is an important factor in their potential to enhance emulsion stability (Aveyard *et al.*, 2002; Tadros and Vincent, 1983; Schulman and Leja, 1954). Solids that tend to stabilize emulsions vary anywhere from  $< 1 \mu\text{m}$  (Levine and Sanford, 1985; Kotlyar *et al.*, 1998) up to a few  $\mu\text{m}$  (Zaki *et al.*, 2000) in diameter. Generally, the most stable emulsions will occur when the interface is stabilized by the smallest particles. For example, Bowman (1967) found that W/O emulsion stability increased when the size of model and tar sand solids decreased from 37 to  $1 \mu\text{m}$ , with a pronounced increase in stability with particles  $< 8 \mu\text{m}$ . Sullivan and Kilpatrick (2002) observed that the water resolution in a model water-in-crude oil emulsion decreased from 83 to 63% when the diameter of added iron oxide particles decreased 0.89 to  $0.026 \mu\text{m}$ . When larger particles such as silica,  $1.45 \mu\text{m}$  montmorillonite clay particles and  $16.65 \mu\text{m}$  sized  $\text{Ca}(\text{OH})_2$  particles were added, no stable emulsions could be created. Binks and Lumsdon (2001) observed that as the size of hydrophobic latex particles decreased from 2.7 to  $0.21 \mu\text{m}$ , the stability to sedimentation of a model water-in-cyclohexane emulsion increased and the average water droplet diameter decreased.

#### **2.4.2.2 Effect of Solids Shape and Density**

Particle density and shape can also play an important role in emulsion stability. Emulsions created with denser particles are expected to be less stable than those created with less dense particles (Schulman and Leja, 1954; Gelot *et*

*al.*, 1984). Tadros and Vincent (1983) suggested that asymmetric particles such as bentonite clays were more effective stabilizers than spherical particles. However, there is also evidence suggesting that irregularities on a surface lessen the emulsifying capability of a particle (Vignati *et al.*, 2003). Sabbagh and Lesser (1998) showed that polyethylene/asphalt emulsions containing teardrop-shaped polymer particles were more unstable than those containing more spherical particles. Cylindrical particles were also observed to aid in stable emulsion formation. Yekeler *et al.* (2004) showed that particle morphology could alter wettability and that smooth particles made up of talc minerals tended to be more hydrophobic.

#### **2.4.2.3 Effect of Solids Wettability**

Wettability is another important factor when considering the capacity of solids to stabilize emulsions. Hydrophilic particles, *i.e.*, those with a contact angle less than  $90^\circ$ , stabilize W/O emulsions (Tambe and Sharma, 1993; Aveyard *et al.*, 2003; Bensebaa *et al.*, 2000; Schulman and Leja, 1954). For example, Gelot *et al.* (1984) showed that Ca-bentonite, a hydrophilic particle, stabilized O/W emulsions whereas carbon black, a hydrophobic particle, stabilized W/O emulsions.

Thermodynamic considerations suggest that the most stable emulsions will result when the contact angle is near  $90^\circ$ , if using “very finely divided” solids (Binks and Kirkland, 2002, Aveyard *et al.*, 2002). Some experimental evidence supports this conclusion (Yan and Masliyeh, 1995), although there is also evidence showing maximum stability at angles other than  $90^\circ$  (Yan *et al.*,

2001; Menon and Wasan, 1986). These various authors have shown that factors such as particle partitioning, surface coverage, and the phase in which the particle is originally dispersed must be considered in addition to contact angle.

### **2.4.3 Crude Oil Rheology**

Emulsion rheology is greatly affected by the oil and water volume fractions and droplet size distribution (Ahmed *et al.*, 1999; Khan, 1996). The droplet size distribution is a function of different parameters, in particular surfactant type and concentration, pH of the aqueous phase, surface tension, mixing energy, ionic strength, temperature, crude oil surfactant chemistry and pressure (Khan, 1996). Salager *et al.* (2001) reported that due to hydrodynamic conditions, water droplets tend to migrate away from the pipe wall and form a lubricating layer at the pipe wall. This may explain why the pressure drop during pipeline transportation is usually lower than that expected from rheological measurements (Nunez *et al.*, 1996).

### **2.4.4 Factors Affecting Rheological Behaviour**

As noted by many (Visintin *et al.*, 2005, Ronningsen *et al.*, 1995, Ronningsen *et al.*, 1992, Farah *et al.*, 2005, Venkatesan *et al.*, 2005), crude oils exhibit complex rheological behaviour that may be strongly affected by the previous mechanical and thermal histories. The presence of wax crystals can lead to a wide range of non-Newtonian characteristics including the presence of a yield stress, pseudo-plasticity (shear thinning), and time-dependent behaviour.

#### 2.4.4.1 Thermal History

Thermal history plays a vital role in the rheological behaviour of crude oil. Paraffinic mixtures display complex rheological behaviour, which changes considerably upon cooling from essentially Newtonian flow at temperatures above the WAT to time-dependent, non-Newtonian behaviour below the WAT. There is also a significant increase in apparent viscosity between the WAT and PP (pour point or gelation temperature) (Visintin *et al.*, 2005). With wax deposits containing both higher molecular weight linear and branched alkanes, WAT and PP generally fall between 20 and 60 °C, respectively (Ronningsen *et al.*, 1991).

Factors to consider in thermal history include the initial temperature to which a sample is heated, cooling rate, final temperature and the storage temperature of the material of interest. The effect of cooling rate of crude oil gels has been investigated by many researchers (Petrellis *et al.*, 1973, Wardhaugh, 1986, Ronningsen *et al.*, 1991, 1992, Chang *et al.*, 2000). An increase in cooling rate (and its possible effect on the wax crystal size and shape) resulted in a decrease in the viscosity of the crude oil gel. The cooling rate also affected the viscoelasticity of crude oils (Huo *et al.*, 2007), with a lower cooling rate likely resulting in a higher storage modulus ( $G'$ ) at a particular test temperature, which led to a higher gelation temperature. Hou *et al.* (2007) proposed that there exists a critical temperature at which the storage modulus, loss modulus, and gelation temperature reach their maximum values

and the gelation take places very easily. This is an interesting concept that certainly warrants further attention.

#### **2.4.4.2 Shear History**

The effect of shear history on the rheological properties has also been studied by numerous researchers (Billington, 1960; Govier *et al.*, 1972; Petrellis *et al.*, 1973; Sifferman *et al.*, 1979; Wardhaugh *et al.*, 1987, 1988, 1991; Lorge *et al.*, 1997; Ronningsen, 1991). Different shear rates, ranging from 1-1000 s<sup>-1</sup> have been investigated for their effects on crude oil viscosity. According to the abovementioned literature, an increase in the shear rate applied to a model system will decrease viscosity and yield stress.

The change in the viscoelastic properties (*e.g.*, G' / G" cross-over points) of crude oil subjected to different shear conditions was investigated by Chang and Boger (1998), who found that the yielding of waxy crude initially occurred elastically, followed by viscoelastic creep and a final fracture. Cooling of crude oil at different shear rates resulted in different rheological behaviours in terms of steady state (viscosity) and viscoelastic properties. Finally, an increase in shear rate while cooling resulted in a lower crude oil gel strength (Chang and Boger, 1998).

#### **2.4.4.3 Time Dependency**

Time-dependent rheological behaviour is common in many industrial fluids (*e.g.*, petrochemicals, cosmetics, pharmaceuticals). It is well-known that the presence of wax in crude oil renders it thixotropic. Thixotropy may be

defined as the continuous decrease in apparent viscosity with time under shear and the subsequent recovery of viscosity when the applied force is stopped. Thus, when a wax crystal network structure is disrupted by a uniform force, its viscosity will decrease until equilibrium is reached with resultant changes in microstructure. When an applied force is removed, Brownian motion will lead to an energetically-favourable rearrangement of the microstructural elements (Barnes, 1997).

Petrellis *et al.* (1973) used a simple hysteresis test to investigate the rheological response of crude oils at small shear rates. The unstressed sample was subjected to small sinusoidal increases and decreases in shear rate. They found that the structure experienced a 'build-up' with the repeated application of shear. This behaviour is common to rheopectic suspensions in which the coagulation and the agglomeration of particles are facilitated by the movement of the fluid, and has not been extensively studied in crude oil. Vinogradov *et al.* (1982) studied the thixotropic and viscoelastic characteristics of highly-paraffinic crude oils at different shear deformations. The time-dependent thixotropic behaviour of highly paraffinic crude oil was also studied by Matveenko *et al.* (1995), who found them to be pseudoplastic with pronounced thixotropy.

#### **2.4.4.4 Effect of Water Droplets**

The properties of the dispersed aqueous phase in crude oil emulsions may have a large impact on the viscosity. Pal (1996, 1997) found that a reduction in droplet size gave a large increase in the viscosity of both

concentrated W/O and O/W emulsions. In addition, non-Newtonian behaviour such as shear-thinning was more pronounced for emulsions with more finely-dispersed droplets.

Another important factor governing the rheological behaviour of an emulsion is the volume fraction of the water droplets ('water cut'). Visintin *et al.* (2008) showed that by increasing water cut to 70%, the PP of a crude oil emulsion increased from 28 °C (8% water) to ~35 °C and the yield stress increased from ~60 to ~550 Pa. Evdokimov *et al.* (2008) studied native crude oil, showing that at low water volume fractions ( $\phi$ ), viscosity was governed by flocculated dispersed water clusters whereas gels made up of monodisperse small droplets were responsible for anomalous viscosity behaviour at  $\phi \approx 0.4$ -0.5. Once formed, these gels retained their structure to  $\phi \approx 0.74$ , and incorporated more water as larger-sized droplets. Water emerged as a separate phase at higher water contents ( $\phi \approx 0.83$ ), causing a reduction in viscosity due to stratified flow (W/O emulsion gel + free water).

Few studies have been conducted on the effect of water on emulsified crude oil wax deposition behaviour, in large part due to the complexity of reproducibly investigating these problems. Hsu *et al.* (1999), who conducted high-pressure flowloop experiments with waxy crude oils to study the effect of water on paraffin deposition under turbulent flow, showed that wax deposition was significantly reduced with the addition of water. Cole and Jessen (1960) used a deposition cell consisting of a cold plate through which an oil-water solution could flow and where the paraffin deposition would occur. The effect

of pipe wall wettability on paraffin deposition showed that, with the presence of water, paraffin deposition on a more water-wet surface was significantly reduced, while no difference in deposition was found for oil-wet surfaces.

## 2.4.5 Modelling Crude Oil Emulsions

Several researchers have investigated models to describe the rheological properties of waxy oils (Davenport and Somper, 1971; Matveenko *et al.*, 1995; Remizov *et al.*, 2000), namely the Casson (1959) model. This model describes the stress-strain relationship of a non-Newtonian fluid as:

$$\tau^{1/2} = \tau_y^{1/2} + \eta_c \gamma^{1/2} \quad (\text{for } \tau > \tau_y) \quad 2.4$$

where  $\tau$  is the shear stress applied to the fluid,  $\tau_y$  is the yield stress of the fluid,  $\eta_c$  is the Casson viscosity coefficient and  $\gamma$  is the resultant strain rate. This model is an improvement on the simple Bingham model for yield stress fluids (Remizov *et al.*, 2000) which describes the stress-strain relationship as:

$$\tau = \tau_y + \eta_B \gamma \quad (\text{for } \tau > \tau_y) \quad 2.5$$

where  $\eta_B$  is the Bingham viscosity coefficient.

The rheological properties of wax-oil gels will depend on the shear and thermal histories to which they are subjected. The composition of the gel also affects the gel properties. Gels with higher solid wax content are expected to have a higher yield stress. In general, the following function can be written to describe the yield stress of wax-oil gels (Matveenko *et al.*, 1995):

$$\tau_y = f(\tau_{gel}(dT/dt), s) \quad 2.6$$

where  $\tau_y$  is the yield stress,  $\tau_{gel}$  is the shear stress applied to the wax-oil mixture during gelation,  $(dT/dt)$  is the cooling rate applied during gelation and  $s$  is the solid wax content of the gel.

Visintin *et al.* (2005) studied the yield behaviour of crude oil showing that their flow behaviour can be characterized with the following equation:

$$\frac{\eta - \eta'_\infty}{\eta'_o - \eta'_\infty} = \frac{1}{1 + \left(\frac{\sigma}{\sigma_c}\right)^m} \quad 2.7$$

where:

$$\eta'_o = \frac{\eta_o}{1 + \left(\frac{\sigma}{\sigma_1}\right)^p} \quad 2.8$$

and

$$\eta'_\infty = \eta_\infty \left[ 1 + \left(\frac{\sigma}{\sigma_2}\right)^s \right] \quad 2.9$$

where the parameters are the zero-shear rate viscosity,  $\eta_o$ , the infinite shear rate viscosity is  $\eta_\infty$ , and the critical stress is  $\sigma_1$ .  $P$ ,  $S$ , and  $m$  are the proportionality constants. The parameters  $\eta_o$  and  $\eta_\infty$  define the two limiting Newtonian behaviours at low and high stresses, respectively, whereas  $\sigma_2$  can be identified with the apparent yield stress.

Overall, this rigorous literature survey has shown that, though extensive research on crude oil has been carried out, there has been comparatively little performed on the role of a dispersed aqueous phase on crude oil emulsion

properties. The objectives mentioned at the end of Chapter 1 will be met by using the experimental approach described in Chapter 3.

# Chapter 3

## Experimental

This chapter introduces the experimental materials and methods used in the analysis of model W/O emulsions and wax-containing oils. Specific measurements associated with each experiment are addressed within the experimental sections of the subsequent chapters. Unless otherwise indicated, all experiments within this thesis were performed in triplicate, as were their respective measurements.

### 3.1 Materials

#### 3.1.1 Mineral Oil

Light mineral oil (Fisher Scientific, Nepean, ON, Canada) was used as the continuous phase of the model crude oil emulsions and wax-containing oils. The density and viscosity of the light mineral oil at room temperature were  $0.85 \text{ kg/m}^3$  and  $0.033 \text{ Pa}\cdot\text{s}$ , respectively. The mineral oil was of  $34.4^\circ\text{API}$  gravity with a molecular weight of 394. Although oils of different viscosity impact the wax crystallization and hence the rheology of crude oil emulsions, this light mineral oil was deemed appropriate for the purposes of this thesis.

Composition-wise, Figure 3.1 shows the high temperature gas chromatogram (GC) of the mineral oil used in the present study. Analysis was conducted using an HP6890 liquid injection gas chromatograph equipped with flame ionization detector (FID). The GC temperature protocol was as follows: after an isothermal period of 5 min at 75 °C, the temperature was increased at 15 °C/min to 180 °C, and then at 5 °C/min to 300 °C. A near-Gaussian distribution of hydrocarbons with a mean carbon number of 25 was found, with most species consisting of between 22 and 34 carbons.

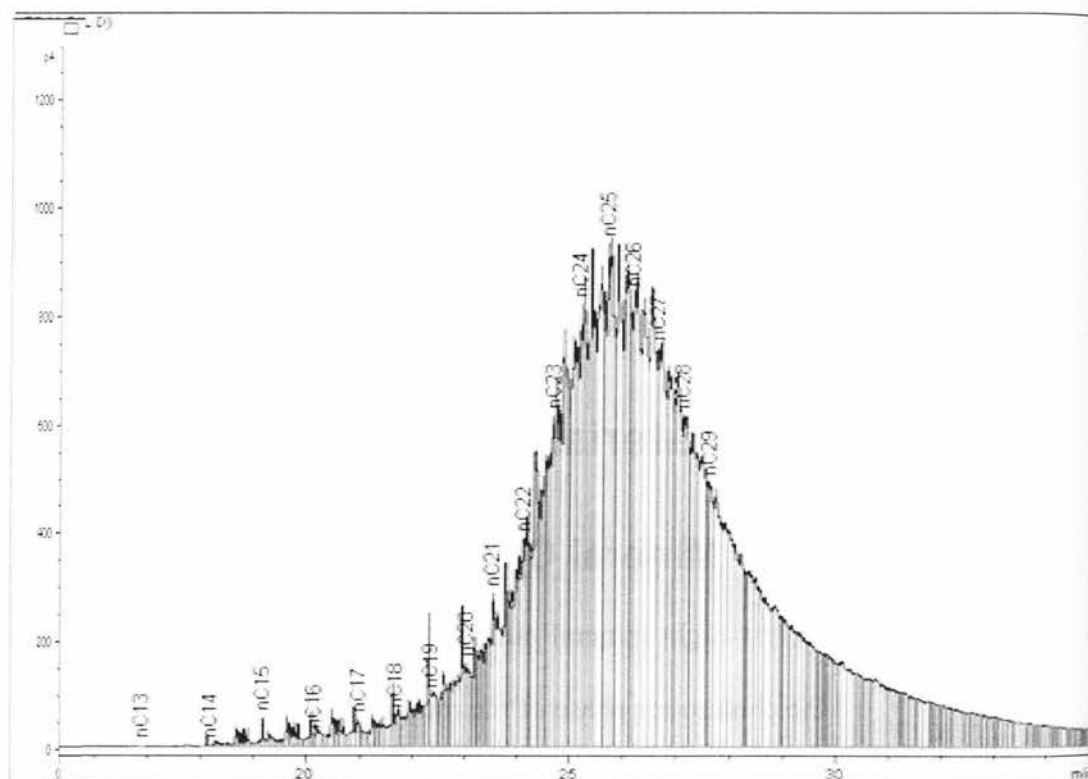


**Figure 3.1** High temperature gas chromatogram of light mineral oil

### 3.1.2 Water

Water used in the preparation of the model crude oil emulsions was double distilled water produced in the Food Research Laboratory at Ryerson University.

### 3.1.3 Surfactant

Polyglycerol polyricinoleate (PgPr) (Abitec, Nealanders International Inc, Mississauga, ON, Canada) was used as the surfactant in the preparation of the W/O emulsions. PgPr was used at concentrations that aid in emulsification, but not in promoting emulsion stability (*i.e.*, do not inhibit flocculation and coalescence). This was necessary to understand the stabilizing effect of the dispersed phase wax crystals.

The critical micelle concentration (CMC) was determined by interfacial surface tension measurements using a DuNouy ring tensiometer (Fisher Tensiomat Model 21, Fisher Scientific, Nepean, ON, Canada). Figure 3.2 shows the evolution in interfacial tension between mineral oil and water as a function of PgPr concentration. The CMC value for PgPr was 0.50%.

The model emulsions consisted of 2.5% PgPr, which was five times the CMC of PgPr in light mineral oil at 25 °C. This PgPr concentration promoted emulsion formation, but not stability.

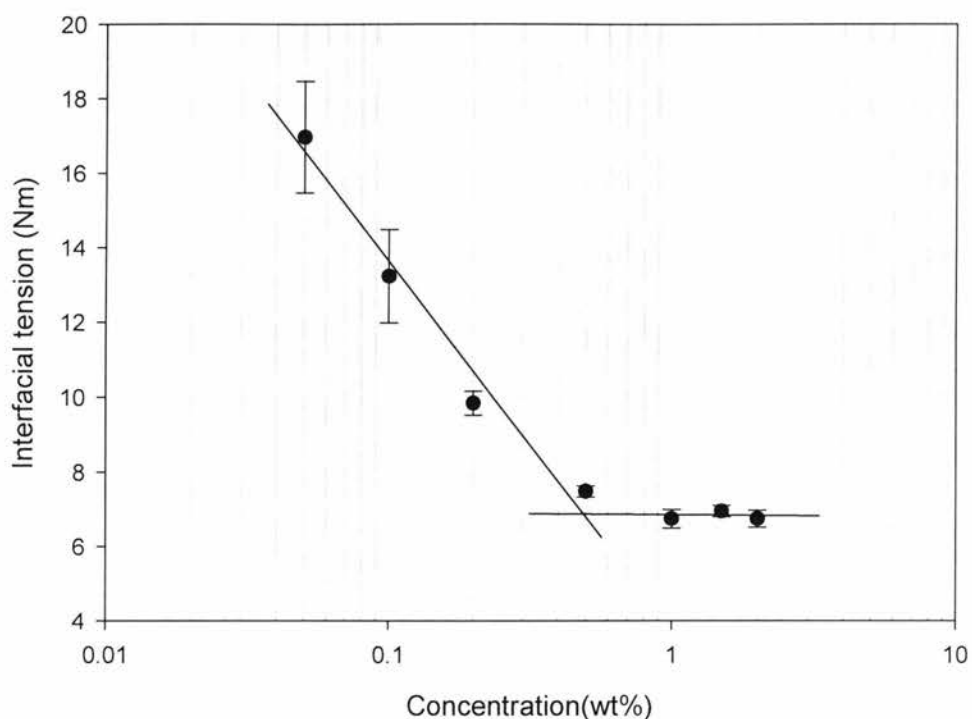


**Figure 3.2** Critical micelle concentration (CMC) determination of PgPr at a planar water/oil interface.

### 3.1.4 Paraffin Wax

The molecular weight distribution of this wax was obtained by a Varian 3800 high temperature gas chromatograph (HTGC) (Figure 3.3). The column used was 30m long, 530mm diameter “Megabore” capillary column. The temperature program used was as follows: 60 °C to 400 °C at 5 °C /min. The carrier gas used was helium at a constant flow rate of 40 L/h and split ratio was 10:1. The wax had a carbon number distribution from C20 to C54 with an average molecular weight of 435.

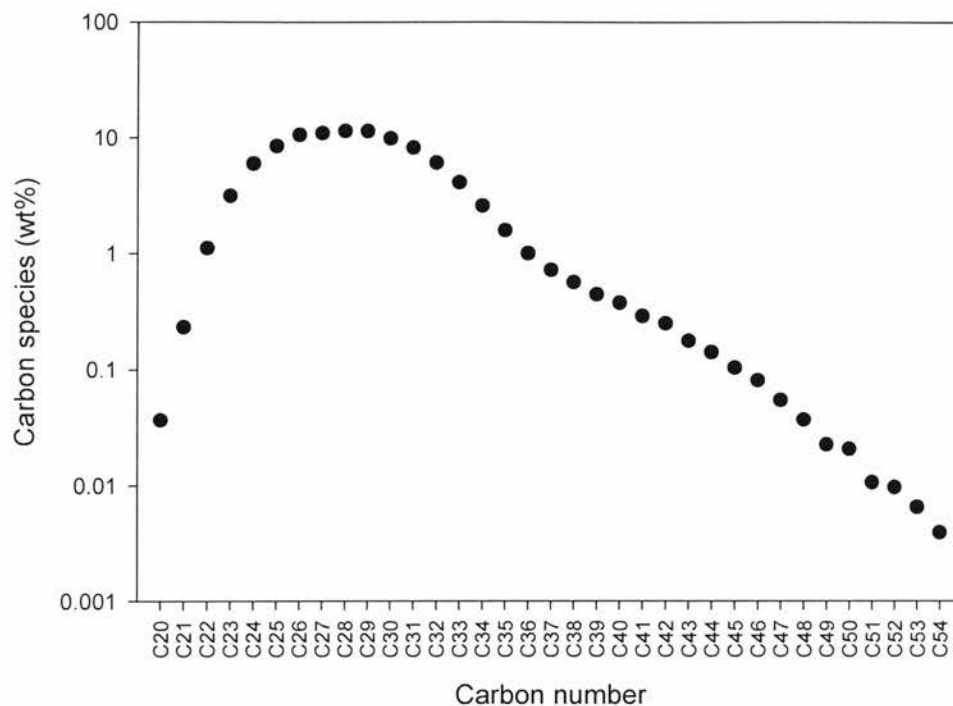


**Figure 3.3** Carbon distribution of paraffin wax using HTGC

## 3.2 Model Crude Oil Emulsion Preparation

Model W/O emulsions consisted of double distilled water, light mineral oil, paraffin wax, and PgPr. Emulsions were composed of 80% (w/w) light mineral oil and 20% (w/w) water. Mixtures of oil, wax and surfactant were heated to 80 °C (above the melting point of wax) for 1 h. The mixture was then cooled to 30 °C and homogenized with water using a hand-mixer (Kinematica, NY, USA) for 30 sec. The pre-mixing stage ensured greater uniformity for the subsequent homogenization step. The mixture was then homogenized with a two-stage valve homogenizer (APV-1000, APV, Concord, ON, Canada) with 4 emulsion recycles. The pressures applied were 5000 Pa in the first stage and 500

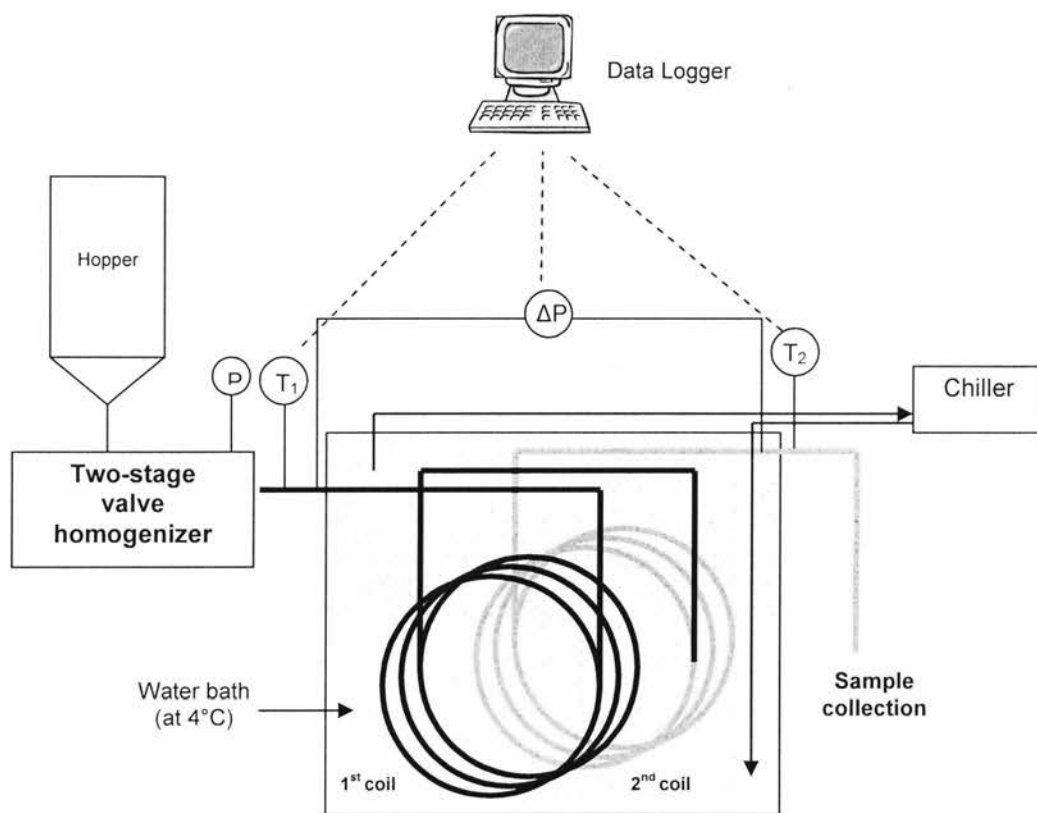
Pa in the second stage. The emulsions were then immediately analyzed using the techniques discussed in section 3.4.

### 3.3 Laboratory Flowloop

A limited number of flowloop experiments were used to provide a very preliminary understanding of wax deposition in pipelines. Figure 3.4 shows the laboratory flowloop set-up used for the study, which was designed and built in-house at Ryerson University in the Food Research Laboratory. It consisted of two in-line detachable 5m tube coils (0.00635m I.D. steel tubing) with thermocouples, a pressure gauge and additional piping attached to a steel frame. When in operation, a data acquisition system (LabView 8.6, National Instruments, Mississauga, ON, Canada) continuously recorded the inlet and outlet fluid temperatures and the differential pressure across the flowloop. The flowloop inlet was directly mated to the homogenizer outlet. Only one flow rate was used, that was generated by the homogenizer's pressure.

For use, coarsely-blended emulsions were placed in the homogenizer hopper (~ 2 kg, 35 °C) and emulsified. This action increased the temperature of the emulsion to ~40 °C. Emulsions were flowed through the flowloop, which was immersed in a waterbath connected to a chiller and maintained at ~ 4 °C. The flow rate of the emulsion in the flowloop was calculated to be ~ 347 ml/min, which was in laminar region ( $Re \sim 3$ ). The flowed emulsions were immediately analyzed for their stability and rheological behaviour, except for

samples collected and used to understand the effect of ageing on rheological behaviour. Samples were collected after passage through 5m or 10m of coil.



- P Pressure sensor for homogenizer
- T1 Inlet thermocouple
- T2 Outlet thermocouple
- $\Delta P$  Differential pressure sensor across the flowloops

**Figure 3.4** Schematic of the laboratory flowloop system

## **3.4 Analytical Methods**

### **3.4.1 Pulsed Field Gradient Nuclear Magnetic Resonance (PFG-NMR)**

PFG-NMR (Minispec Mq, Bruker Canada, Milton, ON, Canada) was used to measure the oil self-diffusion coefficient, solid wax content (SWC) and emulsion water droplet size distribution (DSD). Model emulsion and waxy oil samples were loaded in NMR tubes (diameter = 1cm, height = 15cm) using disposable pipettes (~1.5ml) for the measurements using PFG-NMR. The sample heights in the NMR tubes for the oil self-diffusion coefficient and DSD measurements were 1 cm whereas SWC was measured with a 4 cm sample height.

The use of PFG-NMR to measure molecular self-diffusion enables the determination of emulsion droplet sizes by measuring the restriction of the diffusion of molecules in the discrete phase given the presence of a droplet interface (Tais *et al.*, 2004). This approach permits the characterization of emulsions non-invasively (Hollingsworth *et al.*, 2004).

### **3.4.2 Confocal Laser Scanning Microscopy (CLSM)**

CLSM (Zeiss LSM-510, Carl Zeiss Canada, Toronto, ON, Canada) was used to study the microstructure of the wax crystalline network in model waxy oil and emulsions. The sample temperature was controlled using a Peltier-controlled temperature stage (model TS62 with STC200 controller, Instec, Boulder, CO, USA). Samples were placed in well glass slides (depth = 0.5mm) for microscopy evaluation. Water and oil-soluble dyes (Rhodamine B

and Fluorol yellow 088, respectively) were added to the water and oil phases, respectively and well mixed before homogenization. Previously, it was established that these dyes did not affect emulsion droplet size and stability. In Figure 3.5, the breadth of the droplet size distributions (corresponding to the difference between the 2.5 and 97.5 % values) was somewhat wider in the emulsions containing both dyes. However, no significant difference was found between the 50% (mean diameter) values of the dispersed droplets with and without the added dyes ( $p>0.05$ ).

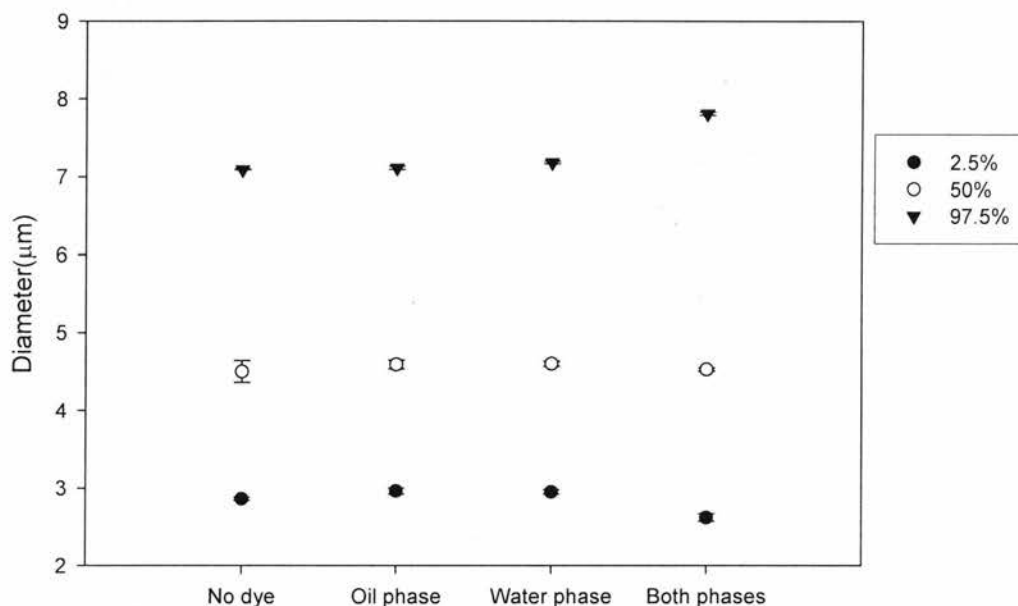


**Figure 3.5** Effect of added dyes on the droplet size distribution of model emulsions. The 2.5%, 50% and 97.5% values are the volume-weighted % of the water droplets smaller than the corresponding droplet diameter.

Micrographs were analyzed quantitatively to evaluate wax crystallization. The features (crystallized wax concentration, crystal size and number of crystals) were analyzed using OEM Reindeer Graphics Fovea Pro 4.0

software, which is a plug-in for Adobe Photoshop. All analyses were based on 20 micrographs for each sample.

### **3.4.3 Polarized Light Microscopy (PLM)**

PLM (Zeiss LSM -510, Carl Zeiss Canada, Toronto, ON, Canada) was used to characterize the wax crystals in the continuous oil phase.

### **3.4.4 Differential Scanning Calorimetry (DSC)**

A DSC (Pyris Diamond model, Perkin-Elmer, Markham, ON, Canada) was used to characterize the wax melting and crystallization behaviour and corresponding changes in enthalpy in the model waxy oil and emulsions. It was also used to determine the WAT. For analysis, samples of 10-20 mg were hermetically sealed in an aluminium pan and weighed. These samples were analyzed in the DSC using set temperature regimes (described below). The crystallization and melting points were taken from the peak temperatures on the thermograms and analyzed using the Pyris data analysis software (v3.5). Prior to any measurement, the DSC was calibrated with an indium standard.

### **3.4.5 Bohlin C-VOR Rheometer**

A Bohlin C-VOR rheometer from Malvern Instruments was used for rheological characterization of the waxy and model emulsions (Malvern Instruments, Westborough, NJ, USA). The Bohlin C-VOR is a high resolution, modular rheometer with triple-mode motor control, which allows for strain, stress or shear rate-controlled measurements. However, only the controlled stress/rate mode was used in this study, *i.e.*, sample deformation was performed

by applying a specified stress/rate and the angular deflection (strain) resulting from the applied stress/rate was measured.

Steady stress was used to obtain the viscoelastic properties of the model crude oil emulsions. A Mooney cell and cup (25 mm diameter, 29 mm height, stainless steel body) was used along with a Peltier baseplate, which precisely controlled temperature. Samples of 2 mL were pipetted in the spaces between the Mooney cell and cup. For yield stress measurements and creep recovery tests, a Vane (V19) geometry (a four-bladed vane) was used. This geometry allows spindle insertion into the material without compromising the sample structure (Wardhaugh and Boger, 1991; Nguyen and Boger, 1992).

### **3.4.6 Statistics**

Statistical analyses were performed with SPSS Statistical Package v8.0.1 using ANOVA and Tukey's analysis (SPSS, Chigaco, IL, USA). Differences were considered significant at  $p < 0.05$ .

# Chapter 4

## Wax Crystallization in a Model Crude Oil

### 4.1 Introduction

Wax deposition on the internal walls of pipelines occurs when the temperature of the external environment is below the WAT of the paraffinic (wax) component of crude oil (Amadi *et al.*, 2005), a situation commonly encountered in offshore and Arctic production (Singh *et al.*, 2000). Because wax deposition leads to progressive restriction of pipeline diameter, there is considerable effort placed on evaluating and minimizing deposit formation.

Compositional analyses have shown that the wax deposits from crude oils contain both higher weight linear and branched alkanes (Ronningsen and Bjorndal, 1991). Such compositional complexity leads to a wide range of WATs, with values for most crude oils between 20 °C and 60 °C.

During wax-oil gelation, there is competition between paraffin crystal growth and the aggregation of the single wax crystallites into a dynamically arrested structure as the associating particles are not initially present in the fluid, but rather form and increase in size at a rate fixed by crystal nucleation and

growth, a physical mechanism which is totally distinct from the diffusion-limited gelation of the system (Vignati *et al.*, 2005).

The purpose of this chapter was to elucidate wax crystallization behaviour and crystal growth in a model crude oil as a function of time. Since crude oil is often recovered in the form of a water-in-crude oil emulsion, wax crystallization in emulsion was also assessed.

## 4.2 Materials and Methods

Model waxy crude oil emulsions were prepared by mixing wax, PgPr and mineral oil at 80 °C for 1 hour followed by static cooling to 25 °C in a temperature-controlled waterbath. Four wax-oil-emulsifier mixtures were prepared: (a) 3% (w/w) wax in mineral oil, (b) 5% (w/w) wax in mineral oil, (c) 2.5% (w/w) PgPr + 3% (w/w) wax in mineral oil, and (d) 2.5% (w/w) PgPr + 5% (w/w) wax in mineral oil.

Model emulsions were prepared by mixing 20% (w/w) water with light mineral oil containing 2.5% (w/w) PgPr and either 3% or 5% (w/w) wax and subsequently subjected to valve homogenization at 5000 psi with 4 cycles. Freshly-prepared emulsions were transferred into NMR tubes for sedimentation and droplet size measurements and tubes were kept in a waterbath at 25 °C.

The samples were analyzed using DSC, CLSM and PFG-NMR. Please refer to Chapter 3 for details on the analysis techniques.

## 4.3 Results and Discussions

### 4.3.1 Wax Crystallization in Wax-Containing Oil

#### 4.3.1.1 Differential Scanning Calorimetry (DSC)

DSC was used to characterize the melting behaviour of the pure wax and wax-oil-PgPr blends mentioned in section 4.2. These samples were placed in DSC pans at 80 °C and stored at 4 °C for 0, 1 or 7 days. Scans were performed from 4 to 70 °C at 5 °C min<sup>-1</sup>.

The pure wax (Figure 4.1) showed two melting peaks at ~45 and ~60 °C, suggesting the presence of two families of species with distinct thermal transitions. In the 5% (w/w) waxy oils (both with and without PgPr), the melting points of the fractions were 23 and 30 °C, respectively (Figure 4.2). The 3% (w/w) wax solutions (both with and without PgPr) showed only one melting peak with a melting point of 22 °C (Figure 4.2), suggesting miscibility of one of the families. The onset of melting temperature of the wax solutions was not affected by the presence of PgPr nor storage time.

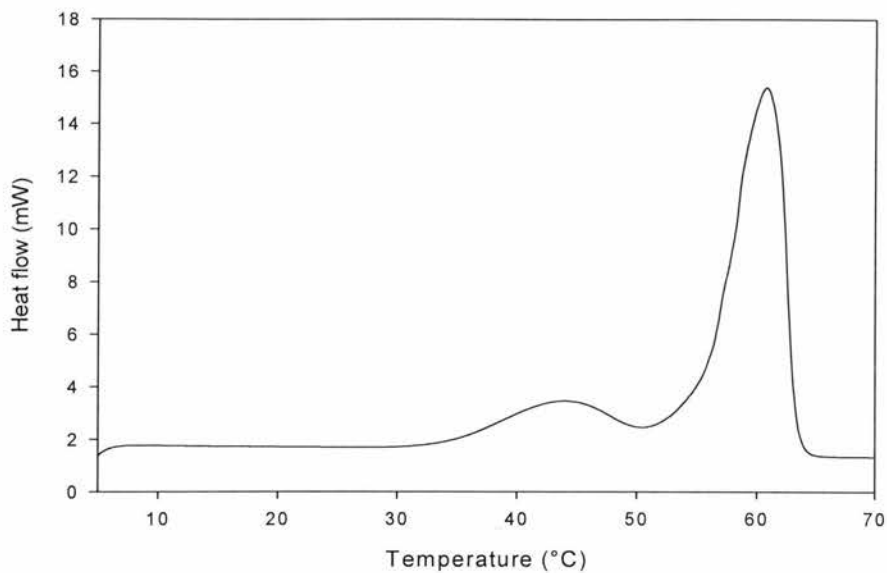


**Figure 4.1** DSC thermogram of pure paraffin wax.

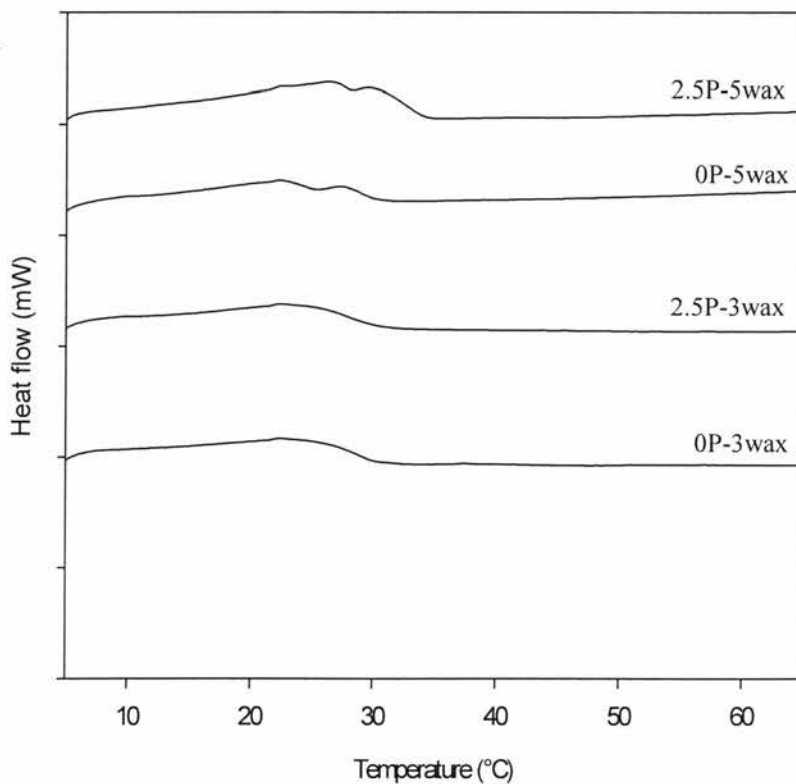


**Figure 4.2** DSC thermogram of mineral oil, wax and emulsifier mixtures (from 4 to 70 °C at 5 °C min<sup>-1</sup>)

The enthalpy of melting increased from day 0 to day 1 for all samples (Figure 4.3), which was likely due to an increase in solids content over time. However, there was no significant difference in enthalpy between days 1 and 7 ( $p>0.05$ ), which suggested that no further increase in wax crystallization took place after 1 day of storage at 4 °C. As well, there was no significant difference in enthalpy of fusion for samples with and without PgPr ( $p>0.05$ ), indicating that the emulsifier had no bearing on solids content.

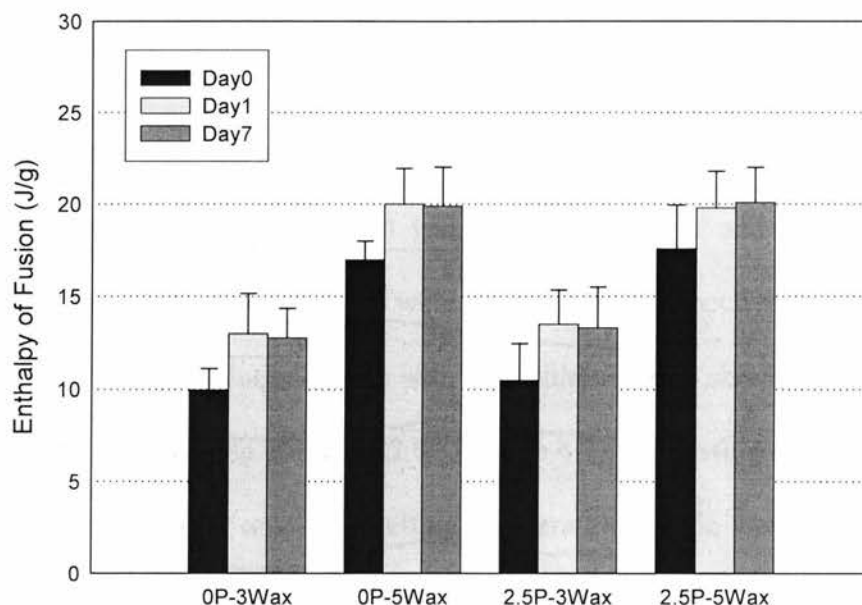


**Figure 4.3** Enthalpies of fusion of wax crystals in oil with and without added emulsifier (from 4 to 70 °C at 5 °C min<sup>-1</sup>)

#### 4.3.1.2 Confocal Laser Scanning Microscopy (CLSM)

CLSM was used to evaluate wax crystal growth in the presence of PgPr. Aliquots of mixed wax-oil-PgPr were transferred into well slides, stored at 25 °C and analyzed on days 0, 1 and 7.

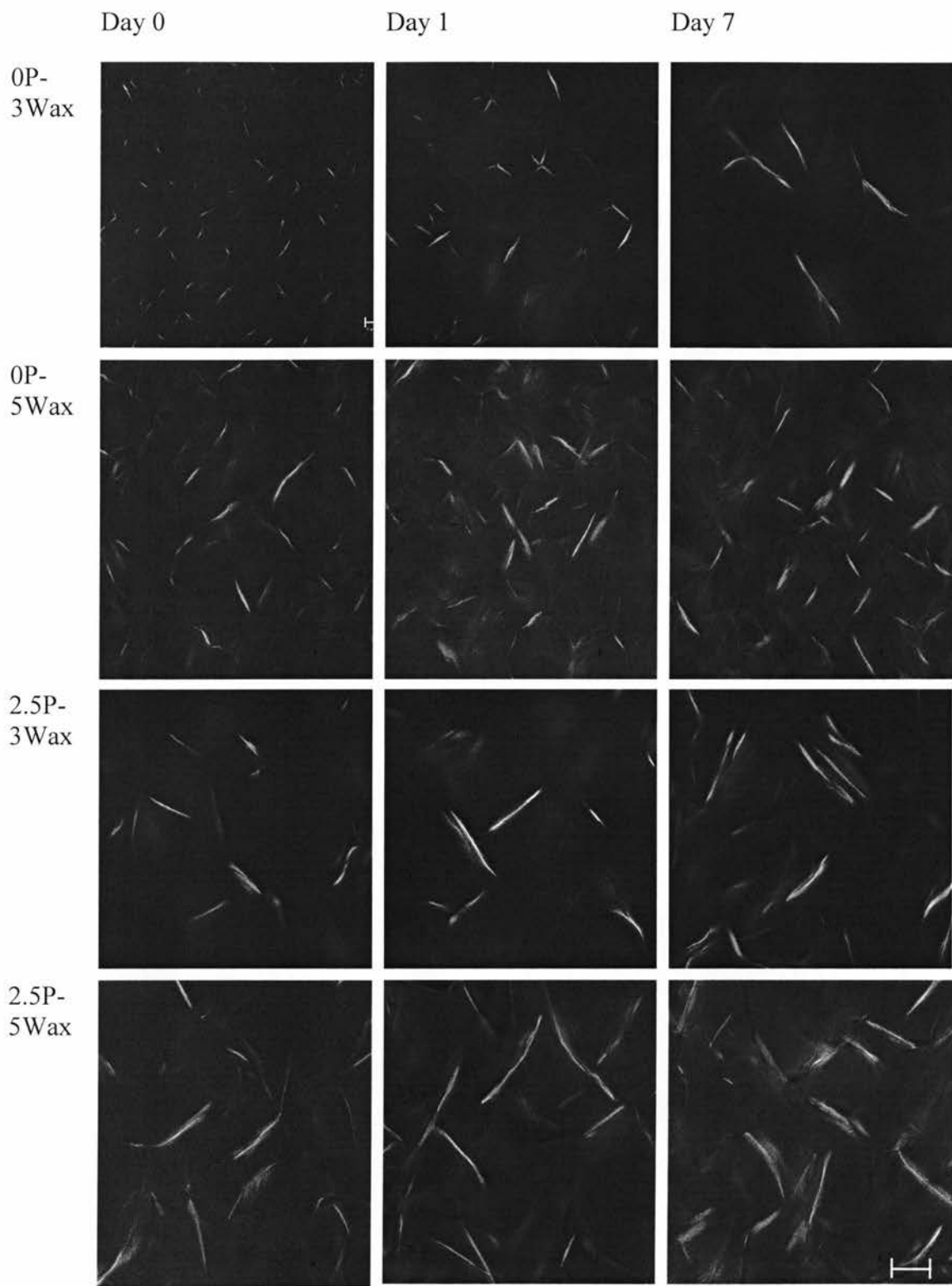


**Figure 4.4** Micrographs of wax-oil-PgPr mixtures ( $T=25\text{ }^{\circ}\text{C}$ ) after 0, 1 and 7 days of storage. Wax crystals appear as white needles dispersed in the oil phase, which appears dark. The size bar represents  $25\text{ }\mu\text{m}$ .

In all samples, the wax crystallized in the form of needles (Figure 4.4), though their shape and spatial distribution was composition-dependent. Figure 4.5 shows the change in crystallized wax concentration for samples over time. On day 0, the crystal concentration for the 3% and 5% (w/w) wax samples were 1.3 and 2.2% (w/w), respectively. There was a significant increase in the wax crystal sizes from day 0 to day 1 ( $p < 0.05$ ) for all samples. However, there was no significant increase in the crystal concentration from day 1 to day 7 ( $p > 0.05$ ), similar to the melting enthalpy results. There was a significant increase in crystal length between days 0 and 7 ( $p < 0.05$ ) (Figure 4.6), with crystals in the samples with PgPr being longer and fewer in number compared to those without PgPr.

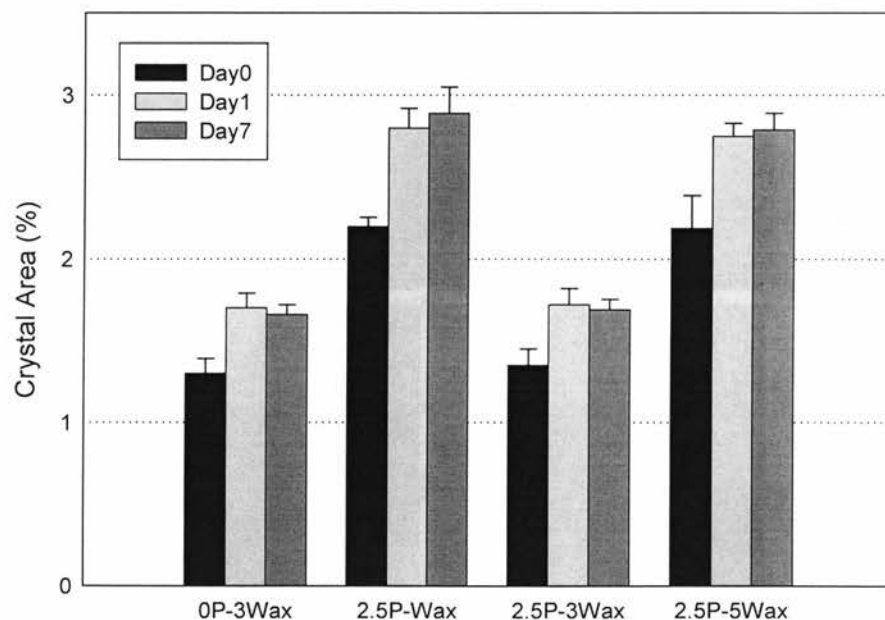


**Figure 4.5** Total crystal area in mixtures of light mineral oil and wax at different wax concentrations and in the absence/presence of PgPr ( $T = 25^{\circ}\text{C}$ ).

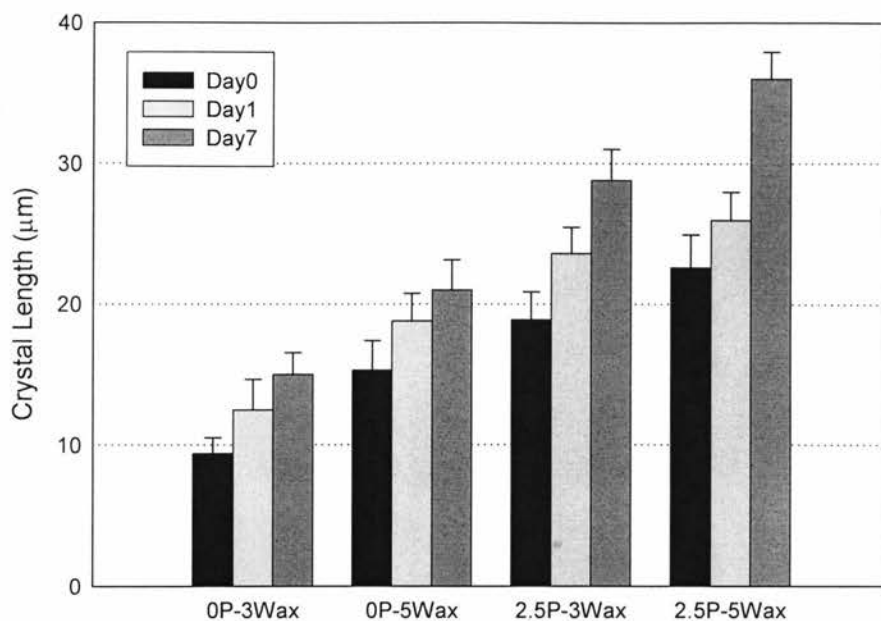


**Figure 4.6** Mean crystal length in mixtures of light mineral oil and wax at different wax concentrations and in the absence/presence of PgPr ( $T=25^{\circ}\text{C}$ ).

#### 4.3.1.3 PFG-NMR results

The self-diffusion coefficient of hydrogen nuclei in mineral oil was measured using pulsed field gradient (PFG)-NMR as a function of storage time. The experiments were carried out for one week and measurements were performed on days 0 (2 h after sample preparation), 1, 2, 4 and 7. Aliquots (1.5 ml) of freshly prepared samples were transferred to NMR tubes and kept at  $25^{\circ}\text{C}$ .

Table 4.1 shows that no significant difference in self diffusion coefficient was observed irrespective of wax content or presence of PgPr ( $p>0.05$ ), suggesting that the mobility of the oil was not affected by the presence of the crystalline wax matrix, at least when the diffusion of its

hydrogen nuclei is concerned, or that the instrumental technique was not sufficiently sensitive for this measurement.

**Table 4.1** Hydrogen nuclei diffusion coefficients ( $10^{-9} \text{ m}^2/\text{s}$ ) for waxy oil.

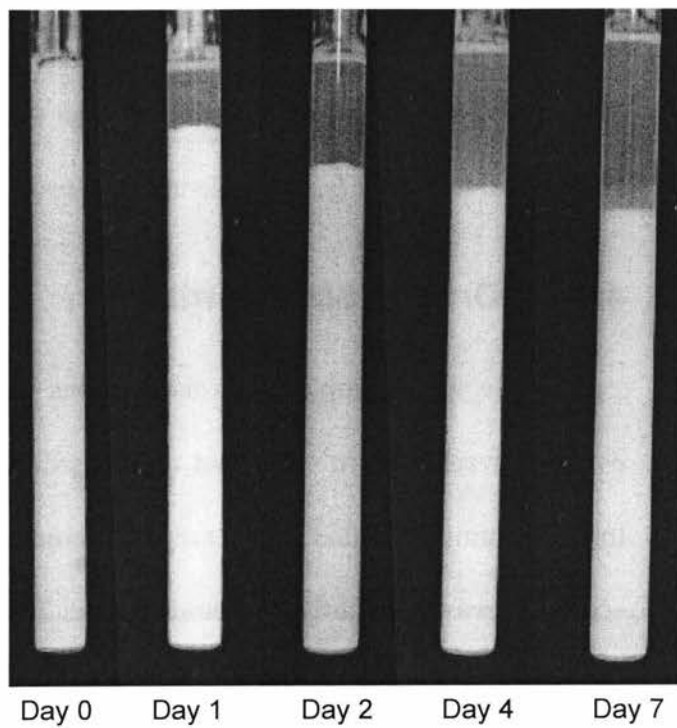
Neat Samples	Day 0	Day 1	Day 2	Day 4	Day 7
0P-0wax	0.035±0.003	0.027±0.002	0.031±0.001	0.027±0.001	0.030±0.001
00P-3wax	0.031±0.001	0.032±0.001	0.033±0.003	0.034±0.001	0.032±0.001
0P-5wax	0.032±0.002	0.030±0.002	0.038±0.004	0.027±0.001	0.031±0.002
2.5P-0wax	0.030±0.000	0.031±0.002	0.034±0.002	0.026±0.002	0.031±0.003
2.5P-3wax	0.029±0.001	0.031±0.001	0.033±0.002	0.027±0.001	0.031±0.002
2.5P-5wax	0.033±0.003	0.032±0.005	0.036±0.003	0.026±0.001	0.031±0.001

## 4.3.2 Wax Crystallization in Emulsion

### 4.3.2.1 Sedimentation Behaviour

Model emulsions were prepared by mixing 20% (w/w) water with light mineral oil containing 2.5% (w/w) PgPr and either 3% or 5% (w/w) wax. Emulsion sedimentation was recorded on days 0, 1, 2, 4 and 7 following homogenization. Figure 4.7 shows the visual appearance of model emulsions over 7 days of storage at 25 °C. The opaque regions of the tubes were composed of the emulsified water and dispersed wax crystals whereas the transparent regions consisted of free mineral oil. Emulsions containing 3% (w/w) wax showed appreciable sedimentation (Figure 4.7a). The extent of sedimentation increased with time over a period of seven days (~ 75% sediment volume). Emulsions with 5% (w/w) wax showed no visible breakdown (Figure 4.7b).

(a)



(b)

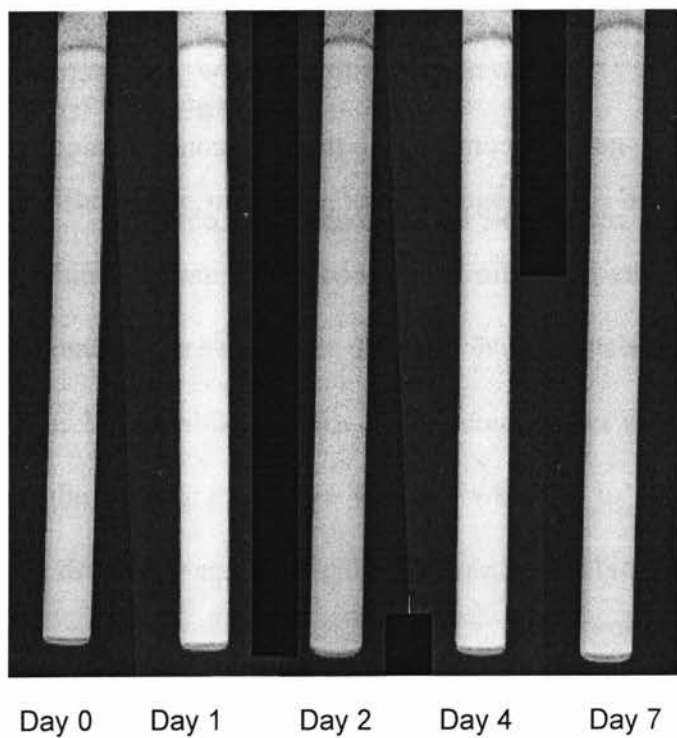


**Figure 4.7** Sedimentation of water-in-oil emulsions containing 2.5% PgPr, 20% water and either (a) 3% wax or (b) 5% wax in the oil phase as a function of storage time at 25 °C.

Based on these results, the wax crystal network formed in the emulsion containing 3% (w/w) wax was either much weaker than in the emulsion with 5% (w/w) wax or there was insufficient wax to prevent sedimentation. With 5% (w/w) wax, the wax crystal concentration prevented large-scale oil separation.

#### **4.3.2.2 Droplet Size Distribution**

The water droplet size distributions of the emulsions were measured over one week. Figure 4.8 shows that regardless of the % wax (w/w) used, the initial volume-weighted mean droplet diameter ( $d_{33}$ ) for both emulsions was  $\sim 5\mu\text{m}$ , increasing slightly with storage time. The  $d_{33}$  of the emulsions containing 3% and 5% (w/w) wax on day 7 was  $\sim 6$  and  $\sim 7\mu\text{m}$ , respectively ( $p > 0.05$ ), indicating little coalescence over 7 days.

Emulsions with 3% (w/w) wax were stabilized by a sparser wax crystal network compared to the emulsions containing 5% (w/w) wax, which was likely responsible for the coalescence observed.

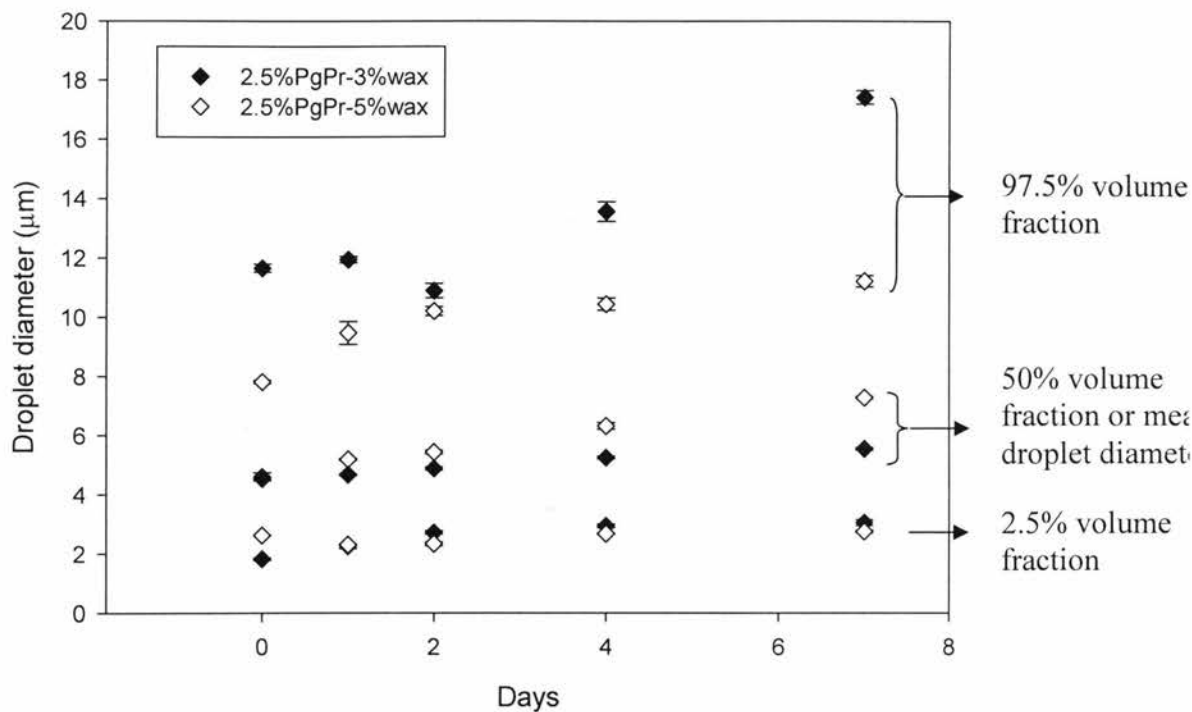


**Figure 4.8** Droplet size distribution of emulsions containing 3% wax and 2.5% PgPr (closed symbol) vs. 5% wax and 2.5% PgPr (open symbol).

### 4.3.2.3 CLSM of Emulsions

Figure 4.9 shows the microstructural changes in the emulsions over 7 days. The background represents the continuous oil phase and black spheres with light grey boundaries are the water droplets. Wax crystals dispersed in oil phase are shown as bright white needles. The average water droplet diameters determined from the micrographs were 4-5 μm, which is in accordance with NMR results. The droplets were not evenly dispersed in oil but were assembled in flocs.

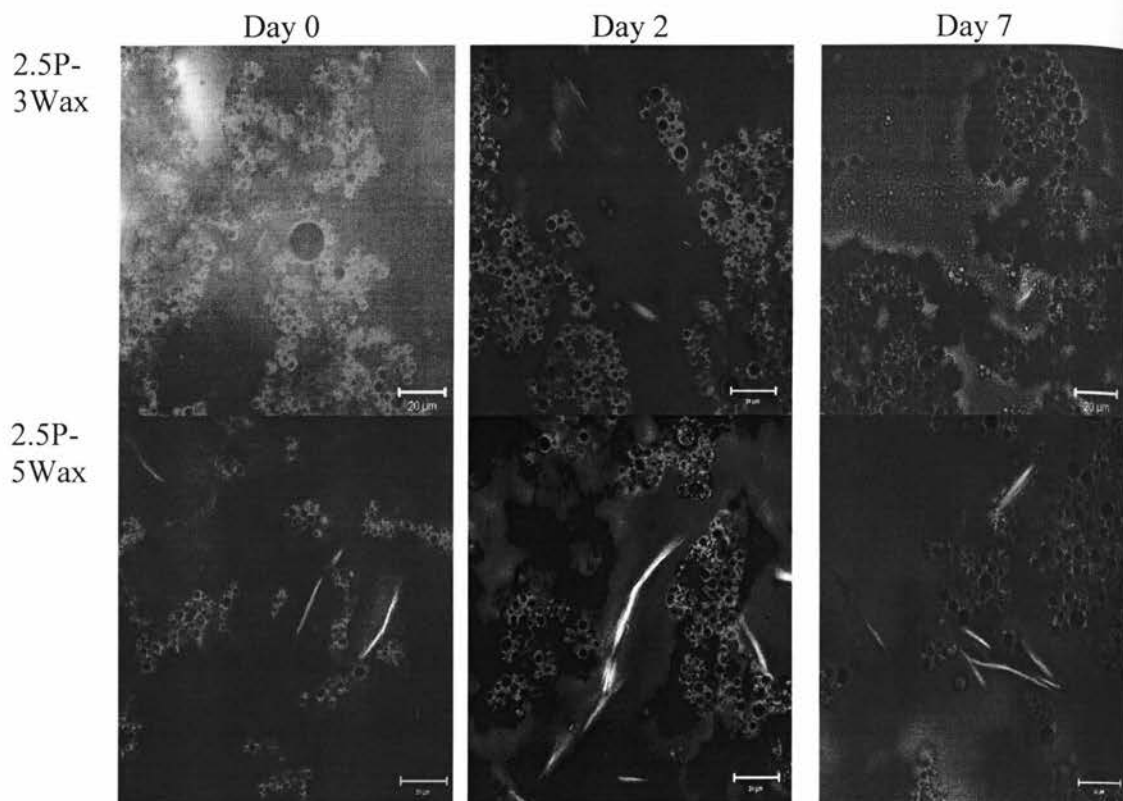


**Figure 4.9** CLSM pictures of model emulsions containing 3 or 5% (w/w) wax. The size bar represents 20  $\mu\text{m}$ .

A significant increase in crystal area was observed in both the 3% (w/w) wax and 5% wax emulsions with time ( $p < 0.05$ ), with a higher density observed in the 5% (w/w) wax emulsion. In both emulsions, wax crystals were generally not associated with water droplets, but were dispersed in the continuous oil phase, likely due to their lack of surface activity and wettability.

## 4.4 Conclusion

As per the first objective (section 1.3), wax crystallization was evaluated in waxy oil and model emulsions consisting of 3% (w/w) or 5% (w/w) wax and with/without PgPr. These samples were analyzed using different techniques, including PFG-NMR, CLSM and DSC.

Wax crystal growth and the resulting network structure were affected by the presence of PgPr, with crystals being more dispersed and less effective at forming a crystalline network in its presence. However, this effect was not evident in the oil diffusion results, as no differences in oil self-diffusion were observed, irrespective of wax content or presence of PgPr.

Emulsions with 5% (w/w) wax were more stable to sedimentation and increases in droplet size than those with 3% (w/w) wax, which was attributed to the larger number of wax crystals in the former. CLSM pictures showed much a larger average crystal size in the 5% (w/w) wax emulsion. Wax crystals were dispersed in the continuous oil phase rather than associated with water droplets.

# Chapter 5

## Baseline Flow Conditions for Model Crude Oil Emulsions in a Lab-scale Flowloop

### 5.1 Introduction

Crude oil is often recovered as an emulsion. Emulsified water adds significant volume to the crude oil can corrode the pipelines and increase transport and refining cost (Hemmingsen *et al.*, 2005). During processing, pressure gradients over chokes and valves introduce sufficiently high shear to emulsify water as dispersed droplets within the oil phase. Together, an emulsified aqueous phase and dispersed wax-like solids greatly affect the rheological behaviour of stagnant and flowing crude oil.

Several attempts have been made to predict wax deposition in pipelines by using laboratory-scale flowloops (Hsu *et al.*, 1999; Burger *et al.*, 1981; Brown *et al.*, 1993). Hsu *et al.* (1999) conducted high-pressure flowloop experiments with waxy crude oils to study the effect of water on paraffin deposition under turbulent flow. They showed that wax deposition was significantly reduced with the addition of emulsified water. However, scale-up of deposition processes studied at a lab-scale usually leads to over-prediction of

wax deposition in the field (Brown *et al.*, 1993), which may be due to differences in wax deposit morphology.

The flow conditions of crude oil in pipelines are often represented by Hagen-Poiseuille's equation (Cheng *et al.*, 1984), which describes slow viscous incompressible flow through a constant circular cross-section. It is commonly used for fluids flowing under laminar flow:

$$\Delta P = \frac{8\mu L Q}{\pi r^4} \quad 5.1$$

where  $\Delta P$  is the pressure drop,  $L$  is the length of pipe,  $\mu$  is the dynamic viscosity,  $Q$  is the volumetric flow rate,  $r$  is the radius and  $\pi$  is a constant.

Shear rate is expressed as the rate at which a shear stress is applied, and is defined as:

$$\gamma = \frac{8V}{d} \quad 5.2$$

where  $\gamma$  is the shear rate,  $V$  is the velocity of fluid, and  $d$  is the internal diameter of the pipe.

In order to understand the complex flow behaviour of crude oil emulsions stabilized by wax crystals, a model W/O emulsion (1:4 water:oil ratio) was studied. A laboratory flowloop was used to perform wax deposition experiments. The focus of this chapter was to determine the operating process flow conditions of the model W/O emulsion in the lab-scale flowloop. This was done in order to mimic the flow conditions of model emulsions in a controlled shear rate/stress rheometer.

## 5.2 Materials and Methods

### *Model Emulsion Preparation*

As per Chapter 3, the model crude oil W/O emulsions consisted of light mineral oil, ultra-pure water and PgPr. A refined paraffin wax (m.p.  $\sim 60$  °C) was used to help stabilize the emulsion and was added molten to the oil mixture prior to emulsification. Mixture of oil, wax (5% w/w) and PgPr (2.5% w/w) were heated to 80 °C (well above the melting point of wax), and then cooled to 30 °C and pre-mixed with the required volume of water with an impeller-type mixer. This coarse emulsification step ensured greater uniformity for the subsequent homogenization step. The mixture was homogenized with a two-stage valve homogenizer (APV-1000, APV, Concord, ON, Canada). Pressures of 5000 Pa and 500 Pa were applied for the first and second stages, respectively. The outlet temperature of the emulsion was  $\sim 40$  °C, due to mild heat buildup in the homogenizer.

The model emulsions were flowed through the laboratory flow-loop (Section 3.3) and the inlet/outlet temperatures and differential pressure generated by the flowing emulsions were obtained from the data logger software (LabView 8.6, National Instruments, Mississauga, ON, Canada). The final emulsions were analyzed for their rheological properties using a controlled shear stress/rate rheometer (Section 3.4.4). Process conditions were determined based on the flowloop dimensions and the flow rate of the model emulsion in the flowloop using Equations 5.1 and 5.2.

## 5.3 Results and Discussion

### 5.3.1 Determination of $\Delta P$ and the Rate of Cooling

In-pipe flow behaviour can be compared with that taking place in a rheometer only if the thermal and shear histories and solidification behaviour of the materials under study are identical in both scenarios. In a rheometer, applying a steady shear stress equal to the flow shear stress of the model emulsion in the pipeline makes the shear history of the two processes nearly identical. In order to have an identical thermal history, an estimation of the cooling rate in the flowloop was determined.

Figure 5.1 and 5.2 shows the inlet and outlet temperatures of model W/O emulsions passed through different lengths of a lab-scale flowloop (5 and 10m). The differential pressure (generated by emulsions' flow) as a function of time is also shown in Figures 5.1 and 5.2. The inlet ( $t=0$ ) temperature of emulsions was set to  $\sim 40$  °C, which was above the WAT of the wax in the model emulsion ( $\sim 30$  °C). As the emulsions passed through the loops ( $\sim 4$  °C), the temperature diminished to 14 and 10 °C for the 5 and 10m lengths, respectively. The length of a typical flowloop experiment was  $\sim 4$  min. The differential pressures (pressure drops) were 240 and 290 psi for the 5 and 10m loop sections, respectively.

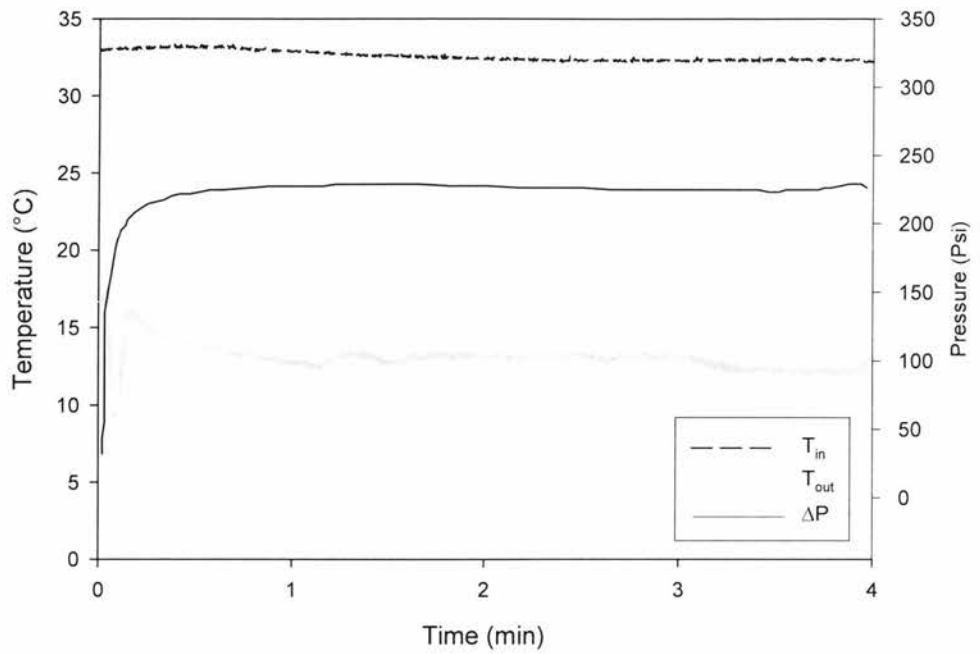


**Figure 5.1** Typical flowloop data for the model crude oil emulsion passed through a 5 m loop.

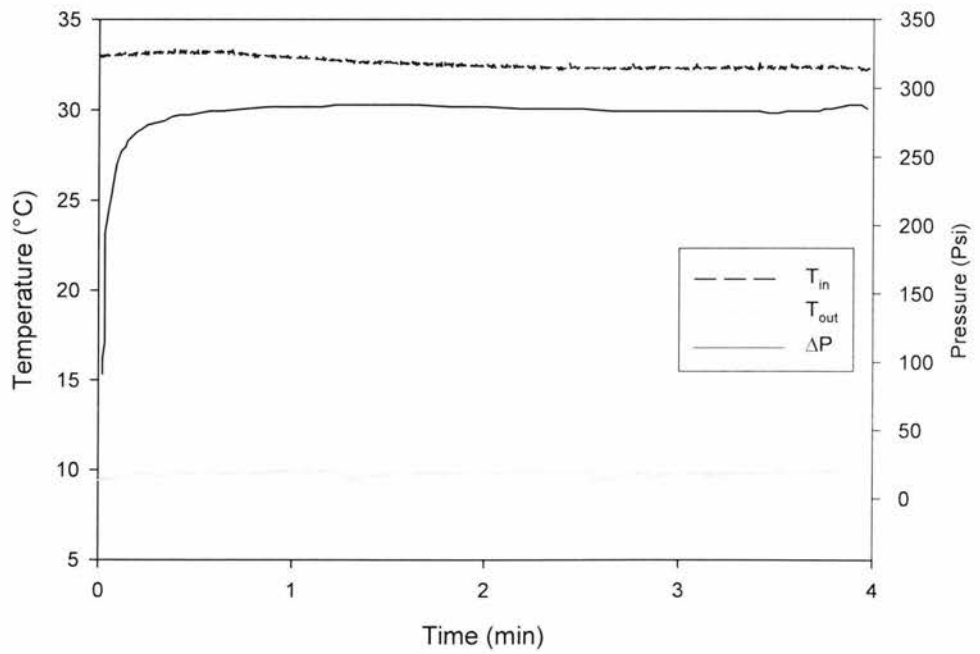


**Figure 5.2** Typical flowloop data for the model crude oil emulsion passed through a 10 m loop.

This shows that there was no wax deposition took place as wax deposition would reduce the radius available for emulsion flow, which in turn would increase the pressure drop across the pipeline with time. This is well represented by:

$$\tau_w = \Delta P x \left( \frac{D}{L} \right) \quad 5.3$$

where  $\Delta P$  = pressure drop,  $D$  = flowloop diameter and  $L$  = length of the pipe

A summary of the process conditions of the flowloop as a function of flowloop length is shown in Table 5.1. These data were recovered from the data logger system after the completion of each flowloop run.

**Table 5.1** Process conditions of the model emulsions as it passes through the flowloop

Flowloop length (m)	$\Delta P$ (psi)	Temperature ( $^{\circ}\text{C}$ )	Rate of cooling ( $^{\circ}\text{C}/\text{min}$ )
5	240 $\pm$ 4.8	14 $\pm$ 0.9	109.5
10	290 $\pm$ 6.1	10 $\pm$ 0.7	8.5

The cooling rates of the model emulsions found was much higher than those encountered in field pipelines. The cooling rate of the fluid is a function of pipe diameter (Equation 5.4). This implies that the cooling rate is inversely proportional to the radius of pipe.

$$\text{Cooling rate} = \frac{D_e}{(1 - \phi_s)\xi} \frac{Nu}{R} (T_o - T_w) \quad 5.4$$

where  $D_e$  is molecular diffusivity of wax in oil,  $\xi$  is the thickness of the gel layer,  $Nu$  is Nusselt number for heat transfer,  $R$  is the radius of pipe,  $T_o$  is the

bulk temperature (oil), and  $T_w$  is the temperature at the pipe wall. With a field pipeline having a much larger diameter than a laboratory flowloop, the effective cooling rate in the latter will be much higher than in the former, under similar operating conditions (Equation 5.4).

### 5.3.2 Theoretical Shear Rate in the Flowloop

The shear rate in the flowloop was calculated from Equation 5.2 based on the pipe diameter ( $4.572 \times 10^{-3}$  m pipe ID) of the flowloop and the velocity of the model W/O emulsion in the flowloop. Table 5.2 shows the data used to calculate the theoretical shear rate in the flowloop.

**Table 5.2** Parameters used in the calculation of shear rate

Flowloop cross sectional area	$1.64 \times 10^{-5} \text{ m}^2$
Flow rate	$6.7 \times 10^{-5} \text{ m}^3/\text{s}$
Velocity	0.41 m/s

The theoretical shear rate in the flowloop was calculated as  $700 \text{ s}^{-1}$ . However, it was not possible to use such a high shear rate in the rheometer due to instrument limitations. Hence, a high shear viscosity plateau was explored, which was found well below  $700 \text{ s}^{-1}$ , as described below.

### 5.3.3 Shear Plateau Determination

Steady-state measurements were made with a shear sweep of the emulsified samples at  $14 \text{ }^\circ\text{C}$  (Figure 5.3) to determine the high shear plateau region. The shear rate was varied from  $0.001$  to  $1000 \text{ s}^{-1}$ . The measuring time for each sample point was set to 10s. The viscosity of the emulsions decreased as the applied shear rate increased (Figure 5.3). Though no plateau was attained

within this range of shear rates, there was minimal change in viscosity with shear rates  $> 200 \text{ s}^{-1}$ . Thus, a rate of  $200 \text{ s}^{-1}$  was used to mimic the shear conditions experienced by crude oil in pipelines for rheological analyses.

Shear rate experiments were performed with two measurement times at each shear rate (10s and 30s), with sequential forward and reverse shear rates of 0.1, 0.5, 1, 5, 10, 50, 100, 500 and  $1000 \text{ s}^{-1}$  on the same emulsified sample. The shear sweep points with both measurement times matched each other, suggesting that either was long enough for the wax to not be in a transient state (Figure 5.3).

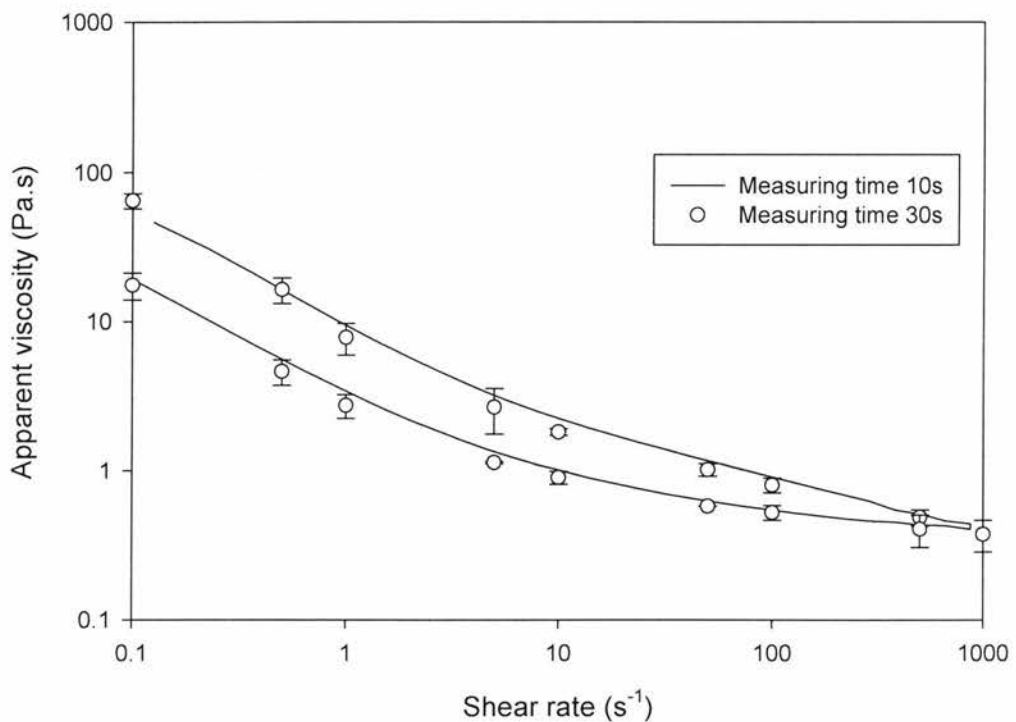


**Figure 5.3** Shear plateau determination with different measuring times for model crude oil emulsions consisting of 5 % (w/w) wax.

Waxy oil is generally thixotropic, *i.e.*, viscosity decreases with time under constant shear (in addition to being shear thinning) (Ronningsen, 1992). Shear thinning can occur if the measurement time is not long enough. Every time the shear rate (and hence flow rate) changes, the sample under investigation goes through a transient state during which measurements should not be made. Thus, the measurement time should at least correspond to the minimal time needed for a sample to attain equilibrium at a given shear rate.

Crude oil viscosity will change with the flow conditions (flow rates, temperature *etc.*) experienced inside pipelines (Chang *et al.* (2000)). The effect of shear rate from  $1 \text{ s}^{-1}$  to  $200 \text{ s}^{-1}$  on the apparent viscosity of the model emulsions cooled from 40 to 4°C at a constant cooling rate of 1 °C/min was evaluated (Figure 5.4). The measurement time was set to 10s.

At higher temperatures, the viscosity was slightly dependent on temperature, but independent of shear rate ( $p < 0.05$ ). Near the WAT, however, the viscosity increased rapidly and became shear rate-dependent as wax crystallization began, with lower shear rates resulting in a higher apparent viscosity ( $p < 0.05$ ). The results also showed the shear thinning behaviour of emulsions, which is common in emulsions given the presence of weakly-interacting particles (droplets, crystals, *etc.*) (Tadros, 1994).

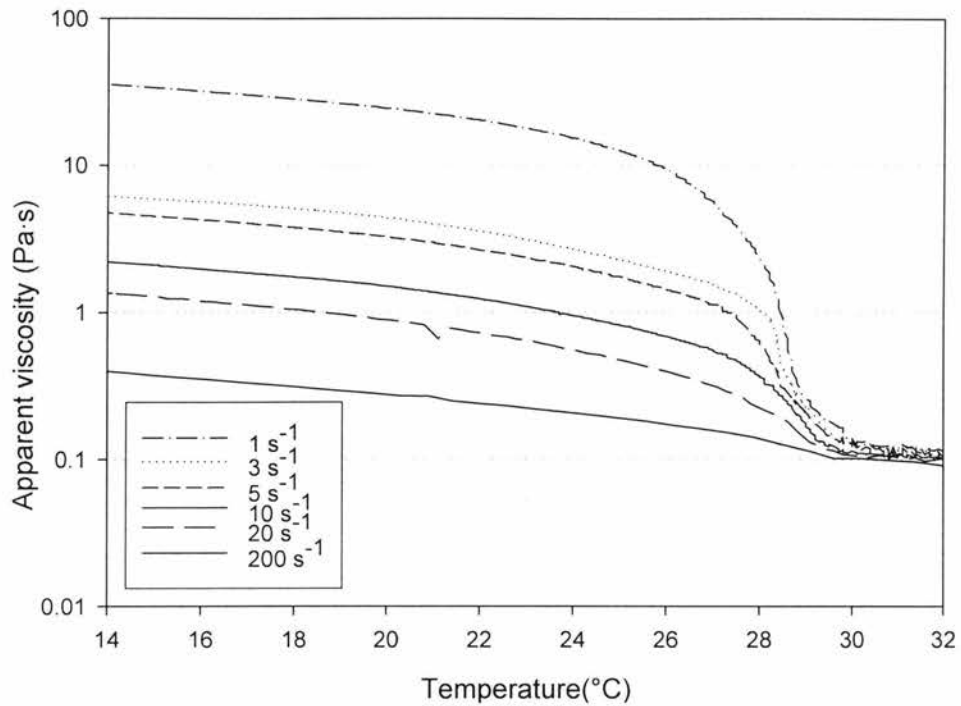


**Figure 5.4** Viscosity of model crude oil emulsions containing 5 % (w/w) wax as a function of shear rate at a cooling rate of 1 °C/min (error bars omitted for clarity).

Shearing an emulsion causes interacting and potentially aggregated particles to be progressively deformed or perhaps disassociate, which decreases the resistance to flow and therefore causes a reduction in apparent viscosity. In Figure 5.4, below the WAT, there was a progressively lower viscosity observed with increasing shear rate, indicating that shear had a substantial influence on the wax crystallization kinetics. Higher shear rates likely resulted in the formation of smaller crystals that were more weakly interacting given the presence of a shear field.

## 5.4 Conclusion

A lab-scale flowloop was designed and used to preliminarily elucidate the flow behaviour of model crude oil emulsions in pipelines. Emulsion flow conditions were ascertained (flow behaviour, temperature and pressure drop, *etc.*) and a protocol to mimic the emulsion flow conditions in a rheometer was developed. Based on these results, a shear rate of  $200 \text{ s}^{-1}$  was used in the subsequent rheological characterization of the model crude oil emulsions.

# Chapter 6

## Rheological Behaviour of Crude Oil Emulsions

### 6.1 Introduction

When crude oil is produced, it is potentially mixed with up to 70% water (Plegue *et al.*, 1986), which is emulsified given the presence of surface-active materials naturally present in the crude (*e.g.*, asphaltenes or resins). Despite their industrial relevance, there are very few published reports on the rheological characterization of crude oil W/O emulsions (Salager *et al.*, 2001; Langevin *et al.*, 2004). Numerous authors (Simon and Poynter, 1968; Rose and Marsden, 1970; Mao and Marsden, 1977; Ronningsen, 1995 and Farah *et al.*, 2005) have found that the best correlation between the relative viscosity ( $\eta_r$ ) of W/O emulsions and the volume fraction ( $\phi$ ) of the aqueous phase in emulsions is an exponential equation, as proposed by Richardson (1933).

$$\eta_r = \exp(k\phi) \quad 6.1$$

where  $k$  is a constant. These findings differ from the classical behaviour expected for an emulsion, *e.g.*, the models of Mooney (1951) or Krieger and Dougherty (1959), which state that:

$$\eta_r = \exp\left(\frac{\alpha\phi}{1 - K\phi}\right) \quad 6.2$$

where  $\alpha$  is a shape factor of water droplets and  $K$  is equal to  $1/\phi_m$  ( $\phi_m$  being the maximum packing concentration of water droplets). Later, Kreiger and Dougherty (1959) modified Mooney's equation to:

$$\eta_r = (1 - K\phi)^{-\alpha/K} \quad 6.3$$

Quintero *et al.* (2008) characterized dilute and concentrated crude oil emulsions and ascertained their viscosity with Equation 6.3. They found that temperature had a strong influence on the emulsions' rheological behaviour due to the presence of a paraffinic gel.

Very little fundamental and applied knowledge is available to explain the complex flow behaviour and pipeline deposition of wax from a mixture of crude oil and water. According to Cole and Jessen (1960), in the presence of water, paraffin deposition on a more water-wet surface is significantly reduced, while no difference in deposition occurs with oil-wet surfaces.

The goal of this chapter was to characterize the rheological behaviour of model W/O emulsions passed through various lengths of a lab-scale flowloop setup (5 and 10m). This chapter is divided into two sections. The first presents the viscosity profiles of the model oil-water-wax system prior to the flowloop run while the second describes the steady-state and dynamic flow behaviour of the model emulsions as encountered in the flowloop.

## 6.2 Material and Methods

### *Model Emulsion Preparation*

As per Chapter 3, the model emulsions consisted of light mineral oil, water (20% w/w) and PgPr (2.5% w/w). A refined paraffin wax (m.p.  $\sim 60$  °C) was used to form the emulsion and was added molten to the oil mixture prior to emulsification. Mixture of oil, wax (5% w/w) and PgPr (2.5% w/w) were heated to 80 °C (well above the melting point of wax), and then cooled to 30 °C and pre-mixed with the required volume of water with an impeller-type mixer for 30 sec. This coarse emulsification step ensured greater uniformity of oil and water phase for subsequent homogenization. The mixture was homogenized with a two-stage valve homogeniser (APV-1000, Concord, ON, Canada). Pressures of 5000 Pa and 500 Pa were applied for the first and second stages, respectively. The outlet temperature of the emulsion was  $\sim 40$  °C, due to mild heat buildup in the valve homogenizer.

The model emulsions were flowed through the laboratory flowloop (Section 3.3) and analyzed for their rheological properties using a controlled shear stress/rate rheometer (Section 3.4.4).

### *Flow of the Model Emulsions in the Loop*

Three flowloop lengths (0, 5, and 10m) were used to analyze the flow characteristics of the emulsion. The “0m flowloop length” emulsion refers to fresh emulsions not passed through the flowloop. The “5m flowloop length” and “10m flowloop length” emulsions refer to the emulsions passed through the 5

and 10m loops, respectively. The outlet temperatures of the emulsions are summarized in Table 6.1.

**Table 6.1** Outlet temperatures of the emulsions passed through different flowloop lengths

Emulsions	Outlet temperature (°C)
0m flowloop length	40
5m flowloop length	14
10m flowloop length	10

### *Rheology*

A Bohlin C-VOR rheometer (Malvern Instruments, NJ, USA) was used to measure the rheological behaviour of the emulsions. The geometry used was a Mooney cell and cup (25 mm diameter, 29 mm height, stainless steel body), unless specified otherwise. The samples (2 mL) were loaded onto the rheometer stage using disposable pipettes. The geometry and pipettes were kept at the measurement temperature prior to starting the tests to minimize any temperature variations. The pipetting was performed with wide orifice tips to minimize sample shearing. The time between the sampling and the measurements were also kept constant in order to avoid any storage time effect on rheological properties. All experiments were performed in triplicate.

### *Viscosity Profiles*

There was a change in the viscosity of the model system with the introduction of each component (oil, water, wax, PgPr). The samples

investigated were pure mineral oil, mineral oil and PgPr (2.5% w/w), mineral oil and wax (5% w/w), a mineral oil and water (20% w/w) emulsion (no wax, no PgPr), and the model W/O emulsion (2.5% w/w PgPr 5% w/w wax). The emulsion with no PgPr and no wax was unstable and separated out into two layers within seconds of preparation. As discussed in Chapter 5, a shear rate of  $200 \text{ s}^{-1}$  was used. The temperature was swept from  $40 \text{ }^\circ\text{C}$  to  $4 \text{ }^\circ\text{C}$  at a rate of  $1 \text{ }^\circ\text{C}/\text{min}$  in the rheometer.

## 6.3 Results and Discussion

### 6.3.1 Viscosity Profiles

Figures 6.1 and 6.2 show the viscosity as a function of temperature for pure mineral oil and the mineral oil-PgPr (2.5% w/w) mixture, respectively. The viscosity changed slowly with temperature and the two systems behaved as Newtonian liquids. The Arrhenius equation for Newtonian fluids was used to describe the temperature dependence of the viscosity as follows:

$$\eta = Ae^{E_a/RT} \quad 6.4$$

where  $\eta$  is the Newtonian dynamic viscosity,  $A$  is a constant dependent on the entropy of activation of flow,  $E_a$  is the activation energy of viscous flow,  $R$  is the universal gas constant and  $T$  is the absolute temperature.

Figure 6.2 also confirms the second characteristic of Newtonian liquids *i.e.*, that viscosity is independent of the shear applied.

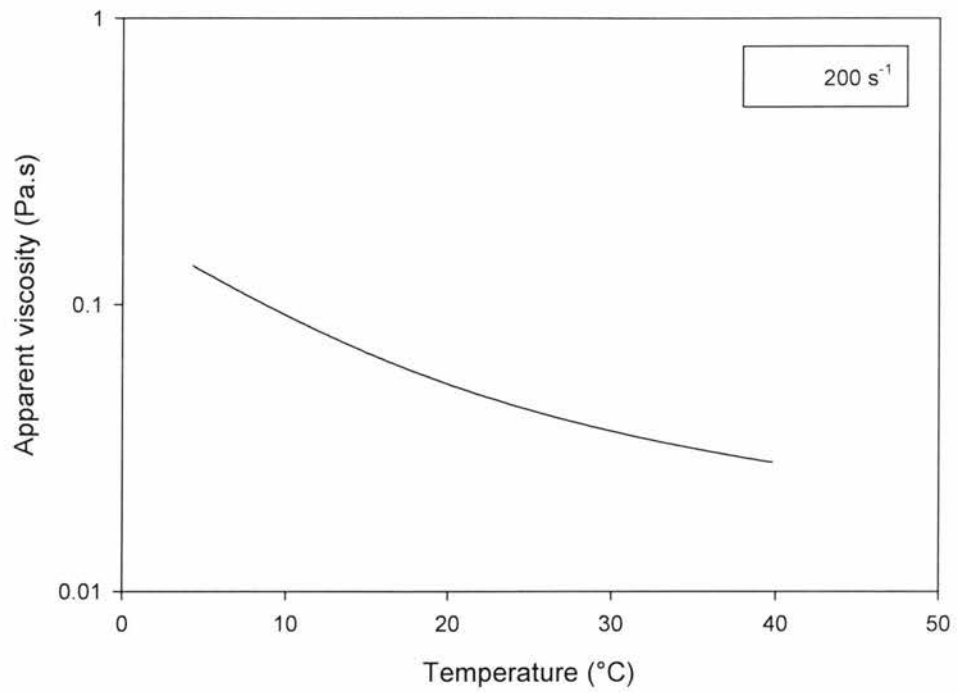


**Figure 6.1** Temperature-dependent viscosity profile of mineral oil.

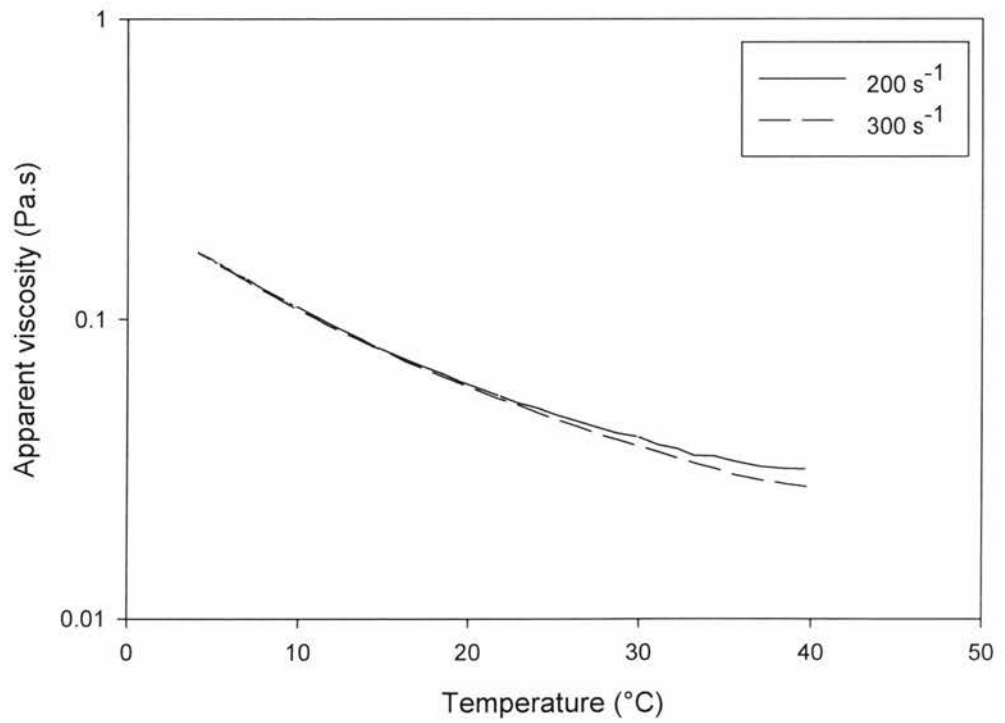


**Figure 6.2** Temperature-dependent viscosity profile of a mineral oil-PgPr (2.5% w/w) mixture.

Figure 6.3 shows the temperature dependence of the viscosity of an oil-wax (5% w/w) mixture and the model emulsion. The viscosity changed slowly with temperature above the WAT, and the waxy systems behaved as Newtonian liquids. Within the Newtonian range, the mixture followed the Arrhenius equation.

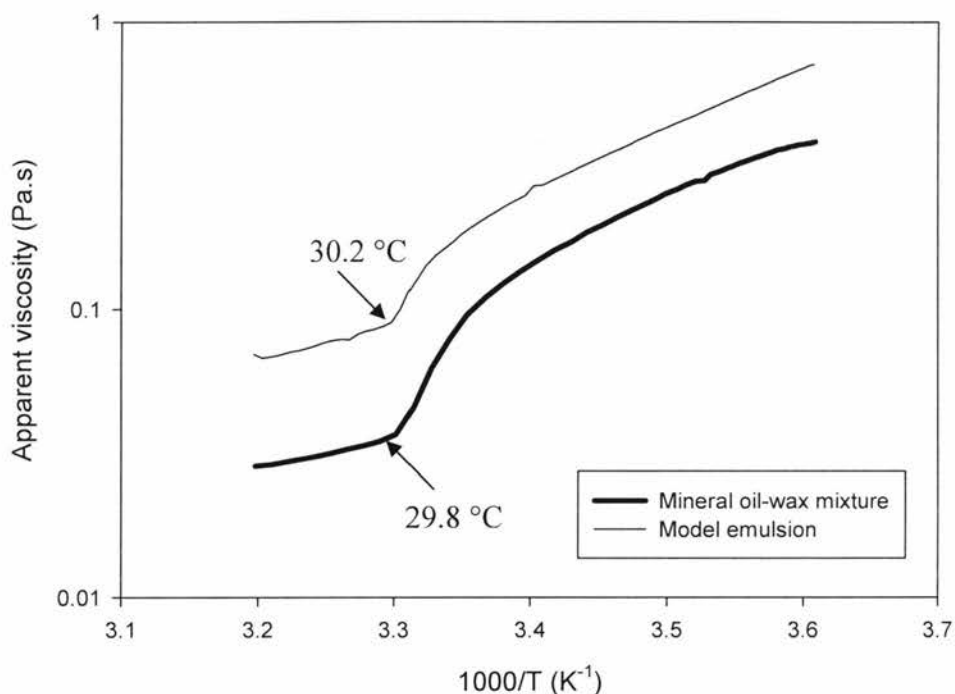


**Figure 6.3** Temperature-dependent viscosity profiles of mineral oil-wax mixture and the corresponding model emulsion consisting of mineral oil and water (4:1) and 5 % (w/w) wax.

The presence of dispersed water droplets increased the viscosity by  $\sim 2x$ . Nevertheless, the viscosities remained low at  $\sim 0.03$ - $0.06$  Pa·s. The viscous flow activation energy ( $E_a$ ) for mineral oil-wax mixture and model emulsion were estimated from the slope of the linear portion of the curve and were  $1.9 \pm 0.2$  and  $2.2 \pm 0.5$  kJ/mol, respectively. These were in good agreement with others

(Ronningsen *et al.*, 1991 and Kane *et al.*, 2004), who reported that the activation energy for oil-wax (10% w/w) samples was  $\sim 2$  kJ/mol.

The WAT for these measurements was defined as the temperature where there was deviation from an Arrhenius response, and a marked increase in the viscosity occurs as wax crystals start to precipitate. The WAT values for the oil-wax mixture and the model emulsion using different techniques are shown in Table 6.2. The WAT found for the oil-wax mixture and the model emulsion using DSC was slightly higher ( $\sim 2$  °C) than with rheometry (viscometry and oscillatory). This was due to the differences in testing conditions, as there was no shear applied during the DSC measurement unlike the rheometry measurements, where a shear rate of  $200 \text{ s}^{-1}$  was applied.

**Table 6.2** Wax appearance temperatures (WAT) using rheometry (viscometry and oscillatory) and DSC.

Sample	Viscometry (°C)	Oscillatory (°C)	DSC (°C)
Oil-wax mixture	29.8±0.5	29.9±0.7	31.6±1.1
Model Emulsion	30.2±0.4	30.3±0.6	32.1±0.8

Also investigated was whether the water droplet size changed due to the application of shear. To see the effect of shear rate ( $200 \text{ s}^{-1}$ ,  $\sim 5$  min) on the water droplets, droplet size distribution (DSD) measurements were conducted at 25 °C (below the WAT) and were compared with the initial DSD at 40 °C (Figure 6.4). There was a slight increase in the 97.5% droplet size ( $p < 0.05$ ) but no significant ( $p > 0.05$ ) increase in the  $d_{33}$  value, which suggested that the emulsion was stable even after the application of shear.

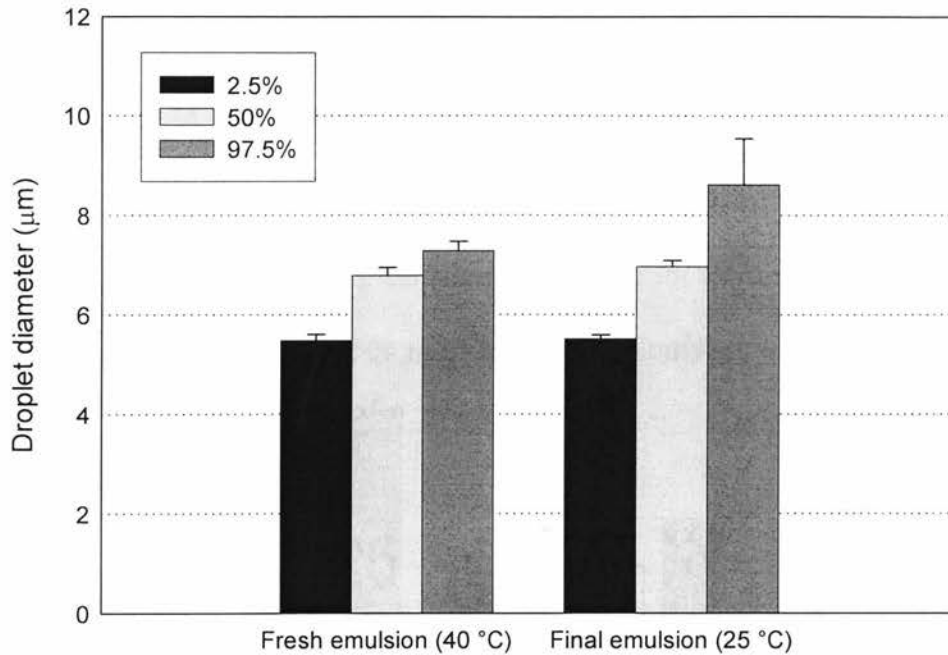


**Figure 6.4** Water DSD of the fresh and final emulsions after the application of shear rate of  $200 \text{ s}^{-1}$ .

### 6.3.2 Flow Behaviour of Model Crude Oil Emulsions in a Lab-scale Flowloop

This section outlines the measurements performed to predict the changes in rheological behaviour of the model crude oil emulsions as a function of three different flowloop lengths (0, 5, and 10m). Emulsions collected from 0, 5, and 10m flowloop sections were measured for their viscosities as a function of temperature. The initial temperatures were 40, 14 and 10 °C (Table 6.1) and the final temperature was 4 °C. Cooling was performed at 1 °C/min.

#### 6.3.2.1 Steady State Rheological Behaviour

Figure 6.5 shows the viscosity profiles of the model W/O emulsions passed through different flowloop lengths as a function of temperature, at a 200

$\text{s}^{-1}$  shear rate. With a decrease in temperature, there was an increase in emulsion viscosity as a result of wax crystallization.

For the fresh emulsions (no flowloop), there was a sharp increase in the viscosity near 30 °C, corresponding to the paraffin wax WAT. The viscosity profiles for all of the emulsions mimicked each other, with the final viscosities for the emulsions cooled from 40 to 4 °C, 14 to 4 °C and 10 to 4 °C being very close.

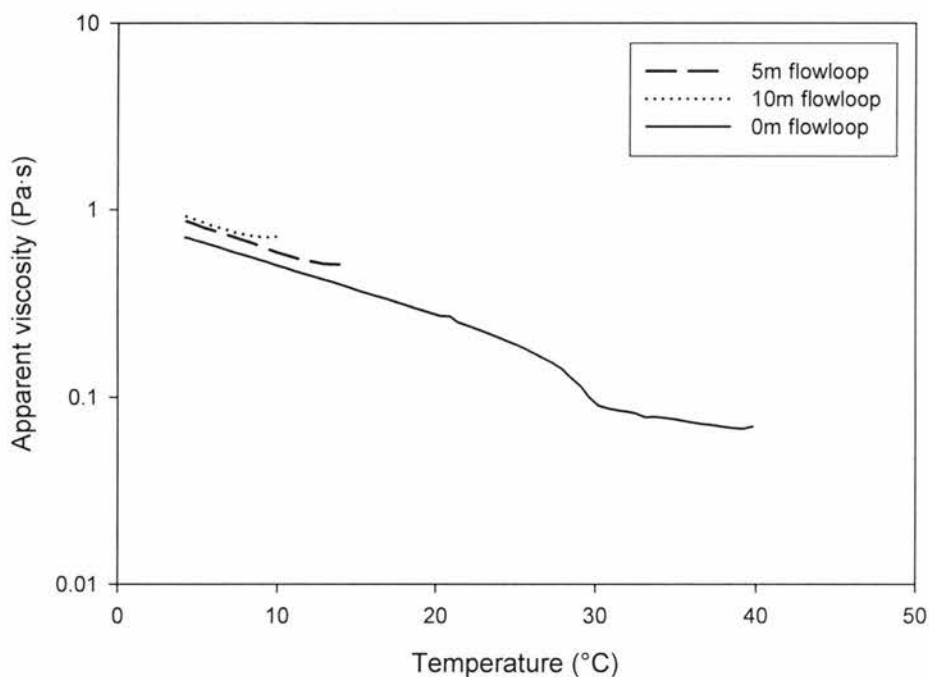


**Figure 6.5** Viscosity profiles of emulsions as a function of temperature (shear rate =  $200 \text{ s}^{-1}$ , rate of cooling =  $1 \text{ °C/min}$ ). Error bars omitted for clarity.

Figure 6.6 shows the droplet size distribution of the fresh model emulsion and its evolution following passage through the 5 and 10m flowloops. The average water droplet size ( $d_{33}$ ) found for the emulsions were  $\sim 7 \mu\text{m}$ . There was no significant difference ( $p > 0.05$ ) found in the  $d_{33}$  of the dispersed water

droplets after passage through the 5 and 10m loops. This also indicates that there no coalescence took place even at a high shear rates ( $\sim 700 \text{ s}^{-1}$ ), as encountered in the flowloop.

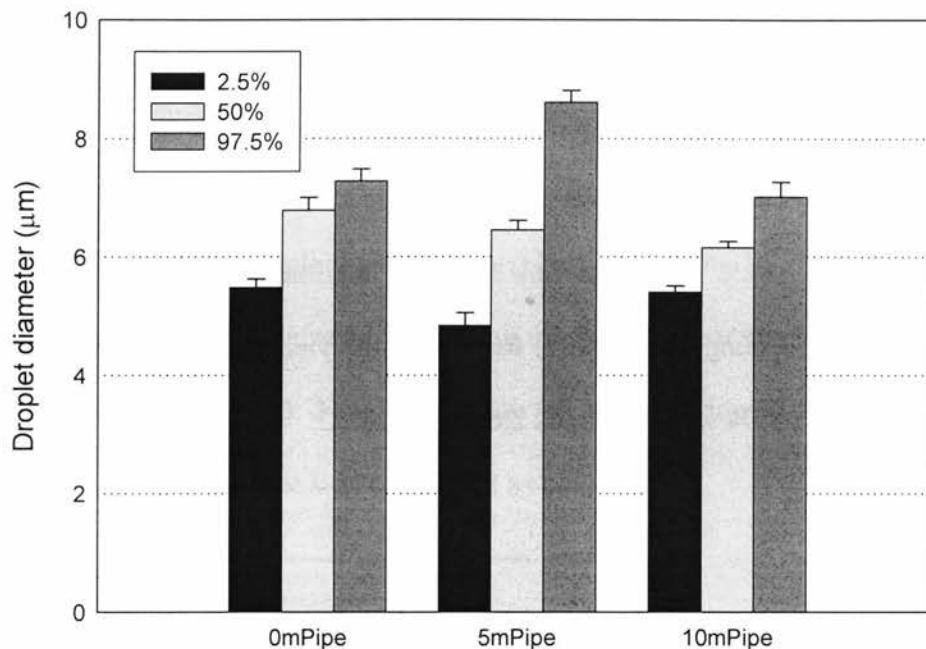


**Figure 6.6** Droplet size distribution of the emulsions' dispersed phase when passed through different lengths of the flowloop.

The effect of transit through the flowloop on the emulsions' yield stress was investigated. Yield stress is often defined as the upper limit of shear stress before flow occurs (Wardhaugh and Boger, 1991; Ronningsen, 1992). Figure 6.7 shows the yield stress of the emulsions passed through different flowloop lengths using the shear sweep method. A vane V19 geometry was used, which is recommended for yield stress measurements (Nguyen and Boger, 1985; Ronningsen, 1992), as it eliminates slippage and sample damage upon loading (Wardhaugh and Boger, 1987).

The yield stress measurements were conducted at 40, 14 and 10 °C for the emulsions flowed through the 0, 5, and 10m loops. There was no yield stress for the 0m emulsions as the measuring temperature (40 °C) was higher than the WAT (30.2 °C). The apparent viscosity of the emulsions increased with an increase in shear, up to a critical stress. Thereafter, there was a decrease in viscosity with shear. That critical stress was taken as the yield stress of the emulsions (Davenport and Somper, 1971; Nguyen and Boger, 1992). The yield stress found for 5m and 10m sections was 0.8 Pa and 1.3 Pa, respectively. Cheng *et al.* (2007) found that the yield stress of a model crude oil (containing ~9% w/w wax) was 2.68 Pa at 28 °C.

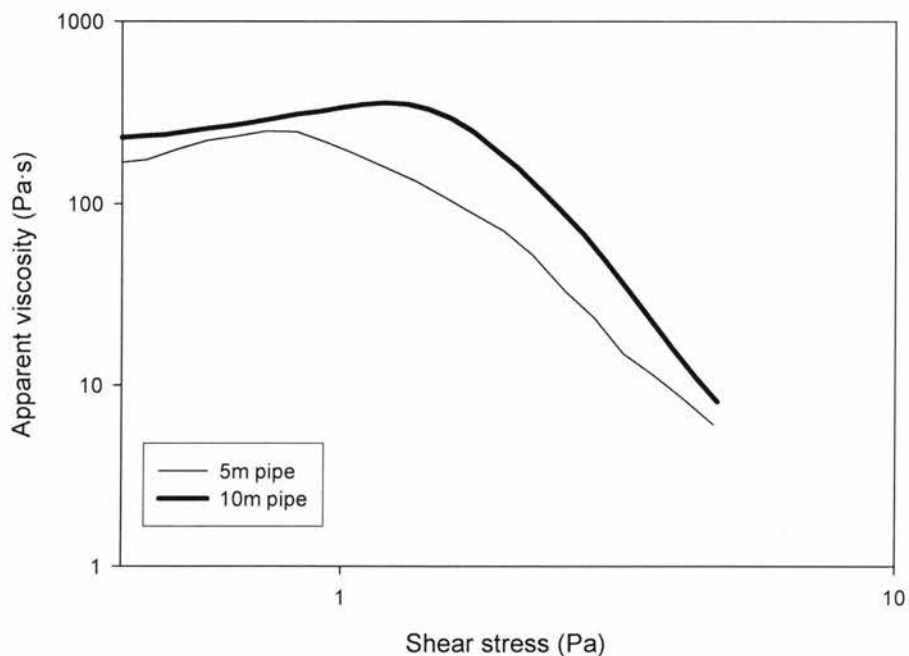


**Figure 6.7** Yield stress determination of emulsions flowed through different flowloop lengths using a shear sweep method (0.5-8 Pa).

However, the yield stress reported by Visintin *et al.* (2008) for model crude oil emulsions (20% w/w water, 9% w/w wax) was ~80 Pa at 5 °C. It was

also shown that the yield stress for model emulsions increased with water content (%).

An alternative technique, creep recovery, was used to verify the yield stress values obtained through shear sweep method. The creep compliance is defined as the measure of a sample's ability to resist an applied shear stress. A high creep compliance indicates a low resistance towards shear stress. Similarly, the recoverable compliance is a measure of the energy not lost as viscous heat during the time of an applied shear stress (Chen *et al.*, 2007). The creep compliance ( $J_c$ ) was obtained by applying a constant shear stress to the samples for a constant time (60s). The deformation ( $g$ ) as a function of time was studied and the creep compliance was calculated as below:

$$J_c(t) = g(t) / \sigma \quad 6.5$$

where  $\sigma$  = shear stress applied. During recovery, the stress was released and the sample's recoverable compliance ( $J_r$ ) was measured for 120s. The recoverable compliance was calculated as:

$$J_r(t) = g_r(t) / \sigma \quad 6.6$$

The creep recovery curves for the emulsions after transit through the 5 and 10m sections are shown in Figures 6.8 and 6.9, respectively. The measurements were carried out by applying a constant stress in the range of 0.1 to 3 Pa.

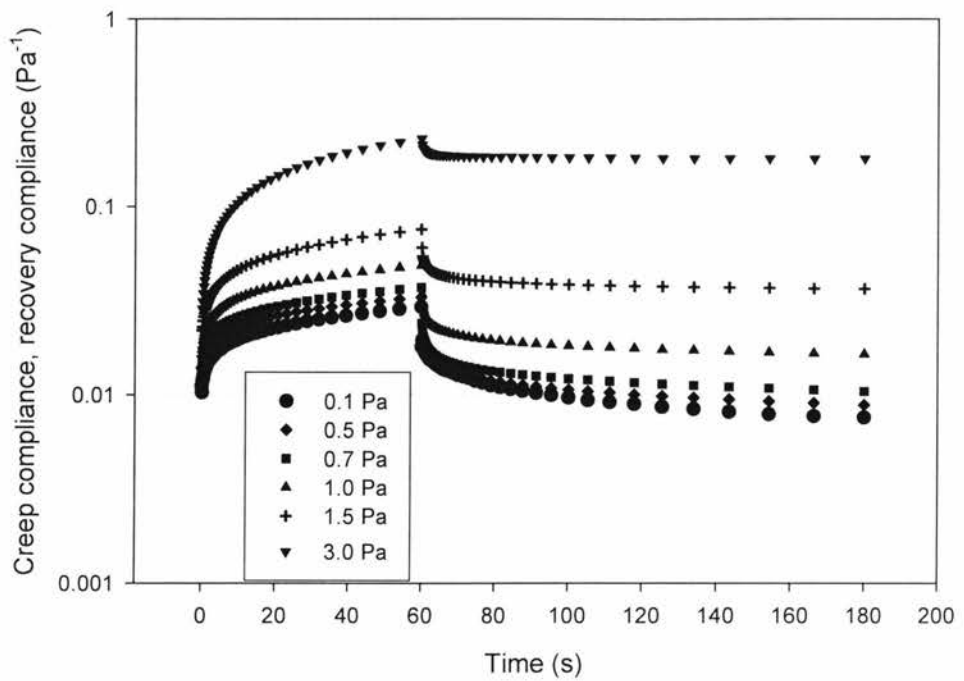


**Figure 6.8** Creep recovery tests for 5m loop-flowed emulsions. Error bars omitted for clarity.

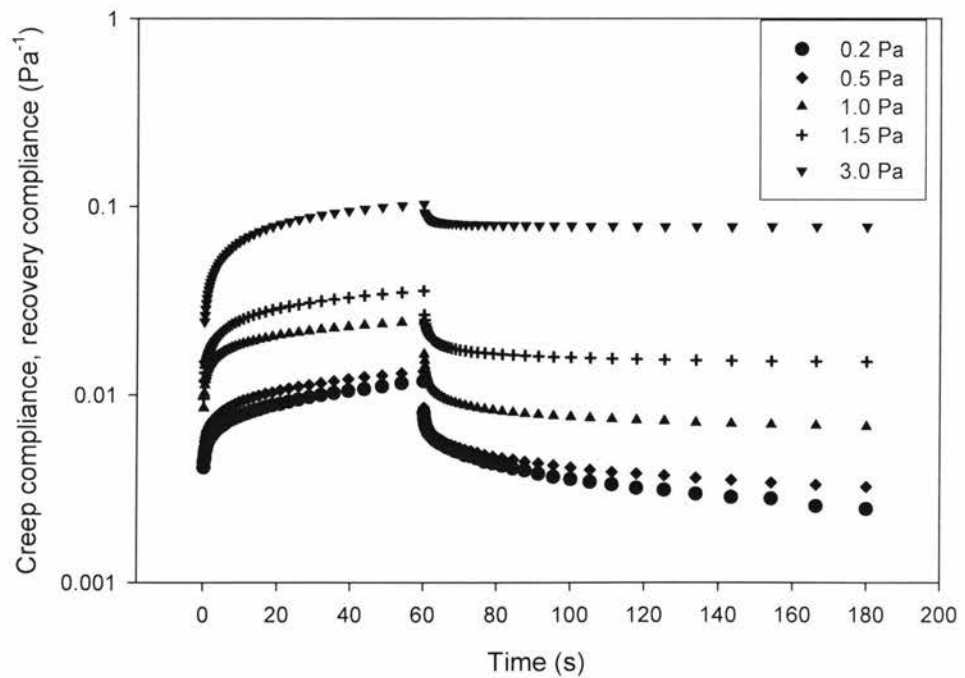


**Figure 6.9** Creep recovery tests for 10m loop-flowed emulsions. Error bars omitted for clarity.

Viscoelastic response at up to a critical stress value (0.7 Pa and 1.0 Pa for emulsions after transit through 5m and 10m pipe, respectively) led to a complete strain recovery, which indicates that these applied stress were below the elastic limit and that the samples responded as elastic solids, with no irreversible deformation. At stresses larger than that critical stress, a significant increase in the strain was observed as the linear viscoelastic regime was exceeded, which indicated breakdown of the wax crystals and/or water droplets in the model emulsions. This critical stress was taken as the yield stress of the materials (Chang and Boger, 1998). Hence, these results show that the yield stress value for the emulsion passed through 5m of loop was ~0.7-1.0 Pa and ~1.0-1.5 Pa. when passed through the 10m loop. The yield stress found using shear sweep and creep recovery methods were comparable with each other.

Steady-state flow curves evaluated for the emulsions having passed through different loop lengths were examined with the Herschel–Bulkley model:

$$\sigma = \sigma_{\text{HB}} + K\dot{\gamma}^n \quad 6.7$$

where  $n$  is a shear rate index,  $K$  is a consistency factor and  $\sigma_{\text{HB}}$  is the yield stress. The symbols in Figure 6.10 are the experimental data while the continuous lines represent the fit with the Herschel–Bulkley model:

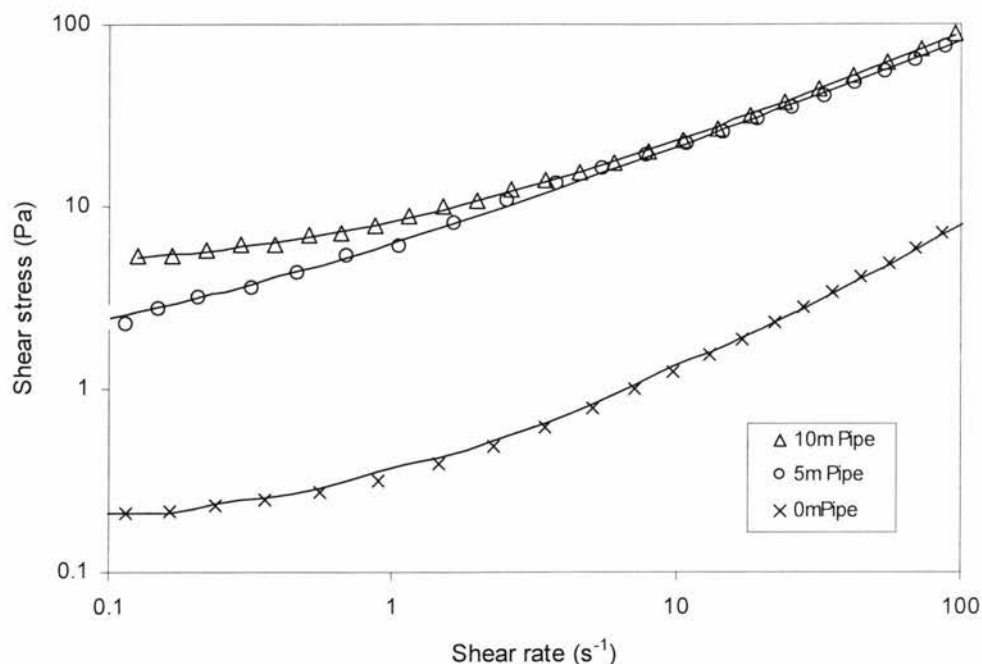


**Figure 6.10** Steady-state flow curves for the emulsions passed through different lengths of flowloop (symbols). The corresponding lines are the Herschel–Bulkley model fit.

The parameters in Equation 6.7 were calculated from the model fit using Polymath software v6.1 (Table 6.3). The yield stress values obtained from the Herschel-Bulkley model were in good agreement with that obtained using the steady-shear sweep method (Figure 6.7).

**Table 6.3** Herschel-Bulkley model parameters for model emulsions

Emulsion	Herschel–Bulkley model parameters			Yield stress [steady stress sweep (Pa)]
	Yield stress (Pa)	$K$	$n$	
0m	0.001	0.144	0.868	0
5m	0.75	4.140	0.648	0.8
10m	1.41	5.15	0.594	1.3

What was the factor that contributed to the change in the yield stress of these emulsions? This was likely related to the amount of wax crystallized

within the emulsions, which was more extensive at lower temperatures (Venkatesan *et al.*, 2005; Visintin *et al.*, 2005). In order to verify this, the solid wax content (SWC) of both emulsions at their outlet temperatures was measured using PFG-NMR. The emulsions' SWCs (Table 6.4) were ~2.1% and ~3.15% (w/w) following transit through the 5 and 10m loop sections, respectively. The amount of wax present in the model emulsions likely led to the observed changes in yield stress.

**Table 6.4** Solid wax content data for emulsions following transit through 5m and 10m loops.

Emulsion	Wax (% w/w)	Yield stress (Pa)
5m	2.10±0.15	0.8±0.01
10m	3.15±0.12	1.3±0.07

### 6.3.2.2 Dynamic Rheological Behaviour

The viscous and elastic responses of viscoelastic systems can be quantified by undertaking dynamic oscillatory measurements. The basis of these measurements is the application of a sinusoidal strain of frequency ( $\omega$ ) to the sample and the measurement of the corresponding stress (Torres *et al.*, 2007). For viscoelastic systems, the stress and strain are out of phase with each other. The phase angle shift ( $\delta$ ) can be measured as the time shift ( $\Delta t$ ) between the amplitudes of the oscillating stress ( $\tau_0$ ) and strain ( $\gamma_0$ ):

$$\delta = \omega \Delta t \quad 6.8$$

From the amplitudes and the phase angle, various viscoelastic parameters may be obtained. These include the complex modulus ( $G^*$ ), the elastic ( $G'$ ) and

viscous components ( $G''$ ) of the complex modulus and  $\tan \delta$ . The complex modulus ( $G^*$ ) is defined as the ratio of the maximum stress  $\tau_o$  and the maximum strain  $\gamma_o$ :

$$G^*(\omega) = \tau_o / \gamma_o \quad 6.9$$

$G^*$  is constant for a given radial frequency,  $\omega$ . The storage and loss moduli are derived from the phase angle and complex modulus:

$$G'(\omega) = G^*(\omega) \cos(\delta) \quad 6.10$$

$$G''(\omega) = G^*(\omega) \sin(\delta) \quad 6.11$$

where  $G'$  is the measure of the energy stored in the material per cycle, whereas  $G''$  is a measure of the energy dissipated as heat (and therefore lost) per cycle.

To obtain these parameters, a preliminary series of measurements were undertaken to identify the linear viscoelastic region (LVR). From this region, constant strain amplitude was selected for a subsequent series of measurements in which the stress amplitude was obtained as a function of changing oscillatory frequency. These data were then subsequently used to obtain the  $G'$  and  $G''$  values of the systems.

The measurements were carried out using Mooney cell geometry (CP 25) with a frequency of 1 Hz. The  $G'$  of the model emulsions was plotted against shear strain (Figure 6.11), which was varied from 0.001 to 1. The  $G'$  values remained constant until the strain induced breakdown of wax crystal network or perhaps deformed the water droplets. For 5m flowed emulsion, the critical strain (onset of decrease in  $G'$ ) was 0.005 and for the 10m flowed emulsion, it was 0.01. The constant  $G'$  regions (LVR) were used to non-

destructively investigate the viscoelasticity of the emulsions as a function of frequency (Tadros, 1990; 1994).

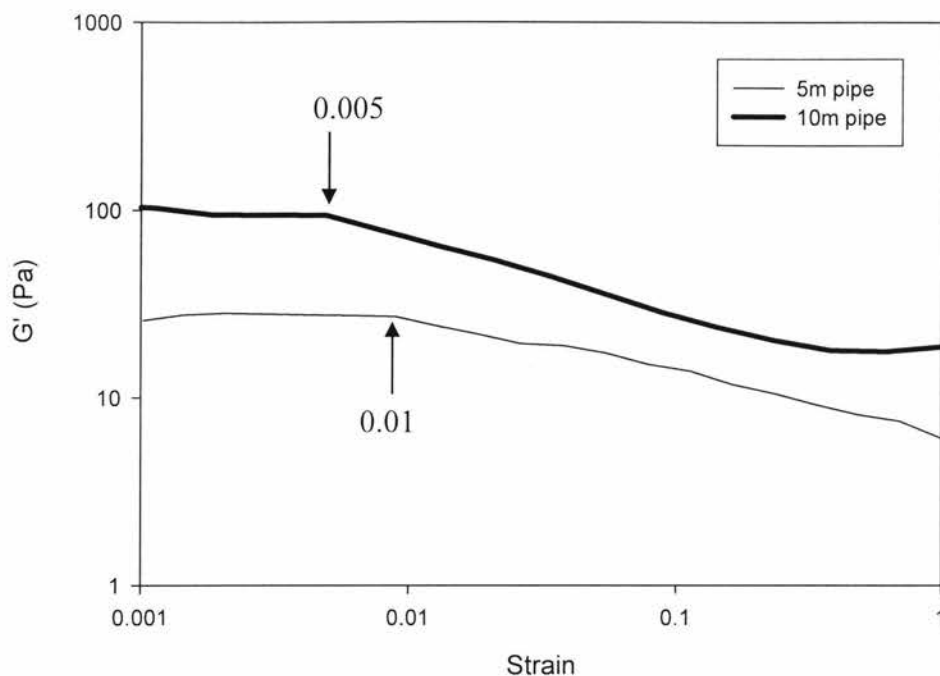


**Figure 6.11** Linear viscoelastic regions of the emulsions flowed through 5m and 10m flowloop ( $f=1$  Hz)

Frequency sweep measurements were performed in the LVR at a constant strain of 0.005 (Figure 6.12). The measuring temperatures were the same as the outlet temperature of emulsions *i.e.*, 14 °C for 5m and 10 °C for 10m emulsions, respectively. The emulsions passed through the 5m loop displayed elastic behaviour below  $\sim 4$  Hz, after which viscous behaviour was observed. Conversely, the emulsions passed through the 10m loop displayed an elastic response below  $\sim 4.9$  Hz. The crossover point ( $G'=G''$ , which shows the transition of a fluid from solid-like to liquid-like behaviour or vice-versa) shifted to a higher frequency with a decrease in temperature (from 14 °C to 10

°C). This was expected as per chapter 4, a more defined crystal network was expected at lower temperatures.

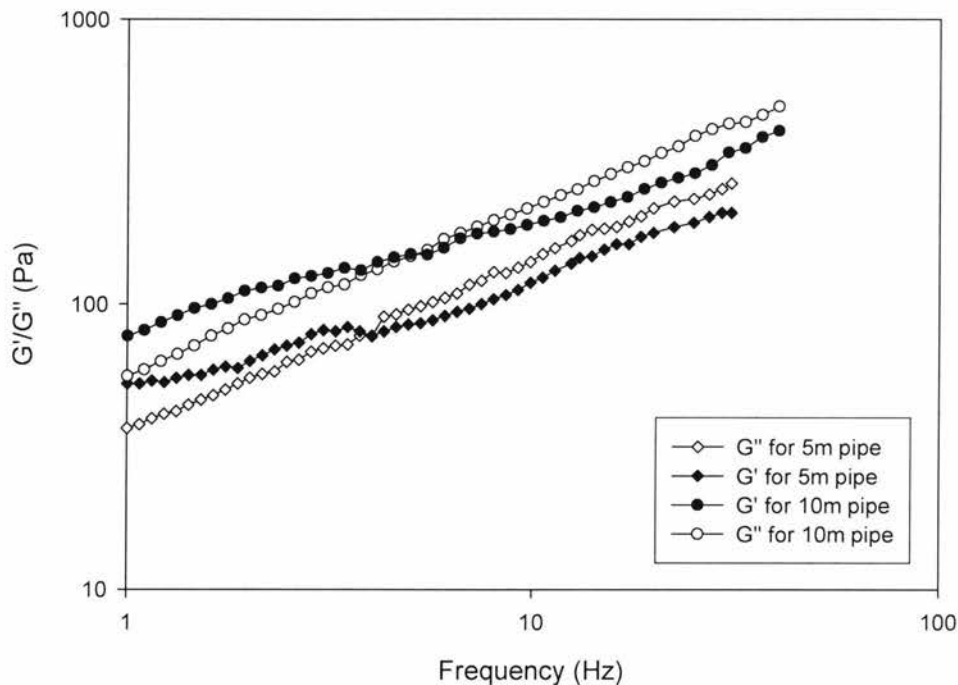


**Figure 6.12** Frequency sweep of emulsions (strain = 0.005). Error bars omitted for clarity.

To view changes in the strength of model emulsions with temperature, dynamic temperature sweeps for both emulsions were conducted. The measurements were conducted at a strain of 0.005 and at a frequency of 1 Hz. The emulsions showed an elastic response under shear stress, showing network development with decreasing temperature. In Figure 6.13, solid-like behaviour was observed for the emulsions in the temperature range of 14 °C to 4 °C, showing strengthening of the wax crystal network with decreasing temperature.

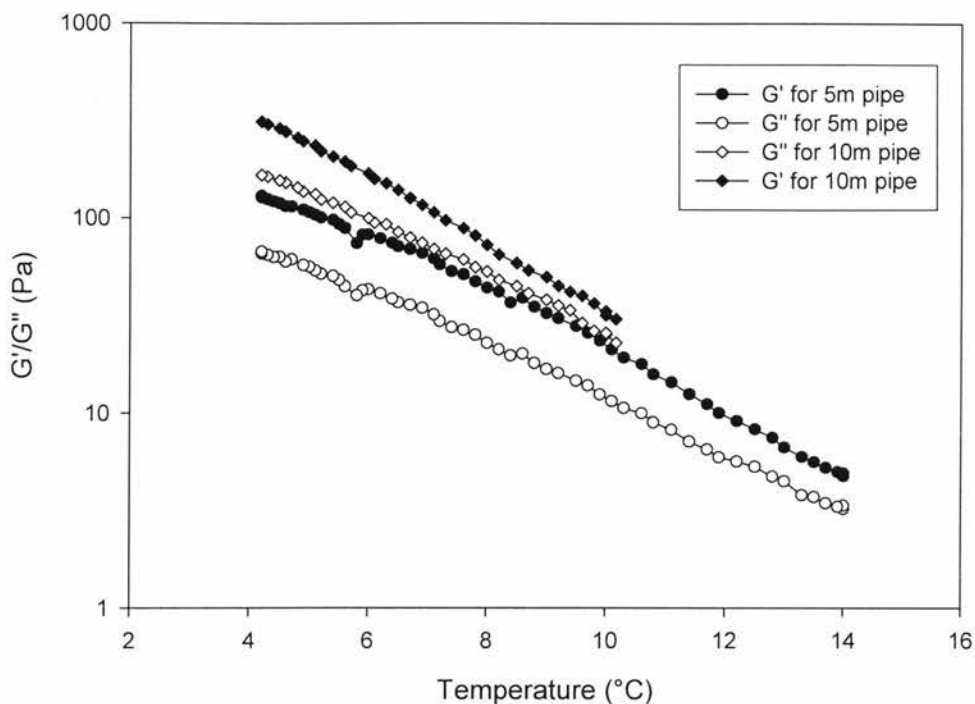


**Figure 6.13** Dynamic temperature sweep of emulsions (strain = 0.005,  $f = 1$  Hz). Error bars omitted for clarity.

The phase angle ( $\delta$ ) can also provide information on the viscoelastic response of an emulsion. In fully elastic networks,  $\delta \sim 0^\circ$ , whereas in purely viscous liquids,  $\delta \sim 90^\circ$  (Chen *et al.*, 2007). For viscoelastic systems,  $\delta$  lies between these values. The closer  $\delta$  is to  $0^\circ$ , the more the emulsion will display an elastic response under shear stress, implying a more developed (or stronger) colloidal network (Chen *et al.*, 2007).

Figure 6.14 shows the change in  $\delta$  with temperature for the 5m and 10m loop flowed model emulsions. The values of  $\delta$  was  $< 30^\circ$  across the entire temperature range, indicating that both the model emulsions demonstrated an elastic response. The model emulsions showed more solid-like behaviour as the

temperature decreased, showing an increase in the strength of wax crystal network.

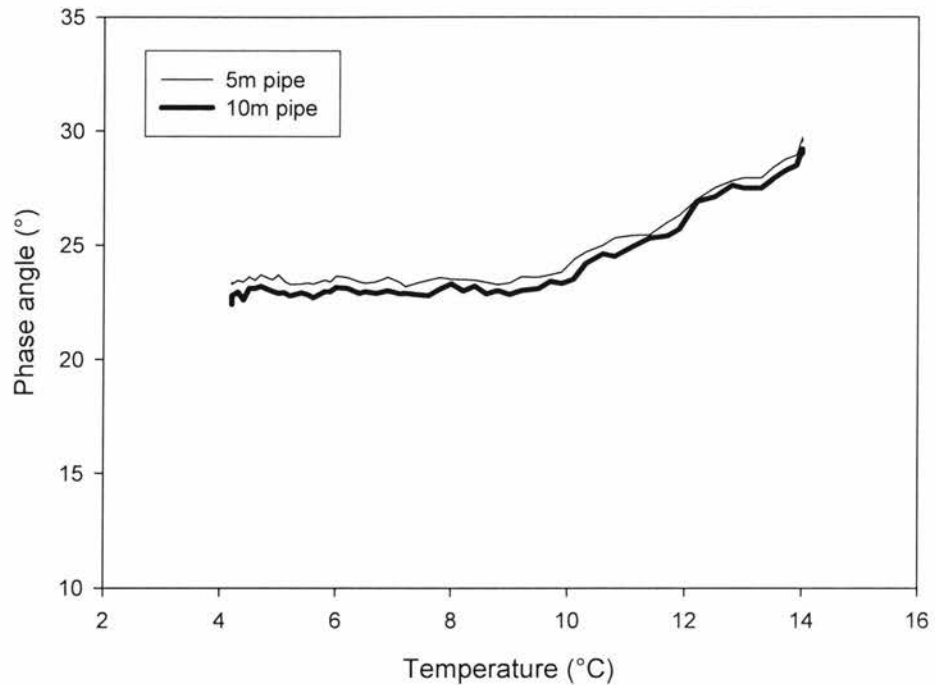


**Figure 6.14** Variation of phase angle with temperature (strain = 0.005,  $f=1\text{Hz}$ )

## 6.4 Conclusions

The results from this chapter met the third objective (section 1.3). Viscosity profiles of the oil-water-wax systems gave insight into the changes in rheological behaviour with the addition of each component to the model system. With the addition of wax to oil phase, the behaviour became non-Newtonian and an increase in viscosity was observed. The presence of water droplets further increased viscosity. Slight differences in the rheological behaviour for model emulsions subjected to different temperature/shear histories.

# Chapter 7

## Yielding and Gelling of Model Crude Oil Emulsions

### 7.1 Introduction

The presence of wax and wax-like species in crude oil imparts complex non-Newtonian fluid flow to the oil, and significant operational problems such as wall deposition and potentially blocked lines (Gill and Russell, 1954; Perkins and Turner, 1971; Uhde and Kopp, 1971; Herring, 1974; Sifferman, 1979; Irani and Zajac, 1982; Wardhaugh and Boger, 1987). The presence of congealed crude oil with a yield stress directly impacts the start-up and restart operations of oil transport through pipelines.

The yield stress concept was first introduced by Bingham and Green (1919) for a class of fluids known as viscoplastic fluids. Many equations have been proposed to describe the relationship between shear stress and shear rate for different viscoplastic materials (Nguyen and Boger, 1983, 1992). In all models, the yield stress was simply defined as the minimum stress required to produce a shear flow, with the material considered solid-like when the applied stress was lower than the yield stress. Thus, the yield stress was thought to be a transition between elastic solid-like and viscous liquid-like behaviour. The difference between the end of elastic behaviour and the start of viscous

behaviour was first described in 1958 by Houwink, who distinguished between elastic behaviour, plastic behaviour and viscous flow (Houwink, 1958).

The early measurements of a yield point for waxy fuel and crude oils were performed with capillaries or large pipelines (Gill and Russell, 1954; Davenport and Russell, 1960; Davenport and Somper, 1971; Knegtel and Zeilinga, 1971; Verschuur *et al.*, 1971; Nguyen and Boger, 1985; Ronningsen, 1992). Both capillary and model pipeline techniques have now been rejected due to uncertainties arising from the known effects of stress concentration, compressibility of the flowloop and the oil, diffusion of the wax-free oil, and contraction of the oil (Gill and Russell, 1954; Davenport and Russell, 1960; Davenport and Somper, 1971; Perkins and Turner, 1971; Verschuur *et al.*, 1971; Wardhaugh and Boger, 1991). Rotational viscometers with concentric cylinder, parallel plates, cone and plate, or vane have also been used to study the yielding of waxy crude oils (Davenport and Somper, 1971; Perkins and Turner, 1971; Sifferman, 1979; Keentok, 1982; Titkova and Yanovsky, 1988; Wardhaugh and Boger, 1991; Ronningsen, 1992). However, no standard test for determining the yielding of waxy crude oils has been adopted by the petroleum industry because of the very poor repeatability in any given instrument and the poor reproducibility between the various tests.

One of the reasons for poor repeatability and reproducibility is that yield values, along with all other rheological properties of waxy crude oils, strongly depend not only on what the sample is experiencing, *i.e.*, temperature and shear rate, but also on what the sample has experienced, *i.e.*, thermal and shear

history. Even small variations in any of the test conditions or history can cause a marked difference in the results. Another important reason for the poor repeatability is that there are various confusing definitions of the yield stress due to a lack of understanding of what yielding actually is. In addition, the usual instrumental effects such as wall slip, instrument inertia, the damping characteristics of the rotation body, and sensitivity to external disturbances have also been identified as possible sources for poor repeatability (Wardhaugh and Boger, 1991; Nguyen and Boger, 1992).

Because a gelled oil may display yield behaviour, significant pressure must be applied to re-start flow; in many operational scenarios, the pipeline may not be able to withstand this pressure. Thus, predicting the conditions for oil gelation and the pressure required to re-start flow are also important in the design of offshore/artic field developments (Chang *et al.*, 1999). Crude oil gelation is associated with phase separation of the wax component, and may take place when as little as 1-2% of wax solids have formed (Ronningsen and Bjorndal 1991, Kane *et al.*, 2003).

How the process of wax crystallization leads to oil gelation and then how the modulus and yield properties of the structural network that develops are related to wax crystallization and its time, stress, and temperature history (Webber, 2001). The purpose of this chapter was to investigate the yielding and gelling behaviour of model emulsions.

## 7.2 Materials and Methods

### *Emulsion Preparation*

As per chapter 3, the model crude oil emulsions consisted of light mineral oil, ultra-pure water and PgPr. From the preliminary experiments, a concentration of 5 times CMC was used for emulsification. Refined paraffin wax (m.p.  $\sim 60$  °C) was used to stabilize the emulsion and was added molten to the oil mixture prior to emulsification.

Mixture of oil, wax (5% w/w) and PgPr (2.5% w/w) were heated to 70 °C (above wax m.p.). The mixture was then cooled down to 30 °C and pre-mixed to form a coarse emulsion. The mixture was then homogenized with a two-stage valve homogenizer (APV-1000, APV, Concord, ON, Canada). The pressures applied were 5000 Pa and 500 Pa in the first and second stages, respectively. The outlet temperature of the emulsion was 40 °C. The emulsions were then flowed through a laboratory flowloop (Section 3.2), if required.

### *Waxy Oil Preparation*

Light mineral oil and wax (5%) were heated to 70 °C for at least 30 min to remove any crystal history.

### *Rheology*

The rheological measurements of the model crude oil emulsions and waxy oils were carried out using Bohlin C-VOR rheometer (Malvern, NJ, USA) with triple-mode motor control, which allows strain, stress, or shear rate controlled measurement to be performed. The temperature was controlled by a Peltier element with an accuracy of  $\pm 0.1$  °C. A solvent trap was used to prevent

evaporation. The samples were loaded into a Cup and Mooney geometry (25mm ID, 29mm height, stainless steel) with a hot pipette and they were temperature-equilibrated for 10 minutes before starting data collection. The reproducibility of all measurements was within 5%. More details on the measurement programs and temperatures are described in “Results and Discussion” section. Some of the micrographs were analyzed quantitatively for wax crystal and water droplet sizes using Fovea Pro 4.0, a plug-in program for Adobe Photoshop. All analyses were based on 20 micrographs of each sample.

## **7.3 Results and Discussion**

### **7.3.1 Yielding of Model Crude Oil Emulsions**

The yield stress of the model emulsions was determined and the effect of different factors (thermal and shear history and ageing) on its value was evaluated. Steady shear sweeps from 0.01 to 5 Pa were used to determine the yield stress values isothermally.

#### **7.3.1.1 Effect of Temperature**

Wax crystal network development was studied as a function of temperature. Figure 6.7 shows the yield stress of model crude oil emulsions flowed through the 5m and 10m loop sections (outlet temperatures of 14 °C and 10 °C, respectively). The yield stress of the model emulsions at 14 °C was ~0.8 Pa, which was slightly lower than that of at 10 °C (1.3 Pa).

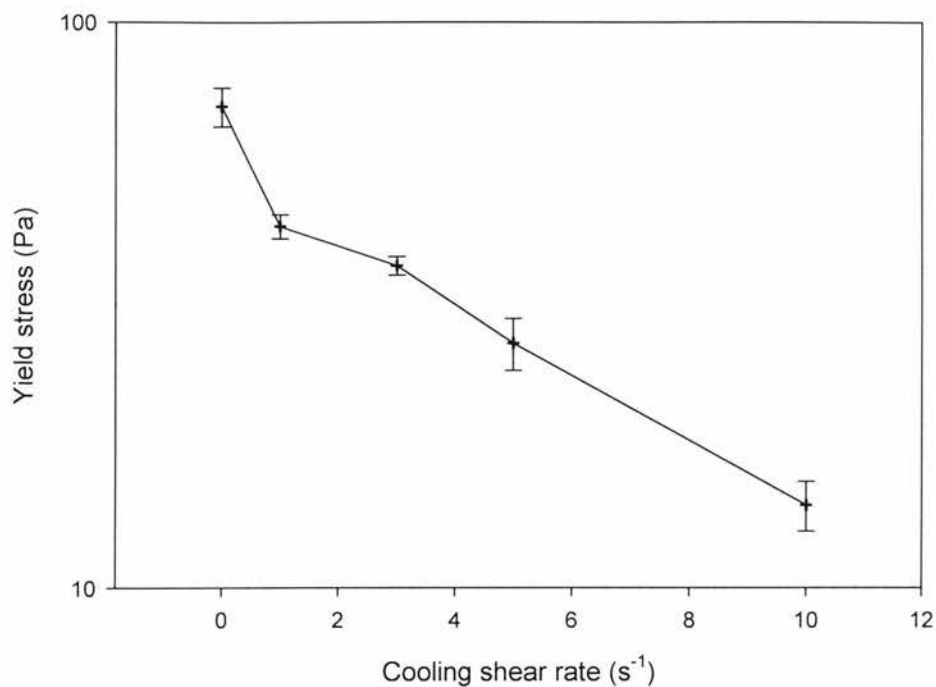
The amount of wax crystallized in the model emulsions was measured using PFG-NMR (Table 7.1). The amount of wax crystallized at 14 and 10 °C was 2.10 and 3.15% (w/w), respectively. Wax crystallization is strongly dependent on the temperature of the model emulsions and this likely caused the differences in yield stress observed.

**Table 7.1** Yield stress of model emulsions vs. wax %

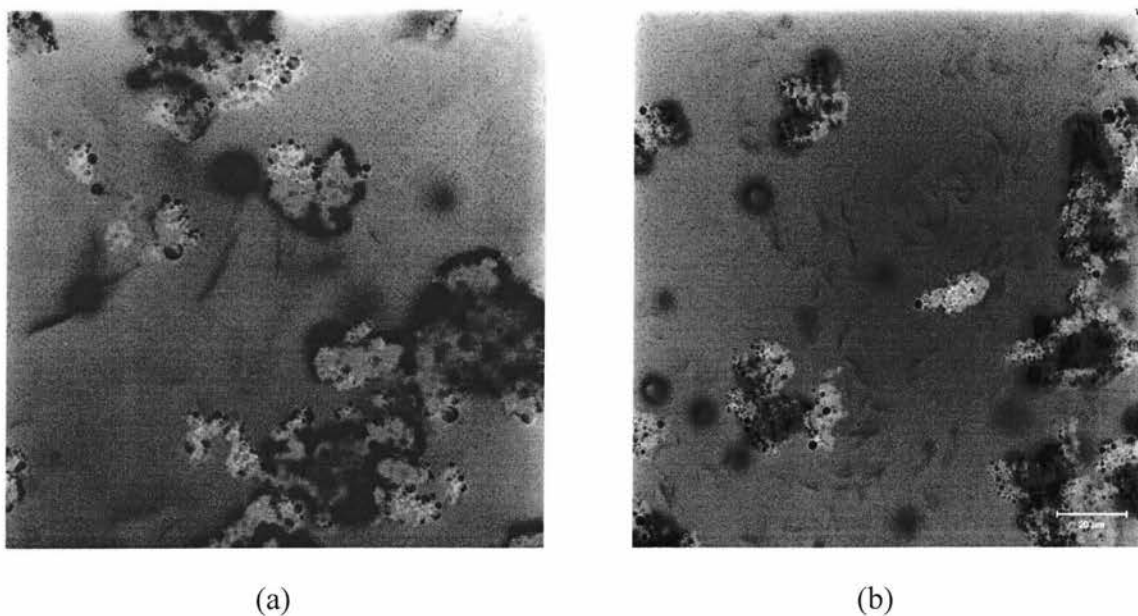
Temperature (°C)	Wax (wt%)	Yield stress (Pa)
10	3.15±0.12	1.3±0.01
14	2.10±0.15	0.8±0.07

### 7.3.1.2 Effect of Shear History

The shear conditions during cooling for wax-containing fluids will influence crystal network formation and consequently yield stress (Chen *et al.*, 2007). Here, freshly-prepared model emulsions were cooled from 40 to 4 °C under static and dynamic conditions at 1 °C/min and subsequently, the yield stress was measured at shear rates of 0 to 10 s<sup>-1</sup>. Figure 7.1 shows that the yield stress (85 Pa) obtained was highest after static cooling (0 s<sup>-1</sup>). It decreased by ~2x when a low shear rate (1 s<sup>-1</sup>) was applied (while cooling) and ~4x when the cooling shear rate was increased to 10 s<sup>-1</sup>. CLSM was employed to gain further insight into the microstructural differences observed with different shear history (Figure 7.2).



**Figure 7.1** Effect of cooling shear rates on the yield stress of an emulsion consisting of mineral oil and water (4:1) and 5 % (w/w) wax to a temperature of 4 °C.



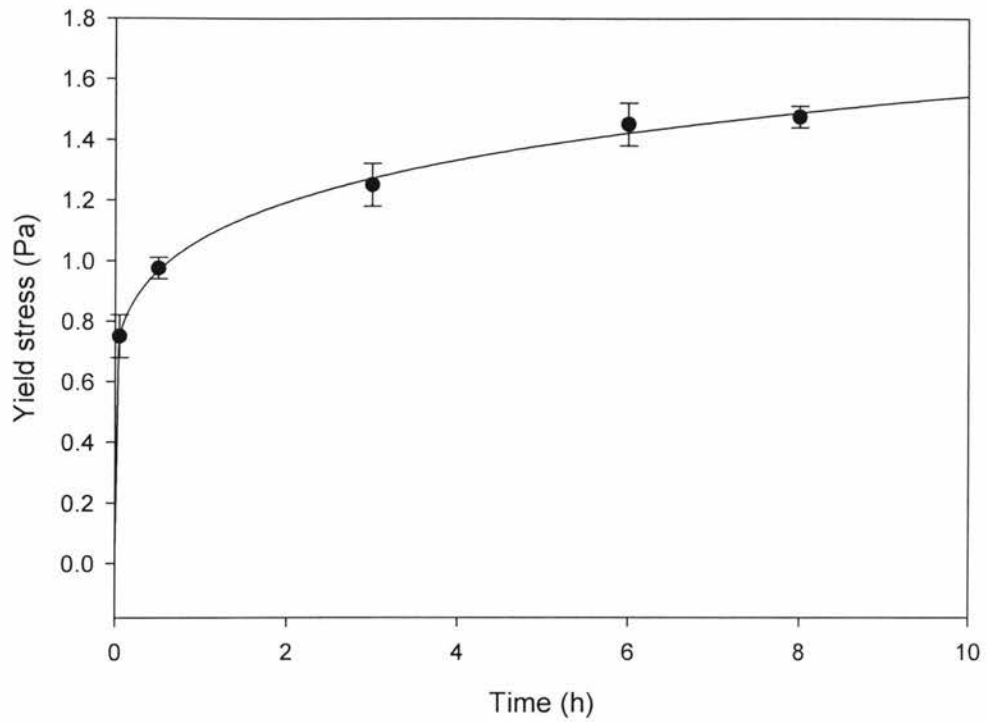
**Figure 7.2** Wax crystal microstructure of the model emulsions with different shear histories (a) 0  $s^{-1}$  (static) and (b) 10  $s^{-1}$ . The scale bars represent 20  $\mu m$ .

Figure 7.2(a) and (b) show the wax crystal microstructure (using CLSM) of model emulsions cooled statically ( $0 \text{ s}^{-1}$ ) and dynamically ( $10 \text{ s}^{-1}$ ), respectively. Wax crystals in the statically cooled samples were larger ( $\sim 18 \mu\text{m}$ ) than those observed with sheared cooling ( $\sim 5 \mu\text{m}$ ). There was no significant difference ( $p > 0.05$ ) found in the droplet sizes ( $\sim 6 \mu\text{m}$ ) of the model emulsions. However, the water droplets were collected into smaller flocs under the influence of dynamic cooling. These differences in wax crystal and water droplet floc sizes possibly influenced the crystal networking and hence the yield stress values of the emulsion.

### 7.3.1.3 Effect of Ageing

The effect of isothermal ageing time on the viscosity of the model emulsion system and on apparent yield stress was evaluated. Emulsions were stored at  $14 \text{ }^\circ\text{C}$  for 8h and their yield stress was measured at 0, 1, 3, 6 and 8h. Figure 7.3 shows the increase in yield stress as a function of age. The yield stress for the emulsion at 0h was 0.8 Pa, which increased with time and reached  $\sim 1.5 \text{ Pa}$  after 8h. The near-plateau of the curve showed that there was little increase in yield stress ( $\sim 1.4 \text{ Pa}$ ) after 6h of storage.

PLM was used to observe any changes in the wax crystal microstructure with ageing and its possible effects on the yield stress of emulsions. Figure 7.4 (a) and (b) refers to the micrographs of the model emulsion at the minimum and maximum ageing times reported above.



**Figure 7.3** Effect of ageing time on the yield stress of emulsion ( $T = 14\text{ }^{\circ}\text{C}$ )

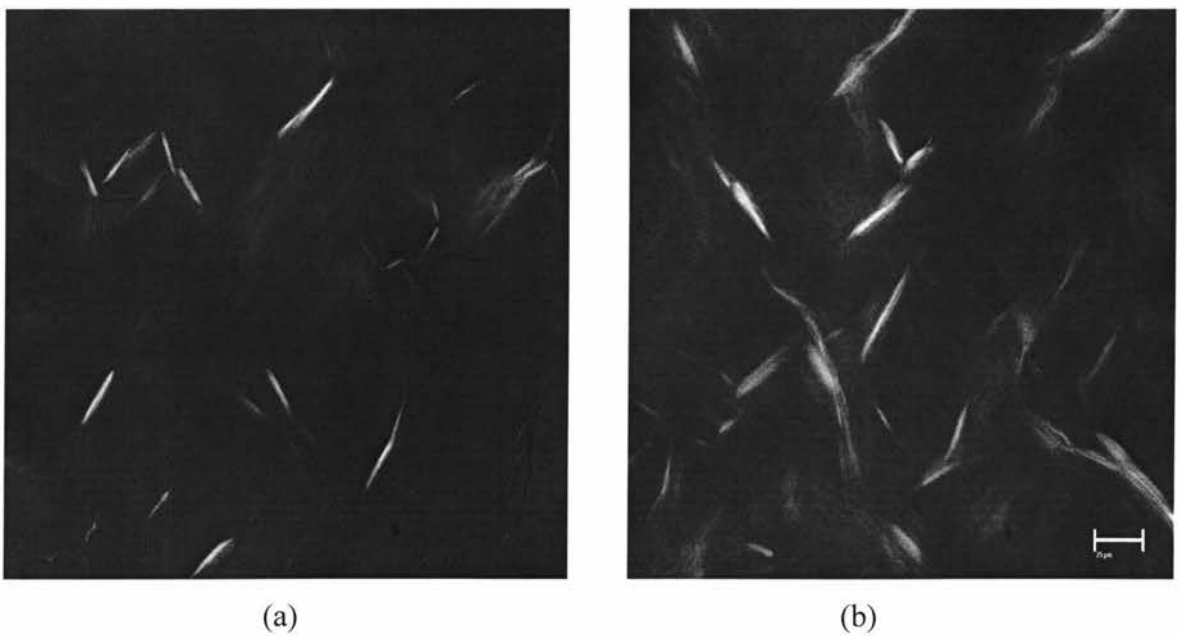


**Figure 7.4** Wax crystal evolution with ageing time (a) 0 hrs (b) 8 hrs. The size bar represents  $25\text{ }\mu\text{m}$ .

The number of wax crystals increased  $\sim 2x$  from 0h to 8h. There was also a slight increase in mean crystal length from 18 to 25  $\mu\text{m}$  over the same timeframe. Thus, it may be inferred that the evolution in wax crystal concentration and size with ageing time were responsible for the change in yield stress observed.

### **7.3.2 Gelation of Model Crude Oil Emulsions**

The gelation temperature is defined as the temperature where there is a crossover between the elastic ( $G'$ ) and viscous ( $G''$ ) moduli, and represents the transition from liquid-like to solid-like behaviour or vice-versa. This section shows the differences in gelation between the model emulsions with/without the presence of water droplets. The effects of rate of cooling and PgPr (surfactant) are also discussed in this chapter. Oscillatory measurements were performed by varying the samples from 40 to 14  $^{\circ}\text{C}$ . The geometry used was Mooney cell (CP 25). The frequency used was 1 Hz and the strain used was 0.005, which was well within the linear viscoelastic region (LVR) (Figure 6.7).

#### **7.3.2.1 Effect of Cooling Rate**

The effect of cooling rate on the gelation of waxy oil and model emulsions was determined using two different cooling rates: 0.05 and 1  $^{\circ}\text{C}/\text{min}$ . Figures 7.5 and 7.6 show the evolution in elastic and viscous moduli as a function of temperature for waxy oil and the freshly-prepared model emulsions, respectively. Both  $G'$  and  $G''$  were nearly constant above the WAT (29-30  $^{\circ}\text{C}$  for model waxy oil and emulsion, respectively). Below the WAT, both  $G'$  and  $G''$  increased with decreasing temperature.

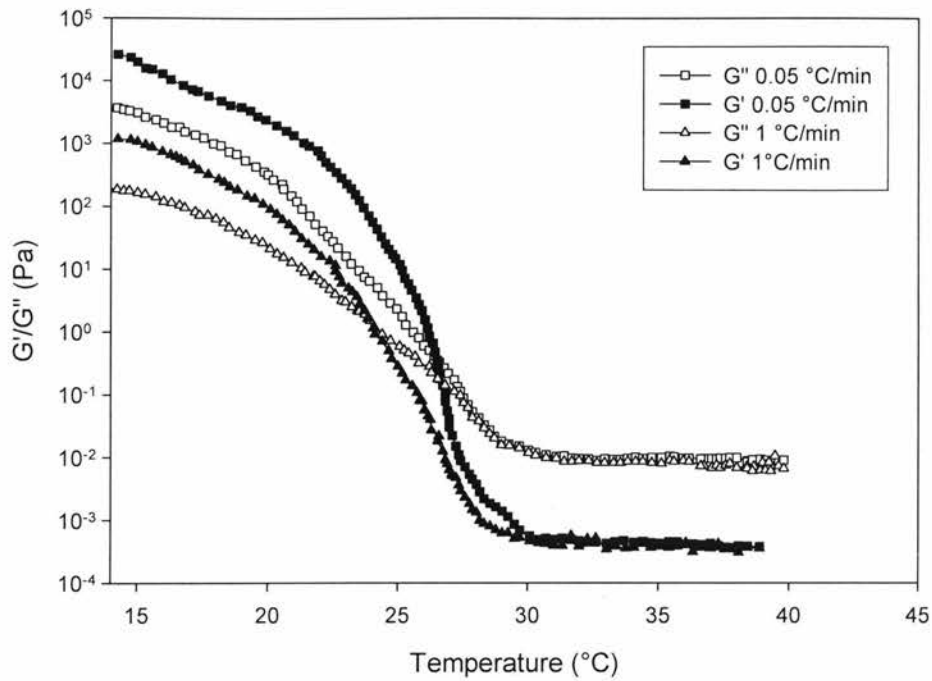


**Figure 7.5** Effect of cooling rates on the gelation of waxy oil (strain = 0.005,  $f = 1\text{ Hz}$ )

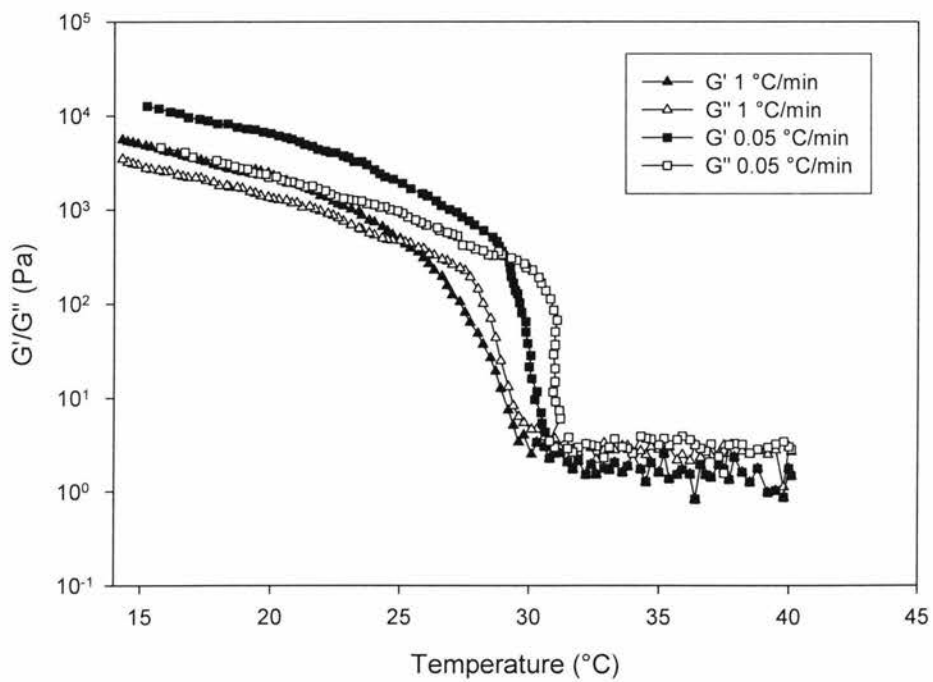


**Figure 7.6** Effect of cooling rates on the gelation of model emulsions (strain = 0.005,  $f = 1\text{ Hz}$ )

Dominant  $G'$  responses were seen at temperatures below the WAT. With the slower cooling rate,  $G'$  values were higher, which is in accordance with the results of Chang *et al.* (2000) and Visintin *et al.* (2005). Furthermore, the crossover point shifted to a higher temperature for both the waxy oil and emulsion with slower cooling rates, suggesting that the structural build-up arising from crystal formation and aggregation was favoured by longer cooling times, which likely strengthened the crystal network.

Figure 7.7 reports the isothermal change of  $G'$  and  $G''$  with time for the different cooling rates after the model emulsion (same emulsions as discussed in the last paragraph), once these had reached 14 °C.

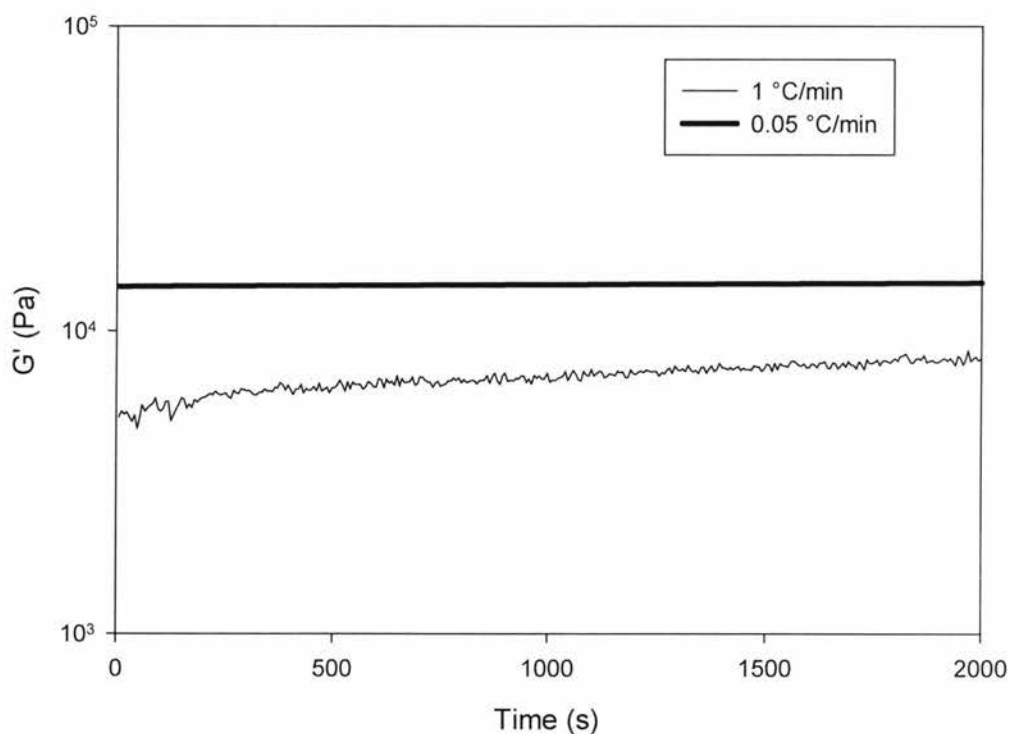


**Figure 7.7** Isothermal change in  $G'$  of emulsion with time ( $T = 14$  °C, strain = 0.005,  $f = 1$  Hz)

Cooling had a great effect on the  $G'$  of the model emulsions, and may have been the result of the larger crystal size observed at lower cooling rates (Rousseau and Hodge, 2005).

### 7.3.2.2 Crude Oil Emulsion vs. Waxy Oil Gelation

The gelation behaviour of the model waxy oil was compared to that of the model emulsion (Figure 7.6). Generally, there was similar behaviour observed for both the samples, whereby gelation temperature increased with a decrease in cooling rate. The gelation points for the model emulsion were slightly higher than for the model oil (Table 7.2).

**Table 7.2** Comparison of gelation points of waxy oil and model emulsion

Sample	0.05 °C/min	1 °C/min
Model emulsion	28.9 °C ± 0.9	25 °C ± 0.8
Model oil	26.5 °C ± 0.6	24.1 °C ± 0.9

### 7.3.2.3 Effect of PgPr

The gelation temperature of the model waxy oil and mineral oil-2.5% (w/w) PgPr mixture was determined at a cooling rate of 1 °C/min. The crossover points found for model oil with and without PgPr were 24.3 and 24.1 °C, respectively (Figure 7.8), showing that PgPr had no effect on the gelation behaviour of model systems ( $p > 0.05$ ). The strength of the model emulsions was higher than the model waxy oil (without PgPr) due to the presence of water droplets.

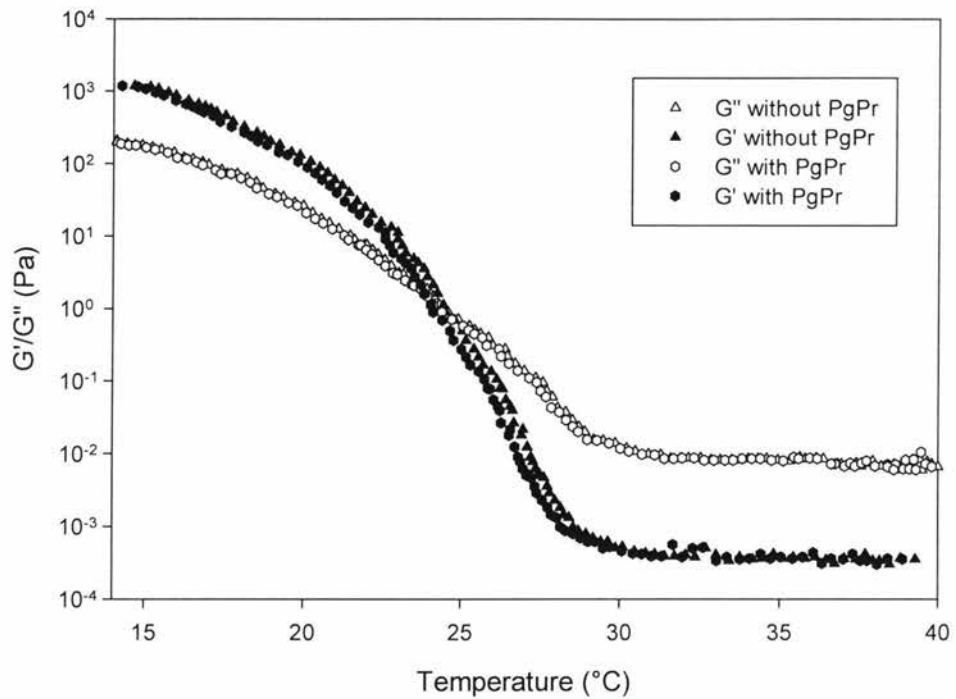


**Figure 7.8** Effect of PgPr on the gelation of waxy oil ( $T = 14\text{ }^{\circ}\text{C}$ , strain = 0.005,  $f = 1\text{ Hz}$ )

## 7.4 Conclusion

In order to meet the fourth and fifth objectives laid out in section 1.3, the effect of different factors on the yield stress of model emulsions was evaluated. The yield stress of model emulsions depended on thermal history, shear history and ageing. The thermal history impacted the amount of wax crystallized thus altering the yield stress of the model emulsions. Shear history influenced wax crystal size and water droplet floc sizes, and possibly crystal network formation. With age, wax crystals increased in size and concentration, which also affected the yield stress of the model system.

The gelation behaviour of waxy crude oil and crude oil emulsions were also determined. The gelation temperature of waxy crude oil was found to be

slightly lower than that of the model emulsion. An increase in gelation temperature was observed with a decrease in cooling rate, which was due to the different crystal sizes produced at different cooling rates.

# Chapter 8

## Conclusions and Recommendations

The research discussed in this thesis was motivated by operational problems associated with the transport and processing of waxy crude oils. An understanding of the flow behaviour of crude oil emulsions is necessary to effectively and efficiently deal with wax deposition problems. The focus of this research was thus to understand the role of a dispersed aqueous phase on the rheological behaviour of model crude oil emulsions stabilized by wax crystals. The knowledge gained from this research may be used as a basis for predicting the strength/extent of wax deposition and the flow characteristics of crude oil emulsions, thereby developing effective remediation strategies. The conclusions from this study and recommendations for future work are presented below.

### 8.1 Conclusions

Wax crystallization was evaluated in different mineral oil dilutions and model emulsion samples with combinations of 3% and 5% wax and with/without PgPr. These samples were analyzed with PFG-NMR, CLSM, and DSC. Wax crystal growth and its structure were found to be affected by the

concentration and presence of PgPr, with crystals more dispersed and less effective at forming crystalline network in its presence.

Emulsions with 5% added wax were more stable to sedimentation and coalescence compared with those containing 3% wax; this could be attributed to stronger wax crystal network formation in the samples with 5% wax. Microscopy confirmed the larger crystal size in the emulsions containing 5% wax. Furthermore, wax crystals were dispersed in the continuous oil phase rather than associated with water droplets.

A laboratory flowloop was designed and used to investigate the flow characteristics of model emulsions. A protocol based on the theoretical shear rate was used to mimic in-pipeline flow conditions in a rheometer.

The viscosity profiles of simple oil-water-wax systems were altered by adding the other components to the model system. For example, with the addition of wax to the oil phase, the mixture transitioned from a Newtonian flow to non-Newtonian and an increase in viscosity was observed. The presence of a dispersed aqueous phase further increased the viscosity of the model system by  $\sim 2x$ .

Changes in the flow behaviour of the model emulsions following passage through the lab-scale flowloop were also investigated, where steady-state and dynamic rheological characterization of the emulsion as function of flowloop length were assessed. The slight differences observed in the rheological properties for emulsions passed through different lengths of the flowloop were attributed to differences in temperature/shear history.

The effect of different factors on the yield stress of the model emulsions was evaluated. Yielding of the model emulsions depended on three factors: thermal history, shear history and ageing time. The thermal history impacted the extent of wax crystallization and hence the yield strength of the wax-stabilized emulsions. The shear history influenced the wax crystal and water droplet floc sizes, and possibly influenced the crystal networking. Evolution in wax crystal size and number with ageing time were likely responsible for changes in the yield stress of the model emulsions.

The gelation behaviour of waxy crude oil and crude oil emulsions were also determined. The gelation temperature of waxy oil was slightly lower than that of model emulsion. An increase in gelation temperature was observed with a decrease in cooling rate, which was likely due to the differences in crystal size seen with different cooling rates.

## **8.2 Recommendations**

Although this research has helped to clarify some of the rheological properties and microstructure of model crude oil emulsions and their relationship to emulsion stability, several new questions arose during the study. The following are recommendations for future avenues of research.

The rheological behaviour of the model emulsions was found to change when flowed through different lengths of a lab-scale 'pipeline'. Wax deposition was not investigated due to the short residence time (~5 min) in the flowloop. The installation of a pump to re-circulate the flowing emulsion is currently

being developed and will be the focus of future investigations on deposition kinetics.

Secondly, microstructural analyses of the model emulsions showed that the wax crystals were independent and not associated with the dispersed aqueous phase. Process parameters should be tailored to permit modulate the interaction between the wax crystals and dispersed aqueous phase to selectively (de)stabilize these emulsions.

Lastly, the rheological behaviour of these crude oil emulsions is based on passage through a ¼” pipe, which is much smaller than that found in actual oilfields. Flow behaviour in larger diameter loops should be attempted, as this would likely affect flow behaviour due to changes in shear and thermal environment.

## References

- Abend S., Bonnke N., Gutschner U. and Lagaly G., *Stabilization of emulsions by heterocoagulation of clay minerals and layered double hydroxides*. Colloid Polymer Science, (1998), 276, 730-737.
- Ahmed N.S., Nassar A.M., Zaki N.N. and Gharieb H.K., *Formation of fluid heavy oil-in-water emulsions for pipeline transportation*. Fuel, (1999), 78, 593-600.
- Ahmed N.S., Nassar A.M., Zaki N.N. and Gharieb K.H., *Stability and rheology of heavy crude oil-in-water emulsion stabilized by an anionic-nonionic surfactant mixture*. Petroleum Science and Technology, (1999), 17, 553-576.
- Amadi, S.U., Dandekar, A.Y., Chukwu, G.A., Khatanlar, S., Patil, S.L., Haslebacher, W.F. and Chaddock, J., *Measurement of the wax appearance temperature of gas-to-liquids products, Alaska North Slope Crude, and their blends*, Energy Sources, (2005), 27, 831-838.
- Aske N., Kallevik H. and Sjoebloom J., *Determination of saturate, aromatic, resin, and asphaltenic (sara) components in crude oils by means of infrared and near-infrared spectroscopy*. Energy and Fuels, (2001), 15(5), 1304-1312.
- Aveyard R., Binks B.P. and Clint J.H., *Emulsions stabilized solely by colloidal particles*. Advanced Colloid Interface Science, (2003), 100, 503-546.
- Azevedo, L.F.A. and Teixeira, A.M., *A critical review of the modeling of wax deposition mechanisms*. Petroleum Science and Technology, (2003), 21, 393-408.
- Barnes, H.A., *Rheology of emulsions – a review*. A: Physicochemical and Engineering Aspects, (1994), 91, 89-95.
- Becher P., *Emulsions: Theory and Practice*. American Chemical Society, (1965), 162, 14-20.
- Bensebaa F., Kotlyar L., Pleizier G., Sparks B., Deslandes Y. and Chung K., *Surface chemistry of end cuts from Athabasca bitumen*, Surface Interface Analysis, (2000), 30, 207-211.
- Binks B.P., Lumsdon S.O., *Pickering emulsions stabilized by monodisperse latex particles: Effects of particle size*. Langmuir, (2001), 17, 4540-4547.
- Bott T.R., *Aspects of crystallization fouling*. Experimental Thermal and Fluid Science, (1997), 14, 356-360.

- Bowman C.W., *Molecular and interfacial properties of Athabasca Tar sands*. Proceedings of 7<sup>th</sup> World Petroleum Congress, Mexico, (1967), 3, 583-603.
- Chang C., Nguyen Q., Dzuy and Ronningsen H.P., *Isothermal start-up of pipeline transporting waxy crude oil*. Journal of non-Newtonian Fluid Mechanics, (2000), 74, 127-154.
- Chen S., Oye G. and Sjoblom J., *Rheological properties of model and crude oil systems when wax precipitate under quiescent and flowing conditions*. Journal of Dispersion Science and Technology, (2007), 28(7), 1020-1029.
- Claudy P., Letoffe J.M. and Chague B., *Crude oils and their distillates-Characterization by differential scanning calorimetry*, Fuel, (1988), 67 (1), 58–61.
- Daniel-David D., Le Follotec A. and Pezron I., *Destabilization of water-in-crude oil emulsions by silicone copolymer demulsifiers*, Oil and Gas Science and Technology, (2008), 63(1),165-173.
- Davenport T.C. and Somper R.S.H., *The yield value and breakdown of crude oil gels*. Journal of Institute of Petroleum, (1971), 55, 86-105.
- Davenport T.C. and Russell R.J., *The full-scale pumping of admiralty fuel oil and its relation to laboratory tests*. Journal of Institute of Petroleum, (1960), 46 (437), 143-160.
- Dickinson E., Ritzoulis C., Yamamoto Y. and Logan H., *Ostwald ripening of protein-stabilized emulsions: effect of trans-glutaminase crosslinking*. Colloids Surface B: Interfaces, (1999), 12, 139-146.
- Elgibaly A.A.M., Nashawi I.S. and Tantawy M.A., *Rheological characterization of Kuwaiti oil-lakes oils and their emulsions*. SPE 37259, (1997), 493-508.
- El-Hattab M.I., *Scale deposition in surface and subsurface production equipment in the Gulf of Suez*. Journal of Petroleum Technology, (1985), 37, 1640-1660.
- Farah M.A., Oliveira R.C., Caldas J.N. and Rajagopal K., *Viscosity of water-in-oil emulsions: variation with temperature and water volume fraction*, Journal of Petroleum Science and Engineering, (2005), 48, 169–184.
- Fechner A., Knoth A. and Scherze I., *Stability and release properties of double-emulsions stabilised by caseinate-dextran conjugates*, Food Hydrocolloids, (2007), 21, 943-952.

Gelot A., Friesen W. and Hamza H.A., *Emulsification of oil and water in the presence of finely divided solids and surface-active agents*, Colloids Surfaces, (1984), 12, 271-303.

Gill F. and Russell R.J., *Pumpability of residual fuel oils*. Industrial and Engineering Chemistry, (1954), 46, 1264-1278.

Guo B., Song S., Chacko J. and Ghalambor A., *Offshore Pipelines*, Gulf Professional Publishing, USA, (2005).

Guo X.H., Pethica B.A., Huang J.S. and Prud'homme R.K., *Crystallization of long-chain n-paraffins from solutions and melts as observed by differential scanning calorimetry*. Macromolecules, (2004), 37(15), 5638-5645.

Herring J.D., *Design Concepts for High Wax Crude Oil Pipelines*. Pipeline Gas Journal, (1974), 4, 34-42.

Hollingsworth K.G., Sederman A.J., Buckley C., Gladden L.F. and Johns M.L., *Fast emulsion droplet sizing using NMR self-diffusion measurements*. Journal of Colloid and Interface Science, (2004), 274, 244-250.

Hou, L. and Zhang, J. *Effects of Thermal and Shear History on the Viscoelasticity of Daqing Crude Oil*. Petroleum Science and Technology, (2007), 25, 601-614.

Houwink R., *Elasticity, Plasticity and Structure of Matter*, (1958), 42, Dover, New York.

Hsu, J.J.C., Elphinstone, G.M. and Greenhill, K.L., *Modeling of multiphase wax deposition*. Journal of Energy Resources Technology, (1999), 121, 81-85.

Irani C. and Zajac J., *Handling of high pour point West African crude oils*. Journal of Petroleum Technology, (1982), 34, 289-298.

Kabalnov A.S. and Shchukin E.D., *Ostwald ripening theory: Applications to fluorocarbon emulsion stability*. Advances in Colloid and Interface Science, (1992), 38, 69-97.

Kane M., Djabourov M. and Volle J.L., *Rheology and structure of waxy crude oils in quiescent and under shearing conditions*. Fuel, (2004), 83 (11), 1591-1605.

Keentok M., *The measurement of the yield stress of liquids*. Rheology Acta, (1982), 21, 325-332.

- Khan M.R., *Rheological properties of heavy oils and heavy oil emulsions*. Energy Sources, (1996), 18, 385-391.
- Knegt J.T. and Zeilinga E., *Field tests with waxy crudes in the Rotterdam-Rhine pipeline system*. Journal of Institute of Petroleum, (1971), 57, 165-174.
- Kok M.V., Letoffe J.M. and Claudy P., *Comparison of wax appearance temperatures of crude oils by differential scanning calorimetry, thermomicroscopy and viscometry*. Fuel, (1996), 75(77), 787-790.
- Kotlyar L.S., Sparks B.D., LePage Y. and Woods J.R., *Effects of particle size on the flocculation behaviour of ultra-fine clays in salt solutions*, Clay Minerals, (1998), 33, 103-107.
- Krieger I.M. and Dougherty T.J., *A mechanism for non-Newtonian flow in suspensions of rigid spheres*. Trans. Society Rheology, (1959), 3, 137-152.
- Langevin D., Poteau S., Henaut I. and Argillier J.F., *Crude oil emulsion properties and their application to heavy oil transportation*. Oil & Gas Science and Technology – Rev. IFP, (2004), 59(5), 511-521.
- Letoffe J.M. and Claudy P., *Crude oils-characterization of waxes precipitated on cooling by DSC and thermomicroscopy*. Fuel, (1995), 74(6), 810-817.
- Levine S. and Sanford E., *Stabilization of emulsion droplets by fine powder*. Canadian Journal of Chemical Engineering, (1985), 62, 258-268.
- Lyklema J., *Adsorption at solid-liquid interfaces with special reference to emulsion systems*, Colloids Surfaces, A: Physicochemical and Engineering Aspects, (1994), 91, 25-38.
- Mao M. and Marsden S.S. *Stability of concentrated crude oil-in-water emulsions as a function of shear rate, temperature, and oil concentration*. Journal of Canadian Petroleum Technology, (1977), 16, 54-59.
- Matveenkov, V.N., Kirsanov, E.A. and Remizov, S.V., *Rheology of highly paraffinaceous crude oil*. Colloids and Surfaces A: Physicochemical and Engineering Aspects, (1995), 101(1), 1-7.
- McLean, J.D. and Kilpatrick, P.K., *Comparison of precipitation and extrography in the fractionation of crude oil residual*. Energy and Fuels, (1997), 11, 570-585.
- Menon V.B. and Wasan D.T., *A review of the factors affecting the stability of solids-stabilized emulsions*, Petroleum Science and Technology, (1988), 23, 12, 2131-2140.

Menon V.B. and Wasan D.T., *Coalescence of water-in-shale oil emulsions*, Separation Science and Technology, (1984), 19(8), 555-574.

Nguyen Q.D. and Boger D.V., *Measuring the flow properties of yield stress fluids*. Annual Review of Fluid Mechanics, (1992), 24, 47-88.

Nguyen Q.D. and Boger D.V., *Yield stress measurement for concentrated suspensions*. Journal of Rheology, (1983), 27(4), 321-349.

Nunez G., Briceno M., Mata C., Rivas H. and Joseph D., *Flow characteristics of concentrated emulsions of very viscous oil in water*. Journal of Rheology, (1996), 40, 405-423.

Oliveira, G.E., Mansur, C.R.E., Lucas, E.F., Gonzalez, G. and DeSouza, W.F., *The effect of asphaltenes, naphthenic acids, and polymeric inhibitors on the pour point of paraffins solutions*. Journal of Dispersion Science and Technology, (2007), 28, 349-356.

Paso K.S., Yi M., Sastry Y., Fogler A.M. and Scott H., *Paraffin polydispersity facilitates mechanical gelatin*. Industrial and Engineering Chemistry Research, (2005), 44, 7242-7254.

Perkins T.K. and Turner J.B., *Starting behaviour of gathering lines and pipelines filled with gelled Prudhoe Bay oil*. Journal of Petroleum Technology, (1971), 23, 301-308.

Petrellis N.C. and Flumerfelt R.W., *Rheological behaviour of shear degradable oils: Kinetic and Equilibrium properties*. Canadian Journal of Chemical Engineering, (1973), 51, 291-301.

Plegue T.H., Frank S., Fruman D. and Zakin J.L., *Viscosity and colloidal properties of concentrated crude oil in water emulsions*. Journal of Colloid and Interface Science, (1986), 114, 88-105.

Richardson, E.G. and Tyler, E., *The flow of liquid suspensions*. Journal of Colloid Science, (1933), 45, 142-151.

Remizov, S.V., Kirsanov, E.A. and Matveenkov V.N., *Structural and rheological properties of microheterogeneous systems 'solid hydrocarbons-liquid'*. Colloids and Surfaces A: Physicochemical and Engineering Aspects, (2000), 175(3), 271-391.

Ronningsen H.P. and Brit B., *Wax precipitation from North Sea crude oils. 1. Crystallization and dissolution temperatures and Newtonian and non-Newtonian flow properties*. Energy Fuels, (1991), 5, 895-908.

Ronningsen H.P., *Correlations for predicting viscosity of W/O emulsions based on North Sea crude oils*. Proc. SPE International Symposium, Oil Field Chemistry, (1995), 100-120.

Ronningsen H.P., Karan K., *Gelling and restart behaviour of waxy crude oils from a North Sea field: A study on the effect of solution gas, mixing with other fluids and pour point depressants*. Proceedings of 10<sup>th</sup> International Conference on Multiphase '01, (2001), Cannes, France.

Ronningsen H.P., *Rheological behaviour of gelled, waxy North Sea crude oils*. Journal of Petroleum Science and Engineering, (1992), 7, 177-213.

Ronningsen H.P., *Rheological properties of water-in-oil emulsions with some waxy North Sea crude oils*, Proceedings of International Congress on Rheology, (1992), 687-697.

Ronningsen, H.P., Sjöblom, J. and Mingyuan, L. *Water-in-crude oil emulsions from the Norwegian continental shelf II. Ageing of crude oils and its influence on the emulsion stability*. Colloids and Surfaces A: Physicochemical and Engineering Aspects, (1995), 119-130.

Rose S.C. and Marsden, S.S. *The flow of north slope crude oil and its emulsions at low temperatures*. Proceedings of the 45<sup>th</sup> Meeting of the Society of Petroleum Engineers, Houston USA, (1970).

Rousseau D., *Fat crystals and emulsion stability – a review*, Food Research International, (2000), 33, 3-14.

Sabbagh A.B. and Lesser A.J., *Effect of particle morphology on the emulsion stability and mechanical performance of polyolefin modified asphalts*, Polymer Engineering Science, (1998), 38(5), 707-717.

Salager J.L., Briceno M.I. and Brancho C.L., *Encyclopedic Handbook of Emulsion Technology*, Marcel Dekker, NewYork, (2001).

Schildberg Y., Sjoblom J., Christy A.A., Volle J.L. and Rambeau O., *Characterization of interfacially active fractions and their relation to water-in-oil emulsion stability*. Journal of Dispersion Science and Technology, (1995), 16(7), 575-605.

Schramm L.L., *Petroleum emulsions - Basic Principles*. Advances in Chemical Series, (1992), 231, 1-49.

Schulman J.H. and Leja J., *Control of contact angles at the oil-water solid interface*. Transactions of the Faraday Society, (1954), 50, 598-605.

Sharma K., Saxena V.K., Kumar A., Ghildiyal H.C., Anurada A., Sharma N.D., Sharma B.K. and Dinesh R.S., *Pipeline transportation of heavy viscous crude oil as water continuous emulsion in North Cambay Basin (India)*. SPE 39537, (1998).

Sifferman T.R., *Flow properties of difficult-to-handle waxy crude oils*. Journal of Petroleum Technology, (1979), 8, 1042-1050.

Simon R.P. and Poynter W.G., *Down-hole emulsification for improving viscous crude production*. Journal of Petroleum Technology, (1968), 20, 1349-1353.

Singh P., Venkatesan R., Fogler H.S., *Formation and aging of incipient thin film wax-oil gels*. AIChE, (2000), 46 (5): 1059-1074.

Sjoblom J., Aske N., Auflem I.H., Brandal O., Havre T.E., Saether O., Westvik A., Johnsen E.E. and Kallevik H., *Our current understanding of water in crude oil emulsions. Recent characterization techniques and high-pressure performance*. Advances in Colloid and Interface Science, (2003).

Smith H.V. and Arnold K.E., *Petroleum Engineering Handbook*, (1987), Bradley Inc., Richardson, TX, USA.

Speight J.G. *The Chemistry and Technology of Petroleum*, Marcel Dekker Inc., (1999), New York, USA.

Stank J. and Mullay J., *Analysis of wax oil mixtures using DSC*. Thermochimica Acta, (1986), 105, 9-17.

Sullivan A.P. and Kilpatrick P.K., *The effects of inorganic solid particles on water and crude oil emulsion stability*. Industrial and Engineering Chemistry Research, (2002), 41, 3389-3404.

Sun R. and Shook C.A., *Inversion of heavy crude oil-in-brine emulsions*. Journal of Petroleum Science and Engineering, (1996), 14, 169-182.

Tadros T.F., *Fundamental principles of emulsion rheology and their applications*. Colloids and Surfaces A, (1994), 91, 39.

Tadros T.F., *Use of viscoelastic measurements in studying interactions in concentrated dispersions*. Langmuir 6, (1990), 28, 100-110.

Tais A.M., Cambert M., Riaublanc, A. and Mariette, F.O., *Effects of casein and fat content on water self-diffusion coefficients in casein systems: A pulsed Field gradient nuclear magnetic resonance study*. Journal of Agriculture and Food Chemistry, (2004), 52, 3988-3995.

Tambe D.E. and Sharma M.M., *Factors controlling the stability of colloid-stabilized emulsions: I. An experimental investigation*. Journal of Colloid Interface Science, (1993), 157, 244-253.

Tambe D.E. and Sharma M.M., *Factors controlling the stability of colloid-stabilized emulsions: I. A model for the rheological properties of colloid-laden interfaces*, Journal of Colloid Interface Science, (1994), 162, 1-10.

Taylor S.E., *Resolving Crude Oil Emulsions*. Chemistry Industrial London, October 19, (1992), 770-773.

Titkova L.V. and Yanovsky Y.G., *Viscoelastic and thixotropic parameters of highly structured grades of petroleum*. Program Trends Rheology, (1988), 2, 305-307.

Torres L.G., Iturbe R., Snowden M.J., Chowdhry B.Z. and Leharne S.A., *Preparation of o/w emulsions stabilized by solid particles and their characterization by oscillatory rheology*. Colloids and Surfaces A, (2007), 302, 439-448.

Uhde A. and Kopp G., *Pipeline problems resulting from the handling of waxy crudes*. Journal of Institute of Petroleum, (1971), 57, 63-73.

Venkatesan, R., Nagarajan, N.R., Paso, K., Yi, Y.B., Sastry, A.M. and Fogler, H.S., *The strength of paraffin gels formed under static and flow conditions*. Chemical Engineering Science, (2005), 60, 3587-3598.

Verschuur E., Den Hartog A.P. and Verheul C.M., *The effect of thermal shrinkage and compressibility on the yielding of gelled waxy crude oils in pipelines*. Journal of Institute of Petroleum, (1971), 57, 131-138.

Vignati E., Piazza R. and Lockhart T. P. *Pickering emulsions: Interfacial tension, colloidal layer morphology, and trapped-particle motion*. Langmuir, (2003), 19, 6650-6656.

Vignati E., Piazza R., Visintin R.F.G., Lapasin R., D'Antona, P. and Lockhart T.P. *Wax crystallization and aggregation in a model crude oil*. Journal of Physics.: Condensed Matter, (2005), 17, 3651-3660.

Visintin R.F.G., Lapasin R. and Vignati E., *Rheological behaviour and structural interpretation of waxy crude oil gels*. Langmuir, (2005), 21(14), 6240-6249.

Wang, Q., Sarica, C., and Chen, T.X., *An experimental study on mechanics of wax removal in pipeline*. Journal of Energy Resources Technology, (2005), 127, 302-312.

Wardhaugh L.T. and Boger D.V., *Flow property measurement of Australian waxy crude oils*. CHEMECA 86, (1986), Adelaide, Australia, 49-53.

Wardhaugh L.T. and Boger D.V., *Measurement of the unique flow properties of waxy crude oils*. Chemical Engineering Research and Design, (1987), 65, 74-83.

Wardhaugh L.T. and Boger D.V., *The measurement and description of the yielding behaviour of waxy crude oil*. Journal of Rheology, (1991), 35 (6), 1121-1156.

Webber R.M., *Yield properties of wax crystal structures formed in lubricant mineral oils*. Industrial Engineering and Chemistry Research. (2001), 40, 195-203.

Wilson V.S., Howes R.W., Van Schie B. and Howes D., *Overview of the preparation, use and biological studies on polyglycerol polyricinoleate (PGPR)*, Food and Chemical Toxicology, (1998), 36, 711-718.

Yan N. and Masliyah J.H., *Characterization and demulsification of solids-stabilized oil-in-water emulsions Part 2. Demulsification by the addition of fresh oil*, Colloids Surfaces A: Physicochemical and Engineering Aspects, (1995), 96, 243-252.

Yan Z., Elliot J.A.W, Masliyah J.H., *Roles of various bitumen components in the stability of water-in-diluted bitumen emulsions*. Journal of Colloid and Interfacial Science, (1999), 220, 329-337.

Yekeler M., Ulusoy U. and Hicyilmaz C., *Effect of particle shape and roughness of talc mineral ground by different mills on the wettability and floatability*. Powder Technology, (2004), 140, 68-80.

Zaki N.N., Ahmed N.S. and Nassar A.M., *Sodium lignin sulfonate to stabilize heavy crude oil-in-water emulsions for pipeline transportation*. Petroleum Science and Technology, (2000), 18, 1175-1193.

Zaki N.N., Maysour N.W.S. and Abdel-Azim A., *Polyoxyalkylenated amines for breaking of water-in-oil emulsions stabilized by asphaltenes and clay*. Petroleum Science and Technology, (2000), 18(9), 1009-1025.